

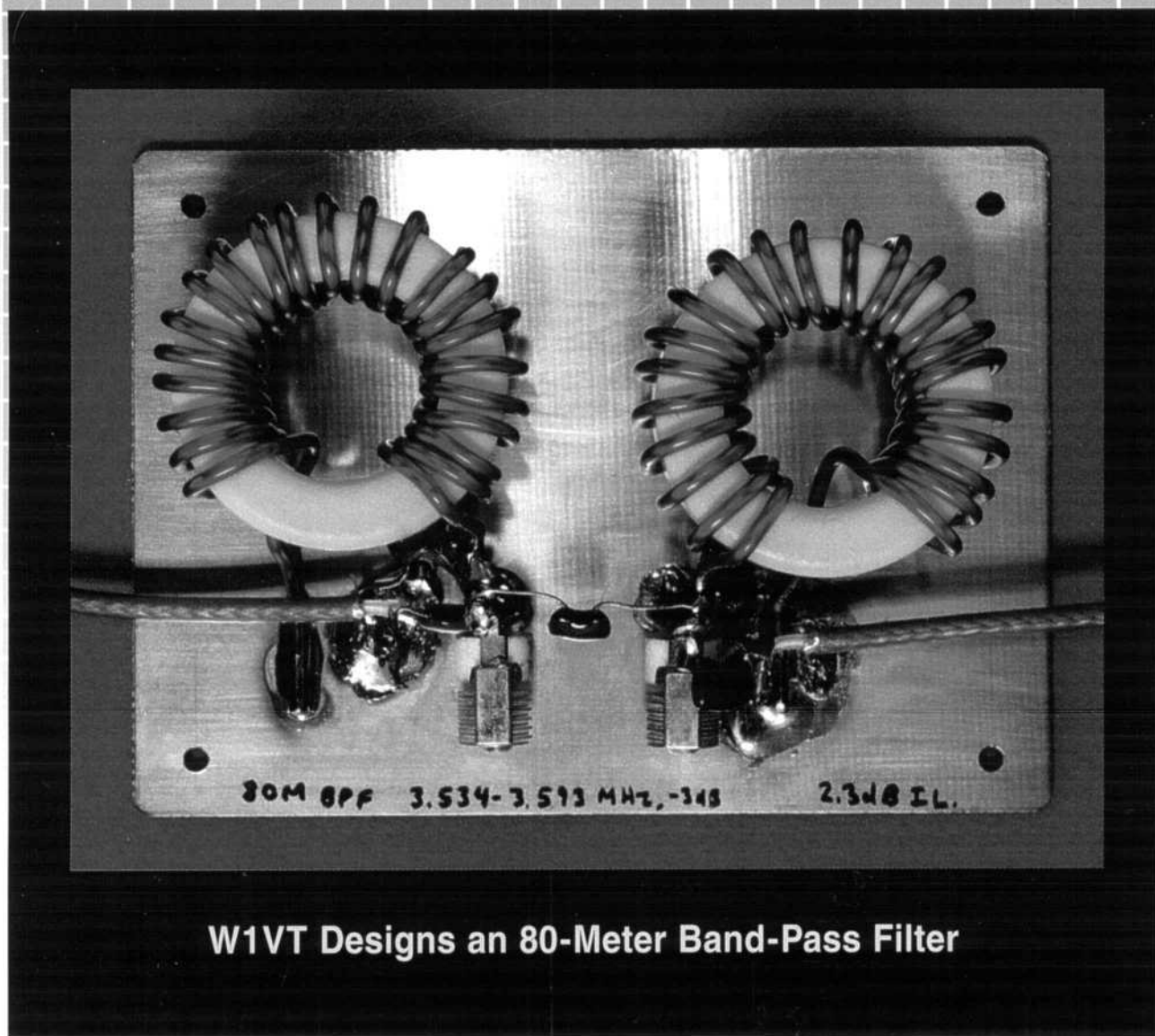
QEX

September/October 1998

\$4



Forum for Communications Experimenters



W1VT Designs an 80-Meter Band-Pass Filter

QEX: Forum for
Communications Experimenters
American Radio Relay League
225 Main Street
Newington, CT USA 06111-1494

QEX

QEX (ISSN: 0886-8093) is published bimonthly in January 98, March 98, May 98, July 98, September 98, and November 98 by the American Radio Relay League, 225 Main Street, Newington CT 06111-1494. Subscription rate for 6 issues to ARRL members is \$18; nonmembers \$30. Other rates are listed below. Periodicals postage paid at Hartford CT and at additional mailing offices.

POSTMASTER: Form 3579 requested. Send address changes to: QEX, 225 Main St, Newington CT, 06111-1494
Issue No. 190

David Sumner, K1ZZ
Publisher

Doug Smith, KF6DX/7 and Rudy Severns, N6LF
Editors

Robert Schetgen, KU7G
Managing Editor

Lori Weinberg
Assistant Editor

Zack Lau, W1VT
Contributing Editor

Production Department

Mark J. Wilson, K1RO
Publications Manager

Michelle Bloom, WB1ENT
Production Supervisor

Sue Fagan
Graphic Design Supervisor

David Pingree, N1NAS
Technical Illustrator

Joe Shea
Production Assistant

Advertising Information Contact:

Brad Thomas, KC1EX, Advertising Manager
American Radio Relay League
860-594-0207 direct
860-594-0200 ARRL
860-594-0259 fax

Circulation Department

Debra Jahnke, Manager
Kathy Capodicasa, N1GZO, Deputy Manager
Cathy Stepina, QEX Circulation

Offices

225 Main St, Newington, CT 06111-1494 USA
Telephone: 860-594-0200
Telex: 650215-5052 MCI
Fax: 860-594-0259 (24 hour direct line)
Electronic Mail: MCIMAILID: 215-5052
Internet: qex@arrl.org

Subscription rate for 6 issues:

In the US: ARRL Member \$18,
nonmember \$30;

US, Canada and Mexico by First Class Mail:
ARRL Member \$31, nonmember \$43;

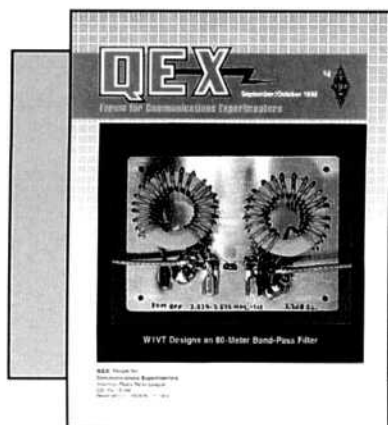
Elsewhere by Surface Mail (4-8 week delivery):
ARRL Member \$23,
nonmember \$35;

Elsewhere by Airmail: ARRL Member \$51,
nonmember \$63.

Members are asked to include their membership control number or a label from their QST wrapper when applying.

In order to insure prompt delivery, we ask that you periodically check the address information on your mailing label. If you find any inaccuracies, please contact the Circulation Department immediately. Thank you for your assistance.

Copyright © 1998 by the American Radio Relay League Inc. Material may be excerpted from QEX without prior permission provided that the original contributor is credited, and QEX is identified as the source.



About the Cover

Zack's 80 meter bandpass filter looks ready for Hallowe'en. Details appear in his RF column.



Features

- 3 ARRL Radio Designer and the Circles Utility, Part 1: Smith Chart Basics**
By William E. Sabin, W0IYH
- 10 Quick, Easy Network Analysis on a PC Using Mathcad**
By Ralph Vacca, W1KF
- 19 Signals, Samples, and Stuff: A DSP Tutorial (Part 4)**
By Doug Smith, KF6DX/7
- 30 A Faster and Better ADC for the DDC-Based Receiver**
By Peter Traneus Anderson, KC1HR
- 33 Low-Noise Front-End Design with ARRL Radio Designer, Example: a 23-cm Preamp**
By John Brown, G3DVV
- 39 A Remote Bandswitch for the "Bug Catcher"**
By Paul I. Protas, WA5ABR
- 44 The CYLOAD Cylinder-Loaded Dipole**
By Hal Wright, W9UYA
- 47 A Concise Calculation Method for Pi-L Networks**
By Karl Gerhard Lickfeld, DL3FM
- 50 Harmonic Filters, Improved**
By James L. Tonne, WB6BLD
- 54 A Test for Ambient Noise**
By Peter Lefferson, K4POB

Columns

- 49 Upcoming Conferences** **57 RF**
49 Conference Proceedings By Zack Lau, W1VT
49 New Products **58 Letters to the Editor**

Sept/Oct 1998 QEX Advertising Index

Alpha Delta Communications: Cov IV
American Radio Relay League: 38, 59,
60, 61, 62, Cov III
ByteMark: 18
Communications Specialists, Inc: 43
Crestone Technical Books: Cov II

HAL Communications Corp: 63
T-Tech, Inc: 63
Timeline Inc: 64
Tucson Amateur Packet Radio
Corp: 43
Z Domain Technologies, Inc: 29



The American Radio Relay League, Inc. is a noncommercial association of radio amateurs, organized for the promotion of interests in Amateur Radio communication and experimentation, for the establishment of networks to provide communications in the event of disasters or other emergencies, for the advancement of radio art and of the public welfare, for the representation of the radio amateur in legislative matters, and for the maintenance of fraternalism and a high standard of conduct.

ARRL is an incorporated association without capital stock chartered under the laws of the state of Connecticut, and is an exempt organization under Section 501(c)(3) of the Internal Revenue Code of 1986. Its affairs are governed by a Board of Directors, whose voting members are elected every two years by the general membership. The officers are elected or appointed by the Directors. The League is noncommercial, and no one who could gain financially from the shaping of its affairs is eligible for membership on its Board.

"Of, by, and for the radio amateur." ARRL numbers within its ranks the vast majority of active amateurs in the nation and has a proud history of achievement as the standard-bearer in amateur affairs.

A bona fide interest in Amateur Radio is the only essential qualification of membership; an Amateur Radio license is not a prerequisite, although full voting membership is granted only to licensed amateurs in the US.

Membership inquiries and general correspondence should be addressed to the administrative headquarters at 225 Main Street, Newington, CT 06111 USA.

Telephone: 860-594-0200
Telex: 650215-5052 MCI
MCIMAIL (electronic mail system) ID: 215-5052
FAX: 860-594-0259 (24-hour direct line)

Officers

President: RODNEY STAFFORD, W6ROD
5155 Shadow Estates, San Jose, CA 95135

Executive Vice President: DAVID SUMNER, K1ZZ

Purpose of QEX:

- 1) provide a medium for the exchange of ideas and information between Amateur Radio experimenters
- 2) document advanced technical work in the Amateur Radio field
- 3) support efforts to advance the state of the Amateur Radio art

All correspondence concerning *QEX* should be addressed to the American Radio Relay League, 225 Main Street, Newington, CT 06111 USA. Envelopes containing manuscripts and correspondence for publication in *QEX* should be marked: Editor, *QEX*.

Both theoretical and practical technical articles are welcomed. Manuscripts should be typed and doubled spaced. Please use the standard ARRL abbreviations found in recent editions of *The ARRL Handbook*. Photos should be glossy, black and white positive prints of good definition and contrast, and should be the same size or larger than the size that is to appear in *QEX*.

Any opinions expressed in *QEX* are those of the authors, not necessarily those of the editor or the League. While we attempt to ensure that all articles are technically valid, authors are expected to defend their own material. Products mentioned in the text are included for your information; no endorsement is implied. The information is believed to be correct, but readers are cautioned to verify availability of the product before sending money to the vendor.

Empirically Speaking

Editing *QEX* for the past year has been a delightful experience. The readership support I have received is outstanding, as shown by the selection of articles now appearing in *QEX*. We've come a long way, but much still needs doing. Unfortunately (for *QEX*), my business affairs have prospered to the point where I can no longer give *QEX* the attention needed. It is time to pass the torch.

Doug Smith has graciously agreed to take over as Editor of *QEX*. He is very well qualified and enthusiastic. I want to thank you all for your support. If you support Doug as well, *QEX* will continue to grow and prosper.

I will not disappear entirely. When I began as Editor, I promised a series of articles on switch-mode power converters. I will keep that commitment and provide some antenna articles, too.—*CUL & 73, Rudy Severns, N6LF*

Rudy, you've clearly brought *QEX* to a higher plateau. To maintain it requires that you grace the pages with those articles you've been promising us! Truly, we all owe you a debt of sincere gratitude. As you and I exchange our roles, your contribution is more critical than ever.

I am the new Editor, Doug Smith, KF6DX, another ARRL "outsider." That is, I'm not at ARRL headquarters. My background is mainly in HF radio, although I enjoy all facets of communications. I am delighted to be part of a magazine that conveys so much good information in each issue, and I will actively support a wide variety of subjects.

My approach will be one of "many small improvements." I'm dedicated to keeping *QEX* at the front edge of technology, while holding a balance between theoretical and practical material. We all like to build! Our Web page will expand to show where we've been and describe the *QEX* editorial approach.

It's easier to write for *QEX* than you might think. I welcome all submissions and inquiries. Don't worry too much about grammar. Write your experiences as best you can, and we'll work with you. We have many expert editors and technical advisors who can help. Pick your passion and start writing. League publications need your contributions!

Several readers have been kind enough to request clarification or

challenge assertions that seem questionable to them. I want such discussion for the "Letters" area of *QEX*. If writing an article seems too challenging for you right now, please send me your comments and suggestions.

As an electrical engineer, I see a widening gap between new technologies and our understanding of them. Even some mature techniques, such as switch-mode power conversion, lack sufficient coverage in Amateur Radio publications. *QEX* is in the unique position to fill this void. We are here to introduce new ideas, debate elegant techniques and document efforts that further the state of the Amateur Radio art. *QEX* lives only to serve as *your* forum to build on our legacy of innovation. Keep those projects going!

In this QEX

This month, we have a wonderful collection. CAD tools have come a long way. What did we do without them? Ralph H. Vacca, W1KF, illustrates some finer points of network-analysis computations on the PC. Bill Sabin, W0IYH, begins a two-part series about the ARRL *Radio Designer* Circles (Smith Chart) utility: how to solve problems in network design.

John Brown, G3DVV, gives us some pointers about low-noise, UHF receiver front-end design, and Dr. Karl Lickfeld, DL3FM, presents his analysis of Pi-L network calculations. James Tonne, WB6BLD, helps you meet FCC harmonic-attenuation requirements. These articles show the tradeoffs facing circuit builders and provide some slick solutions.

Paul Protas, WA5ABR, has a simple construction project that band switches "bug catcher" style mobile antennas from the driver's seat. Perhaps you need a shortened radiator for an attic or small backyard. Hal Wright, W9UYA, provides an experimental loading method for dipoles.

Peter Anderson, KC1HR, shares his work on high-speed ADCs, a key element in any digital receiver. Pete Lefferson, K4POB, examines how externally generated noise affects receiver performance. My own DSP series concludes (at last!) with the offer of a couple of new results. Zack Lau, W1VT, describes an 80-meter bandpass filter. Happy reading and 73—*Doug Smith, KF6DX, kf6dx@arrl.org* □□

ARRL Radio Designer and the Circles Utility

Part 1: Smith Chart Basics

The Smith Chart is a venerable tool for graphic solution of RCL and transmission-line networks. The Circles Utility of ARRL's Radio Designer software provides an "electronic" Smith Chart that is very useful. For those unfamiliar with the Circles Utility, we begin by exploring basic concepts and techniques of matching-network design.

By William E. Sabin, WØIYH

One of the interesting and useful features of the ARRL *Radio Designer* program is the Circles Utility. This two-part article will look at some of the ways of using Circles. A brief overview of basic principles will be followed by some "walk-through" examples that can be used as "templates" or guidance for future reference. The Circles Utility can do the following things:

- Perform Smith Chart operations to design and analyze transmission-line networks and LCR impedance-matching networks. Part 1 of this article deals with these topics.

- Using the Smith Chart, perform

gain-circle operations that are widely used in active-circuit design, especially amplifiers, using S-parameter equations. Input- and output-matching networks can be evaluated. The stability of an active circuit can be evaluated by plotting stability circles. Noise-figure circles (circles of constant noise-figure values) can be plotted. Figures of merit are calculated. We can perform plots of certain quantities over a frequency range. The result is a visual estimate of the performance of the circuit. Part 2 of this article will deal with this.

Smith Chart Basics

It is a good idea to bring up the Circles Utility and perform the following operations as you read about them.

First, to enable Circles, we must enter and Analyze (key F10) a circuit listing of a two-port network as exem-

plified in Fig 1A, a resonant filter circuit that is also an impedance-matching network. The schematic is shown in Fig 1B. Start with the list in Fig 1A, and modify it later as required. I assume the reader already knows how to use the Report Editor to get XY rectangular plots, tables and polar plots versus frequency of such things as MS11, MS21 etc, and how to set the Terminations. An Optimization of the circuit is also performed.

Fig 2A shows how various lines of constant resistance and constant reactance are plotted on the Smith Chart, using the Circles Control Window (we will henceforth call it CCW). The various entries that we type into the CCW text window are just as shown (the " = " is optional and a "space" can be used instead). In particular, pure reactances can only exist on the outer circle of the chart; to move inside, some

resistance must be added. Positive reactance (+X, inductance) is in the upper half, negative reactance (-X, capacitance) in the lower half. High resistance (R, low conductance $G = 1/R$) is toward the right.

You can also create an R or X circle at some specific location. Type "R" or "X" in the CCW, Execute, then place the cursor at the desired location and press the left mouse button. This creates an R or X circle and a label with some specific value.

To remove a single error in an entry, type "DEL" into the CCW, then Execute. To delete two entries, type "DEL 2," and so forth. To get the best accuracy in all of the various operations, click on Settings/Display/Graphics/Line Width and set the line width to "1," the narrowest line.

Fig 2B shows how various lines of constant-conductance and constant-susceptance values are plotted. This chart is a left-to-right and top-to-bottom reverse image of Fig 2A. Positive susceptance (+B, capacitance) is below and negative susceptance (-B, inductance) above the horizontal axis. Both charts always show inductance above the axis and capacitance below the axis. High conductance (G, low resistance, $R = 1/G$) is toward the left.

G and B circles at some cursor location are created by typing "G" or "B," Execute, then place the cursor at the desired location and press the left mouse button.

The Circles Smith Chart is a YZ chart, which means that Figs 2A and 2B and all four of the quantities shown there can be plotted simultaneously on the same chart in two different colors. The term "Z" refers to R and X in *series* and the term "Y" refers to G and B in *parallel*. It's important to keep this distinction in mind, especially when switching between the two. This YZ capability is a powerful feature that we will use often. Also, the Z chart is "normalized" to 1 Ω at the origin. To normalize a 50 Ω system, divide all actual R and $\pm X$ input values by 50. For other values of Z_0 , such as 52 Ω , 450 Ω etc, use Z_0 as a scaling factor. The Y chart is normalized to 1 S (Siemens = 1 / Ω) at the origin. For a 0.02 S (1 / (50 Ω)) system, multiply actual G and $\pm B$ values by 50, or whatever Z_0 is correct. It is very desirable to have a calculator available to normalize values; the computations are no problem once you get the "hang of it." In the interest of simplicity, it is best (at least at the beginning) to use resistive (not complex) values of Z_0 . For a transmission line, a resistive Z_0 means a line with no attenuation (loss).

Fig 2C shows various values of V (SWR) circles, entered as shown. At any point on a particular V circle, a value of RHO, the reflection coefficient, can also be found. For example, at the intersection of $R = 1$ and $V = 8$, the reflection coefficient is 0.77 at 39.17° (angle measured counterclockwise from the horizontal axis). To find this RHO, we use the following procedure:

- Enter the word "RHO" into the CCW and click the Execute button.
- Place the cursor at the intersection of $V = 8$ and $R = 1$.
- Press "M" on the keyboard.
- This places a mark at this location and also puts the complex (magnitude and angle) value of RHO in the CCW.

The following equations give the relationships involved in the RHO and V operations:

$$RHO = \frac{(R + jX) - Z_0}{(R + jX) + Z_0} \quad (\text{Eq 1})$$

where R, X and Z_0 are normalized to 1.0 as discussed previously and

$$V = \frac{1 + |RHO|}{1 - |RHO|}; |RHO| = \frac{V - 1}{V + 1} \quad (\text{Eq 2})$$

where the vertical bars " | " denote "magnitude." From this equation we see that a V circle is also a circle of constant |RHO|, so the V circle is also called a "constant-reflection" circle. Also of considerable interest is the return loss

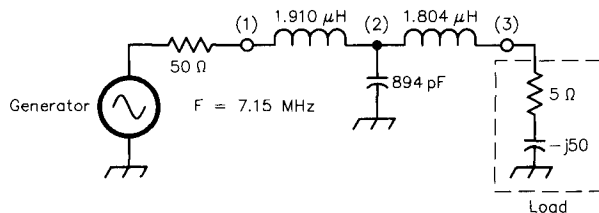
$$RL(\text{dB}) = -20 \cdot \log |RHO| = -20 \cdot \log \left(\frac{V - 1}{V + 1} \right) \text{dB} \quad (\text{Eq 3})$$

Return loss is a very sensitive measure of impedance match that is widely used in test equipment, such as network analyzers. This term means "what fraction of the power that is sent toward the load returns to the generator?" In *Radio Designer*, RL (dB) is the same as MS11 (dB) and MS22 (dB) at the input and output, respectively, of a two-port network. The values of RHO and V can be found for any combination of R and X or G and B, using the cursor method as described.

The Smith Chart is basically a reflection-coefficient (RHO) chart. The distance from the center to the outer circle corresponds to |RHO| = 1.0, which is defined as "complete" reflection of a wave, which corresponds to a short-circuit load ($R = 0$), an open-circuit load ($G = 0$) or a purely reactive load. The chart then assigns the R, X, G and B values in terms of the corresponding complex values of RHO according to the equation

$$Z = Z_0 \cdot \frac{1 + RHO}{1 - RHO}; Y = \frac{1}{Z}; \quad RHO \text{ and } Z_0 \text{ possibly complex} \quad (\text{Eq 4})$$

The method described for RHO, steps 1, 2, 3 and 4, can be



(A)

* Smith chart example

BLK

IND 1 2 L=?1.94198UH? Q=250 F=7.15MHZ
CAP 2 0 C=?860.327PF? Q=10000 F=7.15MHZ
IND 2 3 L=?1.83567UH? Q=250 F=7.15MHZ

TUNER:2POR 1 3

END

FREQ

STEP 7.0MHZ 7.35MHZ 10 KHZ

END

OPT

TUNER R1=50 Z2=5 -50 MS11
F=7.15MHZ MS11=-50

END

* Comments:

- * Set output load in Report Editor to 5 - j50 ohms
- * Set generator in Report Editor to 50 ohms
- * Plot MS11 and MS21

Fig 1—A is a circuit listing for an example two-port network for Smith Chart analysis. B is a schematic of the circuit.

used to find values of Z and Y at some location. Type "Y" or "Z" in the CCW, then Execute, place the cursor at a location and press the "M" key. A marker appears on the chart and the R and X, or G and B, values appear in the CCW. If a marker is not wanted, press the left mouse button instead. This operation suggests an easy way to transform a series R_S and X_S to a parallel R_P and X_P because $R_P = 1 / G$ and $X_P = -1 / B$ at any selected location: Working this backward, we can change parallel R_P to $G (= 1 / R_P)$ and X_P to $B (= -1 / X_P)$, then to R_S and X_S by doing the Y to Z change.

To place a marker at a specific value of $Z = R + jX$ (or $Y = G + jB$) do the following:

- Create the appropriate R (or G) circle and an X (or B) circle, as previously described.
- Place the cursor exactly at the intersection and remove your hand from the mouse.
- Delete the two circles ("DEL 2") if you do not want them to show.
- Press the "M" key. This places a marker at the Z (or Y) location.

Fig 2D shows arcs of constant Q values. Any values of R and +X that lie on the $Q = +2$ line correspond to $X / R = Q = 2$: for example, the intersection of the $R = 1.5$ circle and the $X = +3$ circle. For capacitive values of X, $-Q$ is plotted

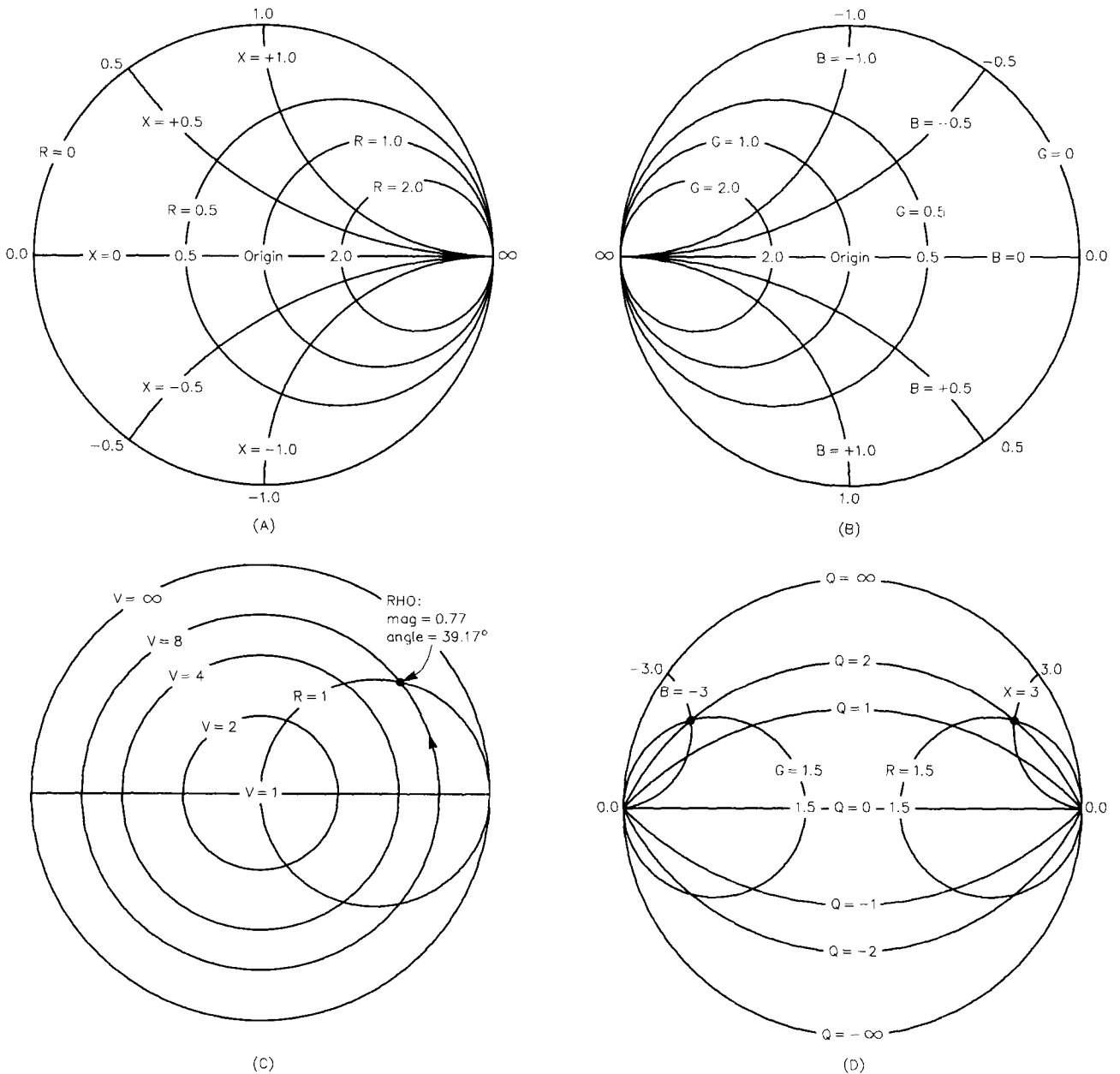


Fig 2—A shows Smith X Chart circles of constant resistance, R, and reactance, X. Positive X is above the horizontal axis. B shows Smith Y Chart circles of constant conductance, G, and susceptance, B. Positive B is below the axis. C shows Smith Chart circles of constant SWR (V) and an example of a reflection-coefficient, RHO, location. D shows Smith Chart arcs of constant Q. Positive values of Q apply to inductive reactance or susceptance. Negative values of Q apply to capacitive reactance or susceptance.

below the horizontal axis. The intersection of $B = -3$ and $G = 1.5$ is also at $Q = B / G = 2$. Q lines are useful in certain applications that are discussed in Part 2 of this article.

The CCW contents and the complete circle that we create can be saved to disk by typing the SPLT command in the CCW. A name for the file is requested. This same file can be recalled from disk by using the RPLT command. The name of the file is requested.

Navigating the Chart

An important topic in Circles operations concerns the ways that we modify the Z , Y , R , X , G and B quantities from one chart location to another. Fig 3A shows an initial value of Z at one location. We want to change Z to any of the values $Z1$ through $Z5$. The value of $Z = R + jX$ is at the junction of the $R = 0.18$ circle and the $+X = 0.26$ circle, where $+X$ is inductive. The following rules are observed in Fig 3A:

The impedance, Z , is at the junction of a constant- R circle and a constant- X circle. To increase X (make the inductive reactance, therefore the inductance, larger), move clockwise along the $R1$ circle to point $Z1$. The change in reactance is $0.91 - 0.26 = +0.65$. (Inductive reactance increases in the clockwise direction.)

The Circles Utility has another option, called DX, which works as follows:

- Enter a frequency in the CCW, for example $FREQ = 7.15E6$, then Execute.

- Type DX into the CCW, then Execute.

- Place the cursor *first* at Z and press the left button.

- Move the cursor to $Z1$ and press the left button again.

- The CCW displays the value of inductance, $L = DX / (2 \pi FREQ)$, that produces the change of reactance from Z to $Z1$ at the $FREQ$ that was entered.

Instead of moving to $Z1$, we can move from Z to $Z2$ along the $R1$ circle. This is a capacitive reactance of value -0.66 . (Capacitive reactance increases $-C$ decreases—in the counterclockwise direction.) The DX option now gives the needed value of capacitance, provided that we place the cursor first at Z , then at $Z2$. We can also move from $Z1$ to $Z2$ for a reactance change of -1.31 .

To increase the value of R , from locations Z , $Z1$ or $Z2$, move counterclockwise along a line of constant X , as shown, if X is positive (above the horizontal axis). If X is negative, the motion is clockwise. The proper directions to reduce R are obvious in Fig 3A.

Having arrived at $Z3$, $Z4$ or $Z5$, the preceding operations can be repeated, and in this manner we can travel around the chart.

Fig 3B shows the travels for the Y chart. The rules are nearly the same as for the Z chart, and the directions are as shown. The differences are:

- Inductive susceptance increases (inductance decreases) in the counterclockwise direction along a line of constant conductance.

- Capacitive susceptance increases (capacitance increases) in a clockwise direction along a line of constant conductance.

- Conductance (G) increases in a clockwise direction along a B line for B less than zero (above the horizontal axis) and counterclockwise along a B line for B greater than zero (below the horizontal axis).

The next task is to move back and forth between the Z chart and the Y chart, using these steps:

- Starting at some Z point, move Z to $Z1$ (Fig 3A). Then, using the CCW, find the value of $Y1$ at this point.

- Then move $Y1$ to $Y2$ (Fig 3B).

- Find the value of $Z2$ at $Y2$ and then move $Z2$ to $Z3$, and so forth until the target is reached.

Many impedance-matching problems start at a load impedance somewhat removed from the center of the chart and work toward the chart center, $R = 1$, $X = 0$ or $G = 1$, $B = 0$. (We assume that the chart center is the impedance that the generator wants to "see." This process models adjustment of an antenna tuner. The target impedance need not be at the chart center. For example, if $Z = 1.1 + j0.05$ or its complex conjugate, place a Z marker there and make that the target. It's equally possible to place the load at or near the chart center and the generator farther out. In that case, we start at the center and work out toward the generator. When we do this reversal of direction, a series inductor

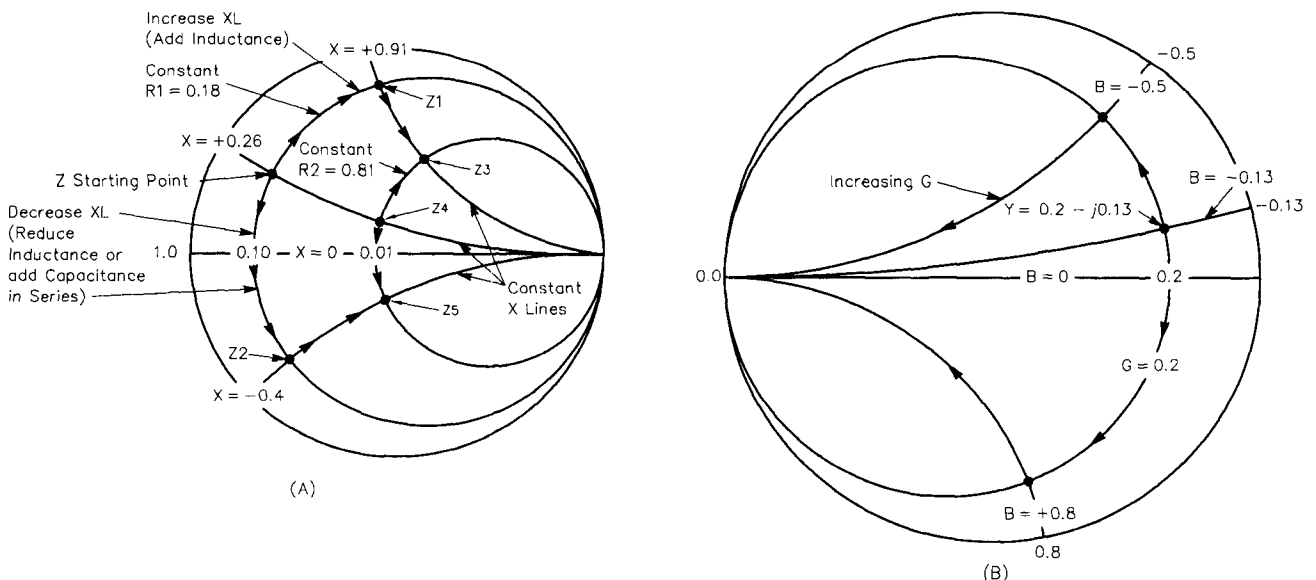


Fig 3—A shows directions of travel on a Z chart for X and R changes by adding or subtracting series XL , XC or R . B shows directions of travel on a Y chart for B changes by adding or subtracting shunt BL or BC .

becomes a series capacitor, and a shunt inductance becomes a shunt capacitance, and so forth.

For example, a 50 Ω load is to be transformed to some complex impedance that a transistor collector (the generator) wants to “see.” Similarly (a little more difficult to visualize but very important) a transistor *input* looks backward toward a transformed 50 Ω (the load that the transistor input sees, looking back). In order to avoid confusion and errors the rule is: Start at the load, wherever it is, and work toward the generator, wherever it is.

The changing of impedance using transmission lines and stubs is covered by three additional Circles functions as follows:

DT finds the electrical length (in degrees) and characteristic impedance [$Z_0(n)$ when normalized to 1.0, $Z_0(u)$ for a 50 Ω line] of a transmission

line that transforms impedance Z_1 to Z_2 . Z_1 and Z_2 can lie on the same V (SWR) circle as shown in Fig 4A, or they may be on different V circles. Use the following approach for the first option: on the same V circle:

- Draw the V circle
- Locate Z_1 and Z_2 on the V circle
- Type DT in the CCW, then Execute
- Place cursor at Z_1 and click left button, then place cursor at Z_2 and click left button again. The clockwise electrical angle is measured. Alternatively, do Z_2 first then Z_1 , in which case the angle is measured clockwise from Z_2 to Z_1 . The complete circle is 180° electrical length.

The information appears in the CCW text window. The physical length is:

$$\text{(meters)} = \frac{(\text{degrees}) \cdot (\text{velocity factor}) \cdot 0.833}{\text{FREQ (MHz)}} \quad (\text{Eq 5})$$

Note also that the two Z points need not be on the same V circle. If they are on two different V circles (but not $V = \infty$) the correct Z_0 of the line and its length (in degrees) will be calculated. Two lines may be required. This valuable feature is often used, especially in microstrip design.

Referring to Fig 2A, the difference between two points on a constant-resistance circle is a value of reactance. After we mark two reactance points on this circle (first the initial value, then the final value), the DXD operation allows us to get this change of reactance with a section of transmission line connected as a stub in series with the line, as shown in Fig 4B. Quite often two stubs—each having one half of the needed reactance—can be installed, one in each wire of a balanced transmission line as shown in Fig 4C. The stub(s) can be:

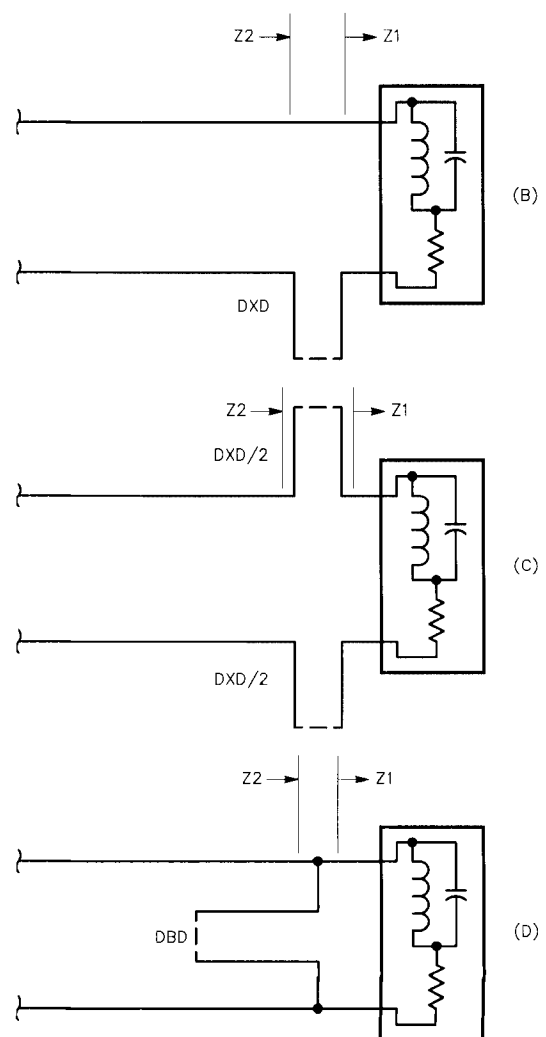
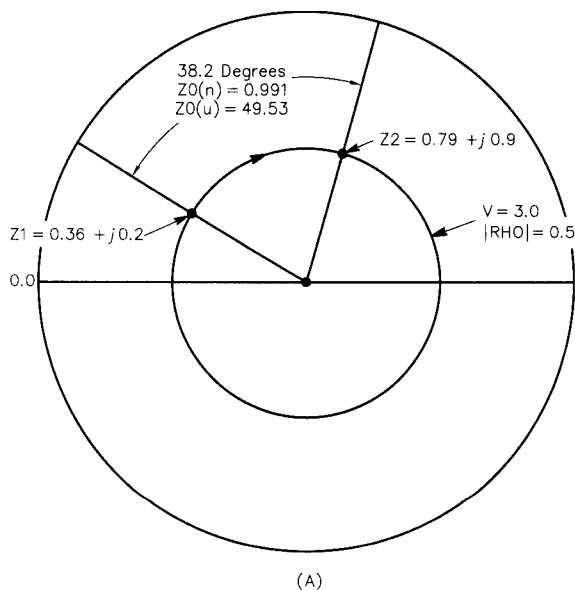


Fig 4—A shows the transmission line required to transform Z_1 to Z_2 along a line of constant SWR, where $V = 3.0:1$ ($RHO = 0.5$). Z_0 (unnormalized) = 49.53 Ω, Z_0 (normalized) = 0.99. B (unbalanced) and C (balanced) show the DXD function; D shows the DBD function.

- A shorted stub (SS) less than $\lambda/4$ is an inductive reactance.

- An open stub (OS) less than $\lambda/4$ is a capacitive reactance.

The CCW asks for one of the following: I ($= Z_0$, impedance of the transmission line), D ($=$ degrees of electrical length) or W ($=$ wavelength). The CCW then tells which stub to use (OS or SS), its reactance and other parameters.

The DBD operation is just like DXD, except that we put two susceptance markers on a constant-conductance circle as in Fig 2B. We then get a parallel stub (OS or SS) as shown in Fig 4D. The reactance of the stub and other parameters are displayed. This kind of stub is widely used.

The combined usage of DT, DXD and DBD in the Circles Utility is a very powerful way to match impedances using transmission lines. By switching from one to another (and between Z and Y) we can travel the chart in transmission-line segments and stubs in a very elegant way. It is worthwhile to keep in mind that the reactances of transmission-line segments vary over frequency in somewhat different ways than ordinary lumped LC components. This can be a factor in designing a network.

Problem Solving

The art and gamesmanship of these matching exercises are to find the minimum number of components, especially lossy inductors. Always keep the possibility of using transmission-line segments in mind because of their high Q (low loss) values. Sometimes a greater frequency-response bandwidth is achieved by using transmission lines than lumped L and C . We also want values of L , C and lines that are realistic, efficient and economical.

Fig 5 (drawn with fine lines to improve accuracy) illustrates the many different possibilities for converting a load impedance Z_{load} to $R = 1, X = 0$. We will use, just as one example, the circuit shown in Fig 1B. Z_{load} is at point A, $0.10 - j1.0$. The first component is a series inductor along the $R = 0.10$ line from A to C. A shunt capacitor moves the impedance along the $G = 0.5$ line from C to I, and a series inductor moves it along the $R = 1.0$ line from I to O (the origin). Fig 1B shows the values calculated in this manner. This circuit would have a very good low-pass filtering property, but requires three components, and at least two of them must be tunable. These values are placed in the circuit listing in Fig 1A and then optimized for best MS11 at 7.15 MHz, using realistic Q values

for the components. MS21 tells the circuit loss in decibels, about 0.35 dB (when MS11 dB is very large). The optimized L and C values are shown. The last inductor "IND 2 3" could have a constant value (remove the question marks from the Netlist), and the other L and C are then optimized.

The first coil from point A could be a fixed value if it gets us beyond point B. This inductance could possibly be built right into the load device (antenna or whatever). A length of transmission line ($Z_0 = 1.0$) could get us from, say point C, along a constant V circle, over to the $R = 1$ circle. A simpler approach could use series inductance up to point B and shunt capacitance from B to O. Better yet, a series coil from A to C and two low-loss capacitors, one in shunt from C to F and one in series from F to O. If the series inductive reactance doesn't go beyond point B at the lowest frequency of interest, however, these schemes won't work. Another interesting idea would be a shunt coil from A to K and a series coil from K to O.

Consider also an inductance from A up to the horizontal axis (the 0.1 mark) and a 9:1 (impedance ratio) ferrite-core transmission-line transformer

from 0.1Ω to 0.9Ω , where a V circle has the low value 1.11. This transmission line should ideally have a Z_0 of 0.3Ω . For a $50\text{-}\Omega$ system, this would correspond to 15Ω . Three small, parallel-connected segments of 50Ω coax would be okay. We can do some fine-tuning with this method. The resistance added by the inductor can be considered for a more-accurate graphical answer. Use the following approach:

- Get a first estimate of the normalized inductive reactance ($= 1.0$) as described above.

- Assume a value of Q_L for the inductor. The R_L of the coil is then $R_L = X_L / Q_L$.

- Add R_L to the resistance $R (= 0.1)$ of the load and relocate point A on the Smith Chart accordingly.

- On the chart, find a better value of the inductor needed to reach the horizontal axis.

- Further repetitions of this procedure are not necessary.

- The 1:9 transformer (assume it to be loss-less) now takes us to a new value, which will still be close to the origin if Q_L is large.

In this example a coil Q_L of 250 would mean a correction of $1.0 / 250 = 0.004 \Omega$,

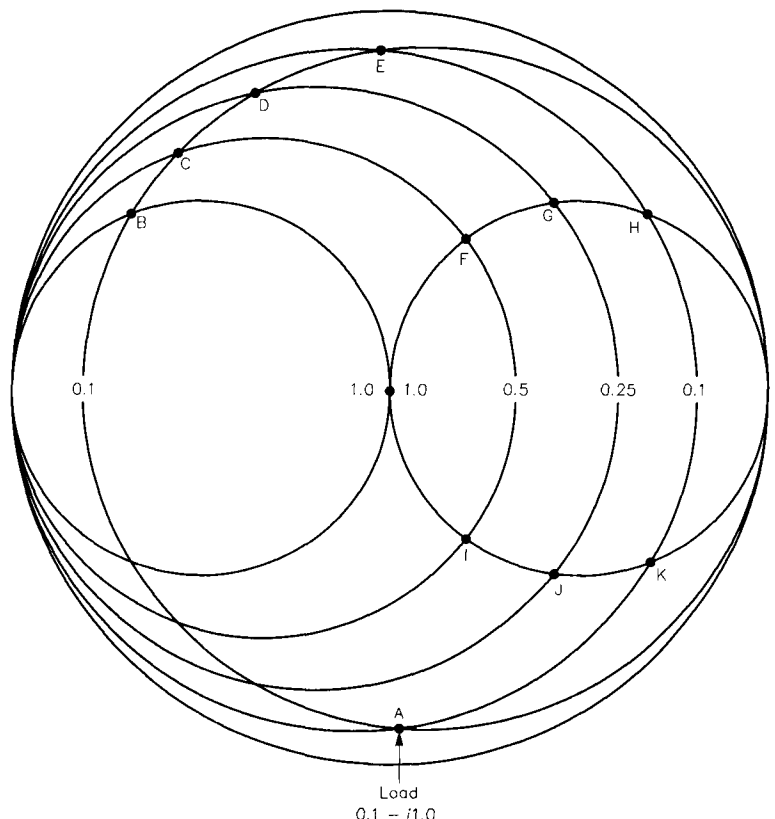


Fig 5—Solution paths for the design example.

which is negligible. In more extreme situations it may be important.

Keep in mind also the discussion regarding the reversal of direction: for example, starting at the origin (the load) and working outward to the generator impedance or possibly its complex conjugate.

The main idea here is to illustrate the power of the Smith Chart in visualizing the myriad possible solutions, each of which has possible merits and possible problems. With such a "shopping list" the designer can make the best decisions. The Circles Utility can then quickly and easily get values for the various components.

Also, a candidate circuit of lines/stubs and adjustable L and C should be tested over a frequency band for "tuning range" of the components. A new Designer file is created as shown in Fig 6 for this purpose. At any arbitrary frequency that is entered into the OPT block, the circuit values are optimized for maximum MS11. The load impedance data is in the DATA block. This data is linked to the ONE circuit element that has been placed in the main circuit block. We can now see what range of L and C values are needed to tune the desired frequency range.

In the example of Fig 6, "IND 2 3" is a fixed value (by assumption, it can't be tuned) and it was necessary to increase its fixed value (see Fig 1A) so that we could tune to the low end of the 7.0 to 7.3 MHz band with reasonable values of the other components. This is typical of problems that we might encounter.

Another interesting exercise is to design a network that has a certain V (SWR) over a certain frequency band (without retuning). Using Eq 3, a V = 2 value corresponds to an MS11 (dB) of -9.5. A V = 1.5 value corresponds to an MS11 (dB) of -14. By observing the plots of MS11 (dB) versus frequency generated by Designer, the -9.5 dB and -14 dB frequency ranges can be easily observed. It is usually necessary to "Rescale" the graph, to see these levels more easily. For further information on the art and witchcraft of broadband impedance matching, see References 2 and 3.

A Minor Bug

The Circles Utility has a problem when performing the DT (transmission line) operation over a small region of a V (SWR) circle close to the horizontal (X = 0) axis (see Fig 4A). Incorrect results may appear, due to a minor glitch in the software. The correct pro-

* Band tuning example

BLK

```
IND 1 2 L=33.92257UH? Q=250 F=7.15MHZ
CAP 2 0 C=2414.698PF? Q=1000 F=7.15MHZ
IND 2 3 L=2.3UH Q=250 F=7.15MHZ
```

* Note that this L is held constant
ONE 3 0 ZDAT

TUNER:1POR 1 0

END

FREQ

```
STEP 6.9MHZ 7.4MHZ 10KHZ
```

END

OPT

```
TUNER R1=50 MS11
F=7.25MHZ MS11= -50
```

END

DATA

```
ZDAT: Z RI
```

* Freq	Real	Imag
7.00MHZ	3	-70
7.10MHZ	4	-60
7.20MHZ	6	-40
7.30MHZ	8	-30

END

* Comments:

- * Put the ONE element in the circuit block.
- * Change TUNER to a 1POR 1 0 (one port) as shown.
- * Set Report Editor to MS11 with TERM=50+j0
- * Put load impedance data in the DATA block, real then imaginary.
- * DATA is interpolated between freq entries.
- * In the OPT block, insert any freq value in the range, one at a time.
- * Analyze, then Optimize at the freq that is in the OPT block.
- * Check to see the min and max values of tuning Ls and Cs that are needed.
- * Check to see that MS11 reaches a very large value.

Fig 6—Net list for band tuning example.

cedure in this situation is to perform DT in two segments. The first segment begins "away from" the horizontal axis and terminates "at" the horizontal axis. The second segment begins "at" the horizontal axis and proceeds to the desired finish point. The total electrical angle of the transmission line is then the sum of the lengths of the two segments. Some practice will make this a simple operation. Two RHO operations on a V circle also provide the DT electrical angle with no error. This problem does not occur often, but you should be aware of it.

Additional Reading

R. Dean Straw, Editor, *The ARRL Antenna Book*, 18th edition, Chapter 28, has an excellent general discussion of the Smith Chart. ARRL Order No. 6133. ARRL publi-

cations are available from your local ARRL dealer or directly from the ARRL. Mail orders to Pub Sales Dept, ARRL, 225 Main St, Newington, CT 06111-1494. You can call us toll-free at tel 888-277-5289; fax your order to 860-594-0303; or send e-mail to pubsales@arrl.org. Check out the full ARRL publications line on the World Wide Web at <http://www.arrl.org/catalog>.

Wilfred Caron, *Antenna Impedance Matching* (Newington: 1989, ARRL), Order No. 2200. This book has very thorough coverage of matching methods using transmission lines and LC components.

W. E. Sabin, W0IYH, "Broadband HF Antenna Matching With ARRL Radio Designer," *QST*, August 1995, p 33.

W. E. Sabin, W0IYH, "Computer Modeling of Coax Cable Circuits," *QEX*, August 1996, pp 3.

W. E. Sabin, W0IYH, "Understanding the T-tuner (C-L-C) Transmatch," *QEX*, December 1997, pp 13.

□□

Quick, Easy Network Analysis on a PC Using Mathcad

*Come see two examples of nodal circuit analysis
made easy by Mathcad's matrix manipulation tools.*

By Ralph Vacca, W1KF

If you dabble in network analysis on your PC, perhaps adding a few more items to your repertoire of methods could get results with minimum time and effort. One of these simplifies the introduction of network information to the PC and produces faster execution times. Next, the advantages of impedance leveling in the design process is introduced and demonstrated with an example for those who may not be familiar with this technique. The last example will demonstrate how the effects of internal voltage-dependent current generators can be easily included by adding the appropriate conductance ma-

trix. However, without the benefit of an example, it is important to add that the matrix method of solution easily allows the application of a current source at one or several nodes and simultaneously determines the voltage at one or more other nodes.

The first method described should reduce the chances of making algebraic errors and produce faster execution times for the frequency response of passive networks. This is accomplished by producing a network matrix $Y(f)$ only by inspection of the network diagram and not by writing KCL equations. There are three main steps in the process that are emphasized in the application of this method. (See Reference 1.)

Before these steps are enumerated, the network matrix $Y(f)$ and its inverse are defined by the following

matrix relations. Where I is the current-source vector and $V(f)$ is the nodal voltage vector:

$$I := Y(f) \cdot V(f) \text{ and } V(f) := Y(f)^{-1} \cdot I$$

Rows and columns of $Y(f)$ are numbered, where n equals the number of nodes, exclusive of the reference node. The row (i) and column (j) indices are: $i := 1 \dots n$ and $j := 1 \dots n$

Three steps are required to perform the "inspection method" for passive¹ networks:

1. Elements along the principal diagonal ($i = j$) of $Y(f)$ are obtained by adding all admittances that are incident at each selected node.

2. Elements above the principal diagonal ($i < j$) of $Y(f)$ are equal to the

¹Notes appear on page 18.

negative of the sum of the admittances that directly connect the selected (i, j) node pair.

3. Elements below the principal diagonal (i > j) of Y(f) are the *mirror image* of those that appear above this diagonal.

You can convince yourself that the network-inspection procedure given in the three steps is valid by writing the KCL equations for a general, n-node network. When doing so, you must use the conventions that currents leaving a node are positive and all nodal voltages are positive with respect to the reference node. Then, by collecting terms that have the same nodal voltage in each of the (n) equations and

forming the Y(f) matrix, you will see that the three steps given in the inspection method yield correct results.

An example will now be given (see Fig 1) to illustrate the "inspection method" as well as "impedance leveling." This filter has provision for unequal input and output terminations. It could be built with two RF transformers having the appropriate coefficient of coupling or as separate inductors with no inductive coupling, as shown in the network diagram given in the example. Three values were selected for the coefficient of coupling to show the effects of over, optimum and under coupling. The example also includes several notes to elaborate

some specific points. In particular, the note concerning multiple sources and nodal outputs is shown at an appropriate place in the example.

The execution time for this example was six seconds,² but it was two seconds for one instead of three values of inductive coupling (k) for the example given here. Another method of analysis that was performed required 150 seconds for the one-coefficient-of-coupling case. This method also used inspection of the network, but did not require that the (i = j) and (i > j) elements be directly given. Elements for the latter case were generated by the program, but with an execution time increase of much more than an order of magnitude!

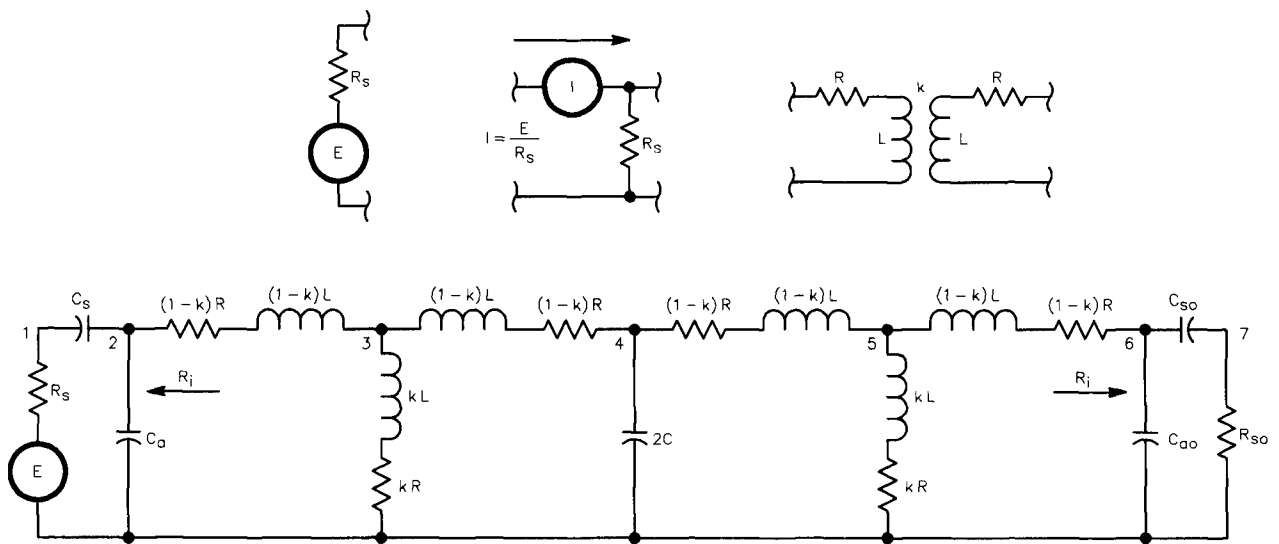


Fig 1—Schematic of example filter.

INPUT DATA $R_s = 50$; $R_i = 2000$; $R_{so} = 200$; $E = 1$; $Q_c = 150$; $\delta = 0.05$; $f_c = 7 \times 10^6$ Hz

R_i = Matched input and output termination of the internal network,

δ = Fractional bandwidth

Note: Select R_i to get more suitable values of L and C. Changing the impedance level of some parts of a network does not alter the frequency response of the network. (See Reference 2.)

$$\omega_c = 2 \cdot \pi \cdot f_c$$

$$C := \frac{1}{\delta \cdot R_i \cdot \omega_c} \quad L := \frac{R_i \cdot \delta}{\omega_c} \quad (\text{see Reference 3}) \quad R := \frac{\omega_c \cdot L}{Q_c} \quad I := \frac{E}{R_s}$$

$$C_s := \frac{1}{\omega_c \cdot \sqrt{R_s \cdot (R_i - R_s)}}$$

$$C_{s0} := \frac{1}{\omega_c \cdot \sqrt{R_{s0} \cdot (R_i - R_{s0})}}$$

$$IL := -20 \cdot \log \left[\frac{\delta \cdot Q_c}{1 + \frac{\delta}{2} \cdot Q_c} \right]$$

approx. IL

$$C_a := C - \frac{1}{\omega_c^2 \cdot C_s \cdot R_s \cdot R_i}$$

$$C_{a0} := C - \frac{1}{\omega_c^2 \cdot C_{s0} \cdot R_{s0} \cdot R_i}$$

$$IL = 2.1 \text{ dB}$$

Impedance level changes at the input and output are discussed in Reference 4.

$$g_s := \frac{1}{R_s} \quad g_{s0} := \frac{1}{R_{s0}}$$

$$\frac{C_s}{10^{-12}} = 72.8 \text{ pF} \quad \frac{C_{s0}}{10^{-12}} = 37.9 \text{ pF} \quad 2 \cdot \frac{C}{10^{-12}} = 455 \text{ pF}$$

$$\frac{C_a}{10^{-12}} = 156 \text{ pF} \quad \frac{C_{a0}}{10^{-12}} = 193 \text{ pF} \quad \frac{L}{10^{-6}} = 2.3 \text{ } \mu\text{H}$$

Minimum frequency: $f_{\min} := 6 \times 10^6 \text{ Hz}$

Maximum frequency: $f_{\max} := 8 \times 10^6 \text{ Hz}$ $n_{\max} := 200$

$$n := 1 \dots n_{\max} \quad r := \log(f_{\max}) - \log(f_{\min}) \quad f_n := f_{\min} \cdot 10^{\frac{r \cdot n}{n_{\max}}}$$

$m := 1 \dots 3$ $k_m := 0.707 \cdot \delta \cdot m$

$k_{\text{opt}} := \sqrt{2} \cdot \delta$	k_m	$L \cdot (1 - k_m) \cdot 10^6 \text{ } \mu\text{H}$	$k_m \cdot L \cdot 10^6 \text{ } \mu\text{H}$
	0.035	2.193	0.08
$k_{\text{opt}} := 0.071$	0.071	2.113	0.161
	0.106	2.033	0.241

The admittance between nodes is now obtained by inspection of the network diagram.

These are shown below with the subscripts that identify them with the node pair.

$$y_{02}(f) := j \cdot 2 \cdot \pi \cdot f \cdot C_a \quad y_{03}(k, f) := \frac{1}{(R + j \cdot 2 \cdot \pi \cdot f \cdot L) \cdot k} \quad y_{04}(f) := j \cdot 2 \cdot \pi \cdot f \cdot 2 \cdot C \quad y_{06}(f) := j \cdot 2 \cdot \pi \cdot f \cdot C_{a0}$$

$$y_{12}(f) := j \cdot 2 \cdot \pi \cdot f \cdot C_s \quad y_{23}(k, f) := \frac{1}{(R + j \cdot 2 \cdot \pi \cdot f \cdot L) \cdot (1 - k)} \quad y_{67}(f) := j \cdot 2 \cdot \pi \cdot f \cdot C_{s0}$$

$$y_{11}(f) := g_s + y_{12}(f) \quad y_{22}(k, f) := y_{02}(f) + y_{12}(f) + y_{23}(k, f) \quad y_{33}(k, f) := y_{03}(k, f) + 2 \cdot y_{23}(k, f)$$

$$y_{44}(k, f) := y_{04}(f) + 2 \cdot y_{23}(k, f) \quad y_{55}(k, f) := y_{33}(k, f) \quad y_{66}(k, f) := y_{06}(f) + y_{67}(f) + y_{23}(k, f)$$

$$y_{77}(f) := g_{s0} + y_{67}(f)$$

Note: When some of the elements of the $Y(k,f)$ Matrix are repeated, the indices of the initial one may be retained when it is more convenient.

ORIGIN =1

$$Y(k, f) := \begin{bmatrix} y_{11}(f) & -y_{12}(f) & 0 & 0 & 0 & 0 & 0 \\ -y_{12}(f) & y_{22}(k,f) & -y_{23}(k,f) & 0 & 0 & 0 & 0 \\ 0 & -y_{23}(k,f) & y_{33}(k,f) & -y_{23}(k,f) & 0 & 0 & 0 \\ 0 & 0 & -y_{23}(k,f) & y_{44}(k,f) & -y_{23}(k,f) & 0 & 0 \\ 0 & 0 & 0 & -y_{23}(k,f) & y_{55}(k,f) & -y_{23}(k,f) & 0 \\ 0 & 0 & 0 & 0 & -y_{23}(k,f) & y_{66}(k,f) & -y_{67}(f) \\ 0 & 0 & 0 & 0 & 0 & -y_{67}(f) & y_{77}(f) \end{bmatrix} \begin{matrix} 1 \\ 2 \\ 3 \\ 4 \\ 5 \\ 6 \\ 7 \end{matrix}$$

$$V(k, f) := Y(k, f)^{-1} \cdot \begin{bmatrix} I \\ 0 \\ 0 \\ 0 \\ 0 \\ 0 \\ 0 \end{bmatrix}$$

Note: More than one current source can be supplied to the network, if that is required, by altering the current-source vector. Also, the voltage at all other nodes can be found by simply changing the subscript on $V(k,f)$ to correspond with the node or nodes selected for examination.

$$dB_{m,n} := 20 \cdot \log(|V(k_m, f_n)_7|)$$

The filter frequency response for different coupling factors is shown in Figs 2 and 3.

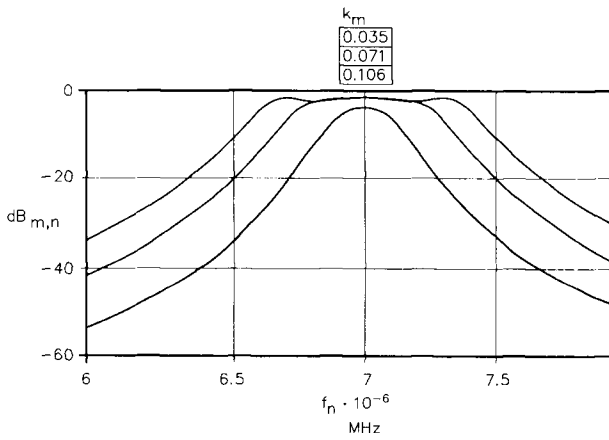


Fig 2—Filter frequency response.

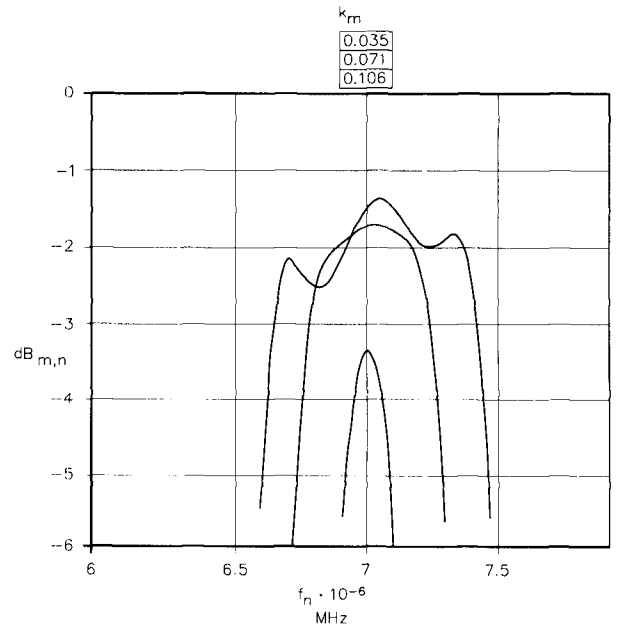


Fig 3—Expanded-scale frequency response.

Table 1
A Demonstration of "Impedance Leveling"

$R_1 \rightarrow$	250	2000	20000	ohms
$C_s \rightarrow$	227	72.8	22.8	pF
$C_a \rightarrow$	1640	156	0.03	pF
$C_{so} \rightarrow$	227	37.9	11.4	pF
$C_{a0} \rightarrow$	1770	193	11.4	pF
$2C \rightarrow$	3640	455	45.5	pF
$L \rightarrow$	0.28	2.27	22.7	μ H

Table 1 gives the values of the network components as R_i changes. Examples of difficult components may be 0.03 pF, 22.7 μ H or 0.28 μ H. Whether they are or are not easy to obtain is in the hands of the designer. It's more important that there is flexibility in getting component values that are more suitable and still maintain the same frequency response with no changes in R_s and R_{so} for all values of R_i that produce positive and real values for the network components. One restriction on R_i appears to be that $R_i > R_s$ and $R_i > R_{so}$. In any case,

negative or complex values for any of the components listed in the table indicate that the value of R_i that produced those results is not permitted.

This last example (see Fig 4) will show how the effects of internal voltage-dependent current generators can also be easily included by inspection. In addition, this example will demonstrate the application of the "alignability" criteria (see Reference 5) in the design of a tuned emitter-coupled amplifier. Analysis of the network begins by first ignoring the internal

current sources (treat them as open circuits—*Ed.*) and following the same three steps as given above for the passive-network case. Then by further inspection of the diagram and arrow directions of each current source, the appropriate sign can be assigned to the relation between the source current and its controlling voltages. At this point, it is now possible to add the effects of the internal current sources by including their transconductance in the $Y(\omega)$ passive matrix. How this is done, will become clear as the example is developed.

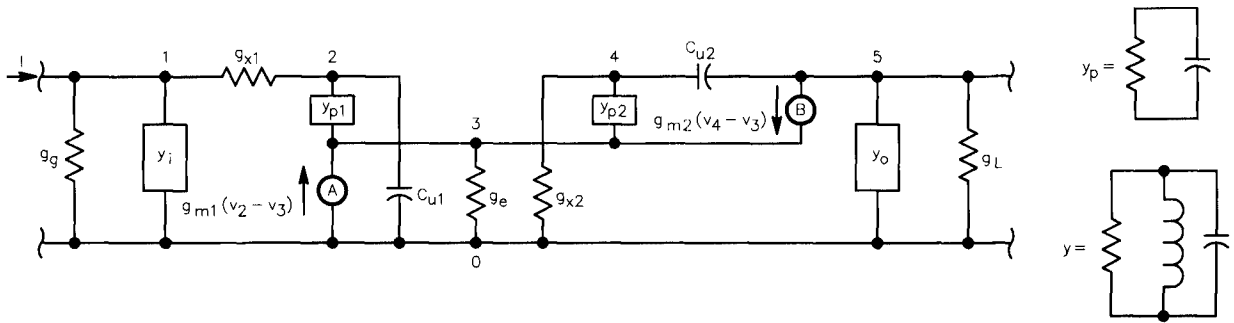


Fig 4—Schematic of network example with voltage dependent current sources.

Minimum frequency: $f_{\min} := 6 \times 10^6$ Hz $n_{\max} := 200$
 Maximum frequency: $f_{\max} := 14 \times 10^6$ Hz

$n := 1 \dots n_{\max}$ $r := \log(f_{\max}) - \log(f_{\min})$ $f_n := f_{\min} \cdot 10^{\frac{r \cdot n}{n_{\max}}}$

INPUT DATA:

$g_{m1} := 0.08$ $g_{m2} := 0.08$ $R_g := 1000$ $L_o := 1 \cdot 10^{-6}$ $f_o := 10^7$ $\omega_o := 2 \cdot \pi \cdot f_o$ $I := 0.0001$

$g_{x1} := 0.00666$ $g_{x2} := 0.00666$ $Q_i := 200$ $L_i := L_o$ $C_o := \frac{1}{\omega_o^2 \cdot L_o}$ $C_i := C_o$

$g_{p1} := 0.0008$ $g_{p2} := 0.0008$ $Q_o := 200$

$C_{p1} := 30 \cdot 10^{-12}$ $C_{p2} := 30 \cdot 10^{-12}$ $R_L := 1000$

$C_{u1} := 3 \cdot 10^{-12}$ $C_{u2} := 3 \cdot 10^{-12}$ $R_o := 2000$

$g_g := \frac{1}{R_g}$ $g_L := \frac{1}{R_L}$ $g_e := \frac{1}{R_e}$ $g_i := \frac{1}{Q_i} \sqrt{\frac{C_i}{L_i}}$ $R_i := \frac{1}{g_i}$ $g_o := \frac{1}{Q_o} \sqrt{\frac{C_o}{L_o}}$ $R_o := \frac{1}{g_o}$

$R_i = 1.257 \cdot 10^4$ $R_o = 1.257 \cdot 10^4$ $C_o = 2.533 \cdot 10^{-10}$

$$\delta_{\max} := \frac{\Delta C_{\max}}{C}$$

$$k_{\max} := 2 \cdot \delta_{\max} \approx 0.1$$

$$k := 0 \dots k_{\max}$$

$$\rho(k) := \left[1 - \delta_{\max} \cdot \left(1 - 2 \cdot \frac{k}{k_{\max}} \right) \right]$$

Enabled =====>
Disabled =====>

Tuning

$$C_o(k) := C_o \cdot \rho(k)$$

$$C_i(k) := C_i \cdot \rho(k)$$

No Tuning

$$C_i(k) := C_i$$

$$C_o(k) := C_o$$

Inspection of Network to Create the Passive Matrix Y(k, ω)

$$y_{u1}(\omega) := j \cdot \omega \cdot C_{u1}$$

$$y_i(k, \omega) := g_i + j \cdot \omega \cdot C_i(k) + \frac{1}{j \cdot \omega \cdot L_i}$$

$$y_{u2}(\omega) := j \cdot \omega \cdot C_{u2}$$

$$y_{p1}(\omega) := g_{p1} + j \cdot \omega \cdot C_{p1}$$

$$y_o(k, \omega) := g_o + j \cdot \omega \cdot C_o(k) + \frac{1}{j \cdot \omega \cdot L_o}$$

$$y_{p2}(\omega) := g_{p2} + j \cdot \omega \cdot C_{p2}$$

$$y_{11}(k, \omega) := y_i(k, \omega) + g_{x1} + g_g$$

$$y_{12}(\omega) := g_{x1}$$

$$y_{22}(\omega) := g_{x1} + y_{u1}(\omega) + y_{p1}(\omega)$$

$$y_{23}(\omega) := y_{p1}(\omega)$$

$$y_{33}(\omega) := g_e + y_{p1}(\omega) + y_{p2}(\omega)$$

$$y_{34}(\omega) := y_{p2}(\omega)$$

$$y_{44}(\omega) := g_{x2} + y_{u2}(\omega) + y_{p2}(\omega)$$

$$y_{45}(\omega) := y_{u2}(\omega)$$

$$y_{55}(k, \omega) := g_L + y_{u2}(\omega) + y_o(k, \omega)$$

ORIGIN = 1

$$Y(k, \omega) := \begin{bmatrix} y_{11}(k, \omega) & -g_{x1} & 0 & 0 & 0 \\ -g_{x1} & y_{22}(\omega) & -y_{23}(\omega) & 0 & 0 \\ 0 & -y_{23}(\omega) & y_{33}(\omega) & -y_{34}(\omega) & 0 \\ 0 & 0 & -y_{34}(\omega) & y_{44}(\omega) & -y_{45}(\omega) \\ 0 & 0 & 0 & -y_{45}(\omega) & y_{55}(k, \omega) \end{bmatrix}$$

Y(k, ω) was constructed by following the three steps for the passive network case. Now, we will show how the effects of the internal current sources are included. These matrices will then include those currents leaving nodes 3 and 5 due to the internal current sources that were initially ignored. Fig 5 is a graph of the voltages at nodes 1 and 5.

Current leaving node 3
from internal source "A"

$$I_{s1} := -g_{m1} \cdot (v_2 - v_3) \square$$

$$I_{s1} := \begin{bmatrix} 0 & 0 & 0 & 0 & 0 \\ 0 & 0 & 0 & 0 & 0 \\ 0 & -g_{m1} & g_{m1} & 0 & 0 \\ 0 & 0 & 0 & 0 & 0 \\ 0 & 0 & 0 & 0 & 0 \end{bmatrix} \cdot \begin{bmatrix} v^1 \\ v^2 \\ v^3 \\ v^4 \\ v^5 \end{bmatrix} \square$$

Current leaving node 3
from internal source "B"

$$I_{s2} := -g_{m2} \cdot (v_4 - v_3) \square$$

$$I_{s2} := \begin{bmatrix} 0 & 0 & 0 & 0 & 0 \\ 0 & 0 & 0 & 0 & 0 \\ 0 & 0 & g_{m2} & -g_{m2} & 0 \\ 0 & 0 & 0 & 0 & 0 \\ 0 & 0 & 0 & 0 & 0 \end{bmatrix} \cdot \begin{bmatrix} v^1 \\ v^2 \\ v^3 \\ v^4 \\ v^5 \end{bmatrix} \square$$

Current leaving node 5
from internal source "B"

$$I_{s3} := g_{m2} \cdot (v_4 - v_3) \square$$

$$I_{s3} := \begin{bmatrix} 0 & 0 & 0 & 0 & 0 \\ 0 & 0 & 0 & 0 & 0 \\ 0 & 0 & 0 & 0 & 0 \\ 0 & 0 & 0 & 0 & 0 \\ 0 & 0 & -g_{m2} & g_{m2} & 0 \end{bmatrix} \cdot \begin{bmatrix} v^1 \\ v^2 \\ v^3 \\ v^4 \\ v^5 \end{bmatrix} \square$$

$$I_s := I_{s1} + I_{s2} + I_{s3} \square \quad I_s := \begin{bmatrix} 0 & 0 & 0 & 0 & 0 \\ 0 & 0 & 0 & 0 & 0 \\ 0 & -g_{m1} & g_{m1} + g_{m2} & -g_{m2} & 0 \\ 0 & 0 & 0 & 0 & 0 \\ 0 & 0 & -g_{m2} & g_{m2} & 0 \end{bmatrix} \cdot \begin{bmatrix} v^1 \\ v^2 \\ v^3 \\ v^4 \\ v^5 \end{bmatrix} \square \quad I_s := G \cdot \begin{bmatrix} v^1 \\ v^2 \\ v^3 \\ v^4 \\ v^5 \end{bmatrix} \square \quad V(f) := \begin{bmatrix} v^1 \\ v^2 \\ v^3 \\ v^4 \\ v^5 \end{bmatrix} \square$$

$$I := Y(k, \omega) \cdot V(f) + G \cdot V(f) \square$$

$$I := (Y(k, \omega) + G) \cdot V(f) \square$$

$$I := Y_s(k, \omega) \cdot V(f) \square$$

$$Y_s(k, \omega) := \begin{bmatrix} y_{11}(k, \omega) & -g_{x1} & 0 & 0 & 0 \\ -g_{x1} & y_{22}(\omega) & -y_{23}(\omega) & 0 & 0 \\ 0 & -y_{23}(\omega) & y_{33}(\omega) & -y_{34}(\omega) & 0 \\ 0 & 0 & -y_{34}(\omega) & y_{44}(\omega) & -y_{45}(\omega) \\ 0 & 0 & 0 & -y_{45}(\omega) & y_{55}(\omega) \end{bmatrix} + \begin{bmatrix} 0 & 0 & 0 & 0 & 0 \\ 0 & 0 & 0 & 0 & 0 \\ 0 & -g_{m1} & g_{m1} + g_{m2} & -g_{m2} & 0 \\ 0 & 0 & 0 & 0 & 0 \\ 0 & 0 & -g_{m2} & g_{m2} & 0 \end{bmatrix} \square$$

$$Y_s(k, \omega) := \begin{bmatrix} y_{11}(k, \omega) & -g_{x1} & 0 & 0 & 0 \\ -g_{x1} & y_{22}(\omega) & -y_{23}(\omega) & 0 & 0 \\ 0 & -y_{23}(\omega) - g_{m1} & y_{33}(\omega) + g_{m1} + g_{m2} & -y_{34}(\omega) - g_{m2} & 0 \\ 0 & 0 & -y_{34}(\omega) & y_{44}(\omega) & -y_{45}(\omega) \\ 0 & 0 & -g_{m2} & -y_{45}(\omega) + g_{m2} & y_{55}(\omega) \end{bmatrix}$$

This detailed development just given for the $Y_s(k, \omega)$ matrix shows how the passive and symmetrical $Y(k, \omega)$ matrix is altered by the internal voltage controlled current source matrices. This much detail is not required in practice, since the effect of

these current sources on the $Y_s(k, \omega)$ matrix can be directly obtained by inspection of the network. In particular, the observation of the arrow direction, terminating nodes (excluding the reference node) and equations for the internal current sources yield all the

information needed to directly modify the $Y(k, \omega)$ matrix. In this example, source currents leaving node 3 modify the passive $Y(k, \omega)$ matrix on row 3, and the source current leaving node 5 modifies the passive $Y(k, \omega)$ matrix on row 5.

$$V(k, \omega) := Y_s(k, \omega)^{-1} \cdot \begin{bmatrix} I \\ 0 \\ 0 \\ 0 \\ 0 \end{bmatrix} \quad \text{Gain}_{dB}(k, n) := 20 \cdot \log \left(\frac{|V(k, 2 \cdot \pi \cdot f_n)_5|}{|V(k, 2 \cdot \pi \cdot f_n)_1|} \right)$$

$$y_{inT}(k, \omega) := \frac{I}{V(k, \omega)_1}$$

$$g_{inT}(k, \omega) := \text{Re}(y_{inT}(k, \omega))$$

$$S_{inT}(k, \omega) := \text{Im}(y_{inT}(k, \omega))$$

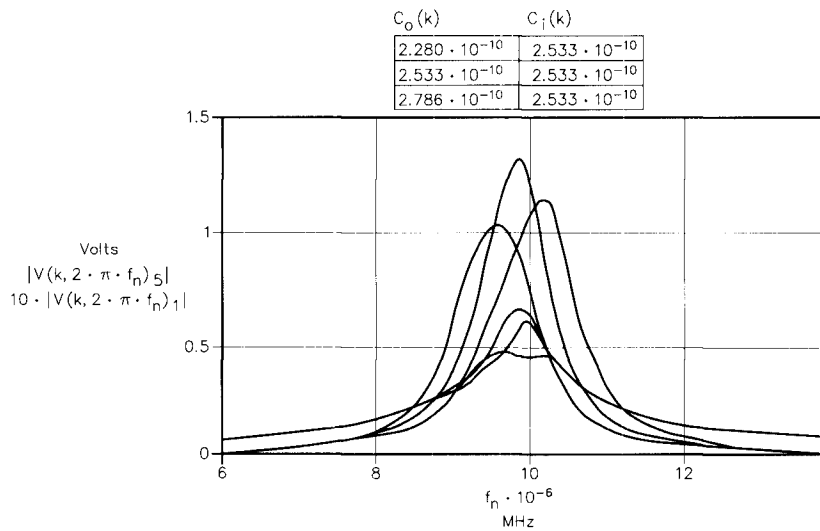


Fig 5—Voltages at nodes 1 and 5.

Fig 5 illustrates the degree to which regenerative action effects the input tuning when only the output is being tuned. In order to more easily discern this phenomena, the input signal scale

has been increased by a factor of 10. This regenerative action is also observed in Fig 6, in the reduction of the input shunt resistance. Indeed, if the gain is increased too much, the resis-

tance is reduced to negative values, producing self-oscillation. Less reaction can be achieved by reducing the gain. The effect of varying C_o and C_i is shown in Fig 7.

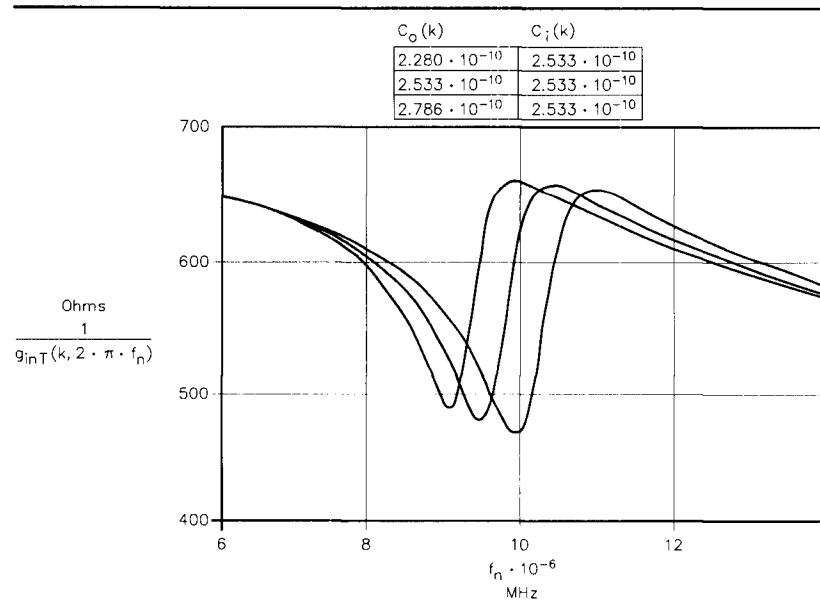


Fig 6—Input shunt resistance.

In the above examples, we have shown how the $Y(\omega)$ and $Y_g(\omega)$ matrices for passive and active networks, respectively, can be constructed by inspection (only) of the network diagrams. It was possible to take full advantage of the passive network case's symmetry and to fully utilize this property for networks using internal voltage control sources as well. The examples also demonstrated the concepts of "impedance leveling" and "alignability," which are useful in the design process.

Matrix inversion is required in the methods of analysis discussed here, but this does not appear to be a disadvantage for many networks, because the matrices are usually very sparse. The maximum order of matrix that can be inverted with the software presently being used (*Mathcad*) is 10. This can handle a 10-node network, not including the reference node. Perhaps, a network with more than 10 nodes can be analyzed by cascading or other means and it may be fruitful to explore them later.

References:

1. E. A. Guillemin, *Introductory Circuit Theory* (New York: John Wiley and Sons, Inc, 1953) p 79, section 5. Regarding the symmetry of parameter matrices.
2. E. A. Guillemin, *Theory of Linear Physical Systems* (New York: John Wiley and Sons, Inc, 1963), pp 192-195: regarding impedance leveling.
3. *Reference Data for Radio Engineers* (New York: Howard W. Sams and Co, Inc, 1975; 6th ed.), pp 8-24,25.
4. W. H. Hayward, *Introduction to Radio Frequency Design*, (New Jersey: Prentice Hall, Inc, 1982), pp 75-82. Regarding impedance-transforming networks.
5. P. E. Gray and C. L. Searle, *Electronic Principles* (New York: John Wiley and Sons, Inc, 1969), pp 605-612: example of tuned RF amplifier with "alignability" as a criterion for design.

Notes

¹Later in this article, we will see how easily the effects of internal voltage-dependent current generators in an active network can be included in the analysis, while still including the symmetry properties of the passive network.

²The PC used was a 486DX4 (100 MHz) with *Mathcad* software.

In the Next QEX

Among other features in the November/December *QEX*, Bill Sabin, W0IYH, concludes his two-part series on the *ARRL Radio Designer* and *Circles Utility* software. Grant Bingeman, KM5KG, presents some practical hot-guy-wire antennas for ham radio and some interesting results. Chris Trask, N7ZWY, examines nonlinear distortion in bipolar transistors, and from across the sea comes an article from Pete Lawton, G7IXH, about a 'fast' digital oscillator stabilizer.

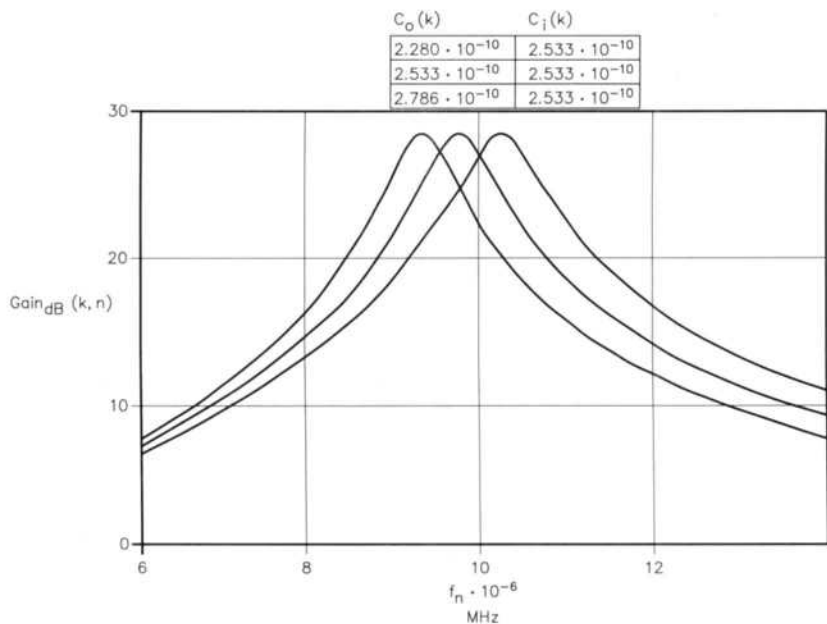


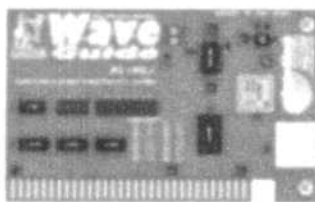
Fig 7—Voltage gain from node 1 to node 5.

DDS from Your PC!

Announcing the new PC-VFO jr!

Digital VFO

Only \$139



PC plug-in card
DC to 54 MHz
.029 Hz Steps
+10 dBm output

Works on any ISA
motherboard

www.bytemark.com/waveguide



800 679-3184

AMIDON, INC.

Committed to Excellence Since 1963



Technical Specifications Online!
www.bytemark.com/amidon

W2FMI BALUNS and UNUNs

Exclusive discussion on the design and implementation of Transmission Line Transformers by the Legendary Dr. Jerry Sevick, W2FMI

www.bytemark.com/amidon/content6.htm



7714 Trent Street
Orlando, FL 32807
407 673-2083 FAX
407 679-3184 Voice

Amidon Master Distributor

Signals, Samples, and Stuff: A DSP Tutorial (Part 4)

Our DSP tutorial winds to an end. As we turn toward home, we finish the Fourier Transform discussion. Along the return path, we'll explore two fascinating parts of modern smart radios: adaptive control systems and remote-control systems. We'll also take a hard look at telephone systems and their bandwidth.

By Doug Smith, KF6DX/7

In the July/August *QEX*, I ended the third part of this series with a promise to provide a method for calculation of the discrete Fourier transform (DFT) that is faster than the so-called fast Fourier transform (FFT). The algorithm and its derivation are provided in this last installment of the tutorial. A unique feature of the algorithm is its error-control mechanism. I'll show that without it, the algorithm would diverge from the correct solution.

As a follow-on to the last issue's discussion of adaptive filtering, I have some notes about other adaptive control systems. I hope readers can dream up a few of their own—try an automatic anti-VOX!

I'll also describe audio digitization at relatively low serial bit rates for use in remote-control systems. Some controversy endures over the correct SNR expression for delta (Δ) modulation. I offer my analysis without making any assumptions about the nature of the audio signal, other than its amplitude.

The Damn-Fast Fourier Transform (DFFT)

Sorry, but I have to take us through the statistical muck

one more time to prove that this Damn-FFT is going to work! It will be worth it, to be sure, since the computational burden will be reduced to be proportional to $2N$, which for large values of N , is quite a bit better than $N \log_2(N)$! We must deal with errors that increase arithmetically, but I'll introduce a straightforward method of limiting them and define the upper bound.

This derivation begins by looking at how DFT results change at each sample time.¹ Say we start with a DFT for an input sequence $x(n)$ at sample time r . Then we compute the DFT for the next sample time $r + 1$ and examine the sequences to see what's changed. For $r = 0$, each DFT sequence expands to:

$$X_0(k) = W_n^{0k}x(0) + W_n^{1k}x(1) + W_n^{2k}x(2) + \dots + W_n^{(N-1)k}x(N-1)$$

$$X_1(k) = W_n^{0k}x(1) + W_n^{1k}x(2) + W_n^{2k}x(3) + \dots + W_n^{(N-1)k}x(N)$$

(Eq 1)

and what's evident is that each input sample $x(n)$ that was multiplied by W_N^{nk} in the summation for $X_0(k)$ is now multiplied by $W_N^{(n-1)k}$ in the summation for $X_1(k)$. So the ratio of the two sequences is nearly:

$$\frac{X_1(k)}{X_0(k)} = \frac{W_N^{(n-1)k}}{W_N^{nk}} = W_N^{-k} \quad (\text{Eq 2})$$

We still have two terms “hanging out” of the relationship, namely the first and the last:

$$W_N^{0k}x(0) = x(0) \text{ and } W_N^{(N-1)k}x(N) \quad (\text{Eq 3})$$

which haven't been accounted for in the ratio. If we first subtract $x(0)$ from $X_0(k)$ before taking the ratio, then add the new term $W_N^{(N-1)k}x(N)$ after, we have the correct result:

$$X_1(k) = W_N^{-k}[X_0(k) - x(0)] + W_N^{(N-1)k}x(N) \quad (\text{Eq 4})$$

Now this can be simplified a little, since:

$$\begin{aligned} W_N^{(N-1)k} &= e^{-\frac{2\pi j(N-1)k}{N}} \\ &= e^{-\frac{2\pi jN}{N} + \frac{2\pi jk}{N}} \\ &= W_N^{-k} \end{aligned} \quad (\text{Eq 5})$$

and substituting:

$$X_1(k) = W_N^{-k}[X_0(k) - x(0) + x(N)] \quad (\text{Eq 6})$$

This is marvelous, because it means for N values of k we can compute the new DFT from the old with N complex multiplications and $2N$ complex additions, or a computational burden proportional to N ! If we begin with $X(k) = 0$ and take the first N values of $x(n) = 0$, we can start the thing rolling—we save computation over the FFT by the factor:

$$\frac{\frac{N}{2} \log_2 N}{N} = \frac{\log_2 N}{2} \quad (\text{Eq 7})$$

which for large values of N is very significant indeed! For example, if $N = 1024$, the improvement is a factor of five. Over the direct DFT, it is a factor of $N^2/N = N$ faster. But there's a catch: An error term will grow in the output because the truncation and rounding noise discussed previously is cumulative. The error will continue to grow unless we do something about it.

The safest way to handle the situation is to effectively reset the variables to zero every N samples or so, and to do this while continually generating output samples.

We'll calculate two DFFTs for all the output points k , with the first of them, $Y(k)$, taking the next N input samples $x(n) = 0$, and the second, $Z(k)$ using unmodified input samples $x(n)$. Beginning at some input sample time r :

For $0 \leq n \leq N-1$:

$$Y_{r+n+1}(k) = W_N^{-k}[Y_{r+n}(k) + x(r+n+N)] \quad (\text{Eq 8})$$

$$Z_{r+n+1}(k) = W_N^{-k}[Z_{r+n}(k) - x(r+n) + x(r+n+N)]$$

After these N iterations, both calculations have identical results except for the greater error in $Z(k)$. At this point, the result of the first calculation $Y(k)$ is transferred:

$$Z(k) = Y(k) \quad (\text{Eq 9})$$

and then the first result is zeroed:

$$Y(k) = 0 \quad (\text{Eq 10})$$

The calculation then continues for another N iterations, at which time the exchange and reset are again done. This places an upper bound on the cumulative error to that associated with $2N$ iterations, but it increases the computational

burden by a factor of two. Now the savings over the FFT is:

$$\frac{\frac{N}{2} \log_2 N}{2N} = \frac{\log_2 N}{4} \quad (\text{Eq 11})$$

which for $N > 16$ represents an improvement.

Behavior of the DFFT Error Term

In this system, we expect the round-off errors to grow linearly in the worst case since we're using the value of $X_{r+n}(k)$, containing an error, to compute the new value of $X_{r+n+1}(k)$. The calculation produces another error which simply adds to the old:

$$X_{r+1}(k) + \epsilon_{r+1} + W_N^{-k}\epsilon_r = W_N^{-k}[\{X_r(k) + \epsilon_r\} - x(r) + X(r+N)] \quad (\text{Eq 12})$$

and the propagation of errors depends on the value of W_N^{-k} . This coefficient might be as large as unity, so after $2N$ iterations, we expect the maximum noise power to be twice that of the direct-form DFT, or:

$$\sum_{n=0}^{N-1} E[\epsilon_n^2] = \frac{2^{(1-2b)}N}{3} \quad (\text{Eq 13})$$

If this were the only source of error, we could track the error term separately—using another set of registers, for example—and use it to steer the output back toward the correct result. Nonetheless, the error in the fixed-point representation of the coefficients W_N^{-k} degrades the signal-to-noise ratio (SNR) as it does in the FFT. This error cannot be represented exactly for all values of k , since the coefficients are *irrational* numbers. That is, sines and cosines. So we suspect that the exchange and reset method is the best we can do.

Fig 1 shows the result of DFFT calculation errors, as obtained from comparison with DFT results for the same input data, over many iterations for $N = 1500$ and with a random input (noise) for $x(n)$. Data and coefficients have 16-bit fixed-point representation, *convergent rounding* has been applied to the coefficients and to the result of each computation. *Block floating-point scaling* has been implemented.² This means that whenever the result of a calculation results in an overflow, the result is divided by two, and a scaling-factor register is updated to reflect the new scale. As indicated in Part 3 of this series,³ the scaling required to prevent overflow increases the output noise beyond the bound of Eq 13. Clearly, the DFFT output error is twice that of the DFT, with an SNR bounded by:

$$SNR_{OUTPUT} = \frac{2^{(2b-3)}}{N} \quad (\text{Eq 14})$$

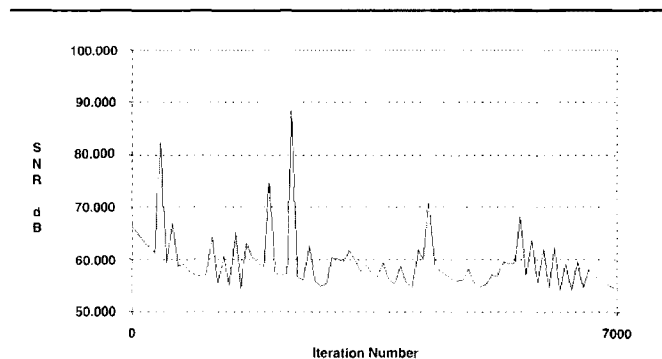


Fig 1—DFFT error noise versus sample time.

The Inverse DFFT (DFFT⁻¹)

There isn't an inverse DFFT (DFFT⁻¹)! The only direct analogy I can find for the inverse case relates to the sample-by-sample nature of the DFFT. In a "real-time" system, only the next output sample need be computed, not the next N output samples. The easiest output term to compute is $x(0)$, since in the summation, all coefficients are $W_N^0 = 1$. The output is then just:

$$x(0) = \frac{1}{N} \sum_{k=0}^{N-1} X(k) \quad (\text{Eq 15})$$

and only one multiplication is involved.

The DFFT should be useful to experimenters who are looking for a quick and simple method of DFT calculation. The application of windowing to the DFFT and further improvements in the algorithm are subjects of ongoing research.

Combining Adaptive Techniques with the DFFT: The Adaptive Line Enhancer

The adaptive, self-tuning filter described previously (see Note 3) can be combined with spectral-analysis techniques to create a very sensitive detector of periodic signals in the presence of noise. The basis for this method is that the Fourier transform of a filter's impulse response $h(n)$ is its frequency response $H(k)$:

$$H(k) = \sum_{n=0}^{L-1} W_N^{kn} h(n) \quad (\text{Eq 16})$$

That is, if we spectrally analyze an adaptive filter's time response, we get a picture of its frequency response. To exploit this combination of the two noise-reduction (NR) techniques, we can apply the DFFT to the filter coefficients $h(n)$ produced by an LMS adaptive filter.

Fig 2 shows an arrangement known as an *adaptive line enhancer*.⁴ Note that the DFFT input isn't a simple, time-

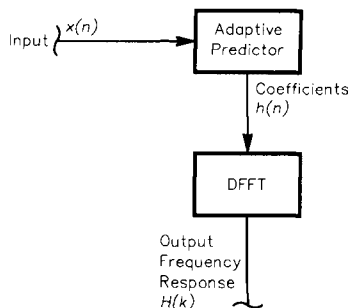


Fig 2—An adaptive line enhancer.

sampled sequence, as it was in the original derivation, because *every value* of $h(n)$ is changing at each sample time. Whereas for some filter of length L , the line enhancer output at time $r = 0$ is:

$$H_0(k) = \sum_{n=0}^{L-1} W_N^{kn} h_0(n) \quad (\text{Eq 17})$$

The output at the next time $r = 1$ is:

$$\begin{aligned} H_1(k) &= \sum_{n=0}^{L-1} W_N^{kn} [h_0(n) + 2\mu e_0 x_0(n)] \\ &= H_0(k) + \sum_{n=0}^{L-1} W_N^{kn} 2\mu e_0 x_0(n) \\ &= H_0(k) + 2\mu e_0 X_0(k) \end{aligned} \quad (\text{Eq 18})$$

This is the DFFT for the adaptive line enhancer. (See Fig 3.) It adds $2L$ complex multiplications and $2L$ real additions to the computational burden of the adaptive noise reduction system, but this sure is a lot better than applying a DFT or even FFT to the filter coefficients. We must use the simultaneous transfer and reset methods of equations 8, 9 and 10 above, because errors build up as before.

This system rivals any spectral-power-measurement algorithm around. If adaptive filtering produces some SNR improvement, then application of the DFFT to the filter coefficients produces an additional improvement.

Further, imagine that the output of the spectral line enhancer was used as the input to a PLL! The SNR could then be whatever was achievable at

the output of the oscillator—a tremendous improvement over the input SNR indeed. Of course, issues of lock time, acquisition range and so on would come into play.

The Direction of Future Research

As industry strives toward the development of hardware capable of sufficient dynamic range to eliminate more of the analog processing stages in receivers, the issues covered above will become increasingly significant. The goal remains the same: To receive a desired signal in the presence of strong undesired signals. We've seen that, in the end, only so much mathematical finesse can be applied to the problem; additional improvements come only through increased processing "horsepower." It's an unfortunate result of the way things are that when the math has exhausted all its avenues of refinement, all effort is expended on increasing the raw speed of calculation. This has the unintended consequence of allowing programmers the luxury of faster machines, of larger data and program spaces and of complacency toward continual upgrades in both of those. The emphasis drifts away from doing things intelligently, and toward brute-force approaches.

This trend is evident in the megabytes of code seen in today's application software. However, this isn't to say, as one patent office commissioner did, that: "Everything that can be in-

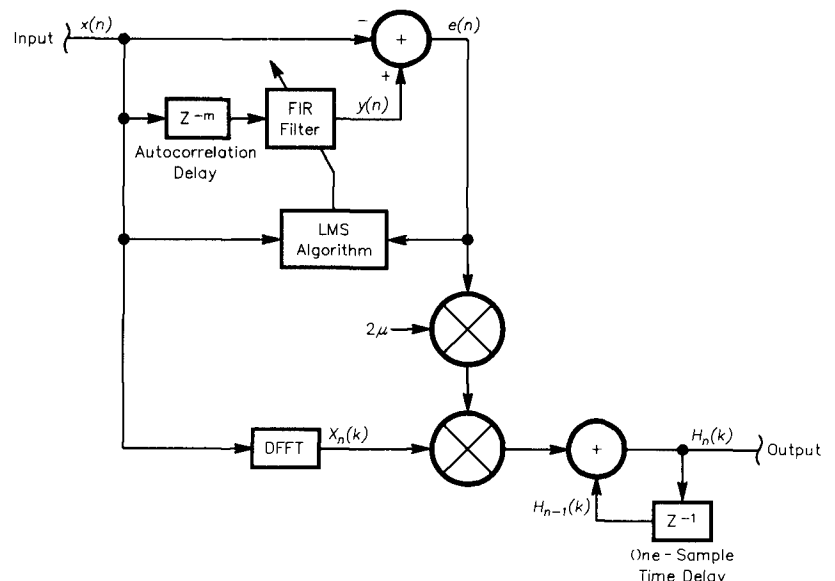


Fig 3—The adaptive line enhancer using the DFFT.

vented, has been invented." It's only a poke at those who forget the importance of questioning everything.

Adaptive Control Systems for Radio Transceivers

Microprocessor control of everything from automobiles to microwave ovens has revolutionized the way we live. It's very much like other innovations throughout history: We didn't know we needed them until they came along and made things so much easier. In fact, it's difficult for many to imagine life without automobiles, microwave ovens or microprocessors; especially, those of the newer generations cannot conceive how it was in the "dark ages."

We do well to study the past, if only to remind ourselves why we did things the way we did and refresh our memories about the mistakes that we made along the way. As is the case for so many human schemes, unintended consequences can be the most memorable part of any invention.⁵ As a good friend is wont to say: "Considering all the problems with these 'new-fangled' computers, I don't think they're here to stay."

But they've sure solved a lot of problems, too. That is the subject of this section, specifically: How computers enhance the performance of radio equipment and make certain things possible that would be excruciatingly difficult without them.

Control Theory

In control theory, the system to be controlled is referred to as the *plant*.⁶ The plant produces some output response to a control input. The thing providing the control input is known as the *controller*. A good example is the automobile, the engine and wheels of which respond to the input commands of the driver. He or she has their hands on the steering wheel, and presumably, their feet near the accelerator and brake pedals. The plant in this case responds to the driver's desire to steer, accelerate or decelerate the car. Most drivers understand this relationship, but there are some who clearly don't!

In a computer-controlled transceiver, the plant responds to input from the operator when it's time to change frequency, mode or alter other parameters. Central to most control systems is the idea of *feedback*, which provides the controller with information about how the plant is responding. In many cases, it's enough to know *whether* the plant has responded. A frequency display or indicator lamp on

a transceiver provides visual feedback about plant response. Many responses are auditory only—the volume control is an example.

As in the case of adaptive filters, feedback provides input to the controller, which then uses some algorithm to produce new control information. The controller's algorithm may be a fixed linear or nonlinear system, or it may be time-varying so that adaptation to changing plant conditions is possible. In the following discussion, we'll address both situations, with emphasis on adaptive DSP technology.

Anatomy of a Computer-Controlled DSP Transceiver

We might be tempted to say that the digital signal processor is the heart of any DSP transceiver, but I'd like to propose that it's the brain. The synthesizer is more like the heart, the transmitter is the vocal chords and the receiver the ears! In the case of a microprocessor-controlled transceiver, almost everything is under the supervision of the processor, so it makes sense that it manages all control commands and feedback. Whether the controls are knobs attached to shaft encoders or keys on a computer keyboard matters not to this deliberation. What *does* matter is that all things impacting transceiver performance *and that can be altered* are implemented by firmware running on a DSP.

For an IF-DSP transceiver, the range of functions falling into this category is immense. In fact, it's prudent to provide as much user control as possible. The challenge is to present the options in a way that is not ambiguous and "user-friendly." Most of us have encountered "user-hostile" operating systems that make ham radio a chore rather than the pleasure it should be. Let's look at some of the basic functions of today's HF rig, and examine how DSP control improves performance.

S-Meter Calibration

Most HF transceivers have an analog gain control (AGC), another example of a feedback control system. It's desirable to meter the signal strength in the receiver, and this is usually done by using the AGC voltage to drive a visual display of some kind. Because of the nature of the physical circuits, gain control is typically proportional to the logarithm of the AGC voltage. Hence, S-meters are calibrated logarithmically—each increment of meter deflection is proportional to a fixed number of decibels.

Analog gain-controlled devices don't repeat exactly from unit to unit. To get an accurate S-meter, it's necessary to characterize each unit separately via a calibration routine. It's easy enough to measure the S-meter's performance, and to build a table of its errors versus input signal strength. We can do exactly this when the S-meter is under microprocessor control.

A correction table is stored in non-volatile memory, and is used to adjust the S-meter values in "real time." During testing, a calibration routine is used to compare the meter reading with the input level from a known-accurate signal generator, and so to generate the table. After many units have been measured, it's found that a small number of S-meter correction curves are sufficient to account for all units; these "boiler plate" tables are used based on individual variations.

Automatic Frequency Calibration and Temperature Compensation

Another benefit of DSP feedback control systems is that it's easy to determine the frequency of a received carrier to within the accuracy of the control system's reference clock. An accurate external reference can be input to the receiver, and its frequency counted by the DSP system. The frequency error is used to generate a correction voltage, which is applied to the voltage-controlled crystal oscillator (VCXO) internal reference. The correction voltage is adjusted until the frequency error is minimized.

This VCXO-control voltage is also varied with temperature to compensate the oscillator's frequency-versus-temperature curve, making it a microprocessor-compensated crystal oscillator (MPCXO). For best accuracy, each unit can be calibrated separately. A table is downloaded and stored in nonvolatile memory representing the variation in control voltage necessary to keep the internal reference's frequency constant. The temperature sensor is located in the oscillator compartment to achieve best tracking.

As each unit is calibrated separately, the shape of the curve in the table accommodates the actual frequency-versus-temperature trait of that particular oscillator. Note that *all* frequency-determining elements in the transceiver are inside the calibration loop, and are therefore compensated to some degree using this technique.

The most convenient way to measure a carrier's input frequency is to translate it down to some IF or audio

frequency, then count the number of zero-crossings per second. As the measured error decreases, the DSP system can automatically narrow the BW of the received signal to improve the SNR and, therefore, the accuracy of the result.

The Receiver as a Spectral Analyzer

As we saw above, various techniques are available to analyze signals in the frequency domain. When tuned to a fixed frequency, however, the bandwidth of the receiver is necessarily limited because of dynamic-range considerations.⁷ With today's frequency-agile synthesizers, it's possible to turn our receiver into a spectrum analyzer.

The receiver is tuned rapidly across the band, and the signal strength is measured at each iteration. A very fast AGC time constant is obviously required. The resolution BW of the measurements can be altered by selecting a different BPF, with the attendant change in sweep speed. The resulting data are graphically displayed, and the operator is given a graphical user interface (GUI) with which to visually select signals, and hence manually tune the receiver.

Adaptive Path-Quality Evaluation and Automatic Link Establishment

Commercial HF operators may not be as skilled as radio amateurs in selecting operating frequencies. Hence, the need for automatic-link-establishment (ALE) systems, which select clear communication frequencies. While I don't expect ALE to catch on in ham circles, certain aspects of it have been in use by amateurs for some 15 years. It's worth examining them as forms of adaptive control.

At the lowest level of ALE architecture is a receiver's frequency-scanning capability. We can scan many frequencies in a relatively short period, look for signals of interest and stop to examine them when appropriate. After all, we're trying to find the best frequency for the communication desired; we'd better have a choice of frequencies, or the exercise would be pointless.

The next level incorporates some form of *selective calling*. We need a signaling method that discriminates between the many stations on the air. Myriad selective-calling schemes have been used over the years in commercial systems; some are more effective than others. The ham community has pioneered quite a few of the digital transmission modes used with radio, and we can easily find examples of se-

lective calling among them. AMTOR, packet, PACTOR, CLOVER, GTOR and now PACTOR II all support selective transmissions. In fact, what transmissions other than news bulletins and CW practice are *not* selective?

At the third level, we integrate the first two levels into a path-quality evaluation (PQE) system. When not in use, all the stations in the network are scanning the assigned frequencies; we then use our selective calling tools to attempt contact with the desired station on the available frequencies, one by one. Connection with the other station results in some acknowledgement that we've been heard. At this point, scanning is suspended, and some exchange of data is made to evaluate the quality of the link. This may be as simple as a signal strength measurement, or may involve appraisal of a data-error rate, or both.

This procedure is known as *polling*. The idea is that after all frequencies have been polled between the two stations, an assessment is made regarding the best frequency to use. Either station can make this judgment, but ultimately one will call the other again on the best frequency to establish com-

munications. In most such systems, the PQE analysis is made at the time when the connection is desired.

Another method of determining connectivity is known as *sounding*. In this procedure, stations not in use periodically broadcast messages intended for the general consumption of all the other stations in the network. Acknowledgment of sounding transmissions is not expected. Those stations that happen to be listening on that frequency evaluate the quality of reception, and make a note of it. When it's time to connect, each station has a much better idea of which frequency is the best.

Here at the fourth level, we pull it all together as an ALE system. After the thing has been operating a while, each station has data about which other stations it can contact. At connect time, therefore, the amount of delay until communications are established is at a minimum. The operator enters the selective calling code for the station with which communications are desired, and the system uses its "learned" information to make contact on the best frequency. This information is slowly changing, of course. We'll also throw in a busy-channel detector, which pre-

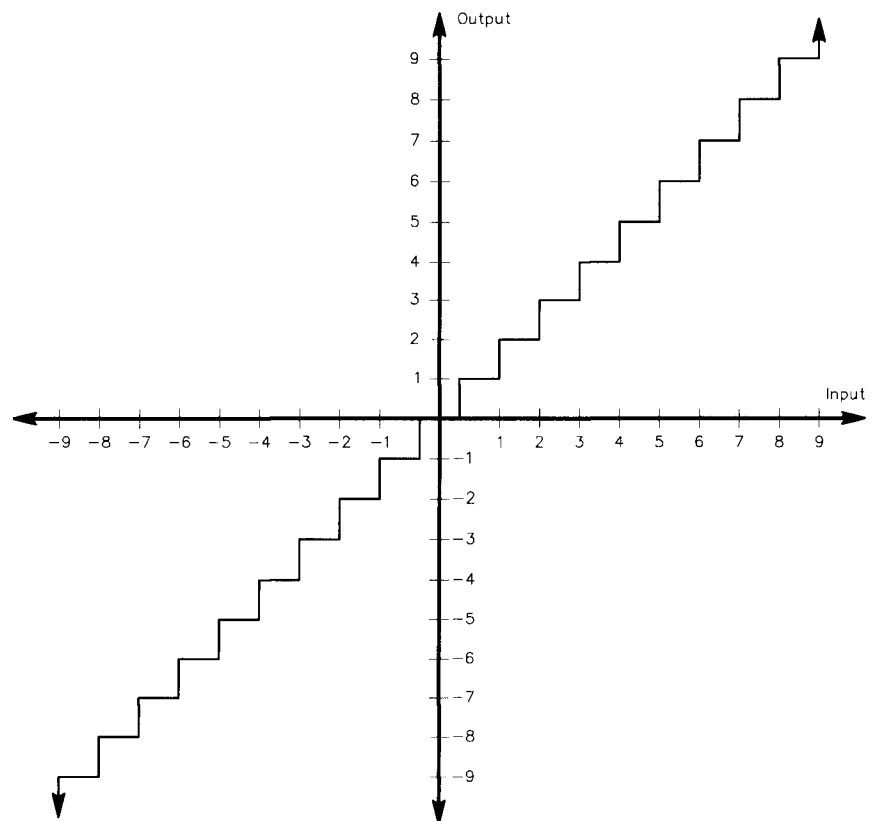


Fig 4—Uniform quantizer transfer characteristic.

vents stations from transmitting on frequencies that are already in use.

At level five, we add the ability to exchange information about network connectivity; that is, we allow the stations to periodically report to each other which others they can hear. Imagine that station A can communicate with station B, and station B can also communicate with station C, but that A cannot directly talk to C. When A attempts to contact C, the connection will fail; B then intervenes and relays the traffic from A to C.

Higher ALE levels implement the capacity to *store and forward* traffic. Stations in the network save copies of messages intended for other stations that are busy or temporarily unavailable. Later, when a connection can be established, the messages are delivered.

Standards have evolved based on these strategies, among them the AX.25 packet protocol, FED-STD-1045, 1046, 1047 etc. The advantage of standards is that they take the best of all the various techniques and meld them into a logical format. Amateur Radio has done well in fostering its packet standards. We could establish similar standards for the other digital modes and promote our ability to respond when the world needs us, such as during a major disaster or other emergency. I feel strongly that to advance the cause of Amateur Radio is not only to push the state of the art, but also to use our technology in times of need. How much more traffic could have been passed after the Mexico City earthquake with such a system?

I'll use the rest of my space here to discuss the remote control of radio equipment, as this is also important to emergency preparedness in many ways. It's also of interest to those of us in antenna-restricted areas—it's becoming so common these days!

Remote-Control Systems for Radio

This really is a hot topic because of its bearing on communication effectiveness in general. Hams who live in antenna-restricted areas (as I do) must find some means of getting on the air without upsetting their neighbors. Antennas are viewed as an eyesore by an increasing number of neighborhood associations, but it's RFI that really gets us in trouble. Remote location of the transceiver solves both problems. Commercial systems must often crowd many transmitters into a small area, so they're forced to distantly locate the receivers. Finally, the situation

wherein many operators share a single transceiver occurs in both the commercial and amateur services. Repeaters on the VHF and UHF bands are examples.

No matter who is using the equipment, the requirement exists for a control link. Part 97 of the FCC Rules⁸ states that there shall be a control operator present at the control site at all times. While the automatic message store-and-forward system described above stretches the rules to their limits, I think we can see that a radio without a control operator is like a sailboat without a skipper. All kinds of things go wrong with radios that require the attention of human beings! In remote control, we're just extending the control site to a point distant from the transceiver. Complete control is still possible, and the system is secure as long as it can "fail safe."

The Control Path

For a control link, two media present themselves: The public switched telephone network (PSTN) and a direct VHF, UHF or microwave radio link. It would be nice if whatever method we select were applicable to either form of remote link. It's also desirable that both control data and audio traverse the link in both directions simultaneously; ie, in full duplex. Especially in the case of a remote radio link, it's tempting to use two channels: one for the control data, and one for the audio. When considering the PSTN, however, this isn't very attractive. Telephone bills never stop coming, so it sure would be nice if we could implement the whole system on a single line.

Starting in 1996, interest in simultaneous voice and data transmission intensified. Driven by the demand for "teleconferencing," numerous companies introduced digital simultaneous voice and data (DSVD) modems. These were followed by so-called analog simultaneous voice and data (ASVD) modems, which touted improved audio quality while maintaining moderate data-transmission bandwidth. Neither of these technologies is compatible with the formats emerging for digital audio transmission over the Internet.

Meanwhile, telephone companies are grappling with a connectivity problem of their own: How can they accommodate an ever-increasing number of calls, from both voice and modem users, without increasing the number of physical lines? The tremendous increase in traffic caused by the Internet began to place a strain on the existing PSTN.

PSTN Traffic Capacity and Quality: The Bandwidth Boondoggle

This issue of traffic capacity is an enormous one for the telephone companies and for those of us wishing to pass large amounts of information through the telephone lines. As I began looking into this, several crucial questions emerged: Who or what sets the available bandwidth on the PSTN? Can the telephone companies change the bandwidth without notice?

In both wired and wireless communications, digital transmission modes are becoming more prevalent.⁹ Digital formats have clear advantages over analog. The first, most obvious of these is noise immunity in detection; a detector has only to determine whether the received datum was a one or a zero. Another advantage is that error detection and correction can easily be applied to digital data. Whereas we want to pass both digital control information and audio in our remote-control application, it makes sense to use an exclusively digital mode on the remote link. It's easier and more secure to digitize the audio, and recover it error-free on the other end, than it is to devise analog control methods for a complex transceiver. Also, the data are more easily encrypted for security. The telephone companies discovered the benefits of digital transmission long ago, and while it might surprise some, virtually *all* telephone calls are digital during most of their journey.

In going digital, the folks at the telephone company (remember, it used to be just one company) found that when speech was digitized, it took up a heck of a lot more bandwidth than in analog form. Consider a speech signal occupying a bandwidth of about 3 kHz. Digitize it using 8 bits, or 256 quantization levels, at a rate just above the Nyquist limit, say 8 kHz. The bit rate is then:

$$\begin{aligned} \text{bit rate} &= \left(\frac{8 \text{ bits}}{\text{sample}} \right) \left(\frac{8,000 \text{ samples}}{\text{second}} \right) \\ &= 64 \times 10^3 \frac{\text{bits}}{\text{second}} \end{aligned}$$

(Eq 19)

Now the BW is about 10 times what's required for the actual information, but this is basically the phone company's standard. The format does have the advantages of noise immunity and the ability to *time-division multiplex* the data with those of other telephone calls. The quality of this *uniform quantization pulse-code modulation (PCM)* scheme would leave something to be desired, since its dynamic range (DR),

the ratio of a full-scale signal to the smallest quantization step, using signed, fixed-point math, is only:²

$$DR = 2^{(b-1)} \approx 6.02(b-1) \text{ dB} \approx 42.2 \text{ dB} \quad (\text{Eq 20})$$

and its maximum SNR for a sine wave input:

$$SNR_{MAX} = 2^{\left(\frac{b-3}{2}\right)} \sqrt{3} \approx 6.02(b-1) + 1.76 \text{ dB} \approx 43.9 \text{ dB} \quad (\text{Eq 21})$$

A uniform "quantizer" has the transfer characteristic shown in Fig 4.

*Compression Techniques:
Non-Uniform Quantization*

To improve things, we decide to take our 256 quantization levels and distribute them over the range of amplitudes such that resolution for low-level signals is increased at the expense of high-level signals. This results in a non-uniform quantization transfer characteristic, such as that shown in Fig 5. The net effect is to increase the DR for a given number of bits, and to improve the SNR for low-level signals. Alternatively, we could reduce the number of bits, and therefore our occupied bandwidth, while maintaining the same DR as before. The main drawback of non-uniform quantization is a lower limit for the maximum SNR. Eqs 20 and 21 are no longer valid.

In most non-uniform quantization systems, the transfer curve is somehow logarithmic; ie, the quantizer output is proportional to the log of the input. In North America and Japan, *μ-law* quantization is used, wherein for $|x| < 1$ and $\mu \gg 1$:

$$f(x) = \text{sign}(x) \frac{\ln(1 + \mu|x|)}{\ln(1 + \mu)} \quad (\text{Eq 22})$$

$\mu = 255$ for North America. The DR expression must now be rewritten to reflect the new transfer function $f(x)$. Setting Eq 22 equal to the smallest-possible positive output step $1/2^{b-1}$ yields the smallest-possible positive input signal which can be resolved:

$$\frac{1}{2^{b-1}} = \frac{\ln(1 + \mu x)}{\ln(1 + \mu)}, \text{ for } x > 0 \quad (\text{Eq 23})$$

$$x_{MIN} = \frac{(1 + \mu)^{\frac{1}{2^{b-1}}} - 1}{\mu} \quad (\text{Eq 24})$$

This is smaller than $1/2^{b-1}$, and for $b = 8$ and $\mu = 255$, the DR is now:

$$DR = x_{MIN}^{-1} = 20 \log \left(\frac{\mu}{(1 + \mu)^{\frac{1}{2^{b-1}}} - 1} \right) \text{ dB} \approx 75 \text{ dB} \quad (\text{Eq 25})$$

Derivation of the SNR is inherently much more difficult. Degradation of the peak SNR occurs because of the coarse quantization used for large-signal amplitudes, where finely spaced levels aren't otherwise necessary. An input that is near the boundary of two coarsely spaced quantization levels is liable to jump rapidly between those levels, producing a lower-frequency noise component at the "jitter" frequency. At low input amplitudes, quantization uses more levels, and improves the SNR there over uniform quantization. The basic idea is to hold SNR constant over the range of input amplitudes. We can analyze the SNR for μ -law quantization as a function of input level in the same manner as in the derivation of statistical truncation or rounding errors given previously. This time, however, we'll use terms for the RMS noise voltages instead of the powers.

As before, the noise voltage is the expected value of the quantization er-

ror over the "distance" between two adjacent quantization levels. Between two adjacent output quantization levels $n/2^{b-1}$ and $(n + 1) / 2^{b-1}$, the quantizer is liable to produce noise proportional to the difference between the corresponding *input* levels. After Eq 24:

$$x_n = \frac{(1 + \mu)^{\frac{n}{2^{b-1}}} - 1}{\mu} \quad (\text{Eq 26})$$

and

$$x_{n+1} = \frac{(1 + \mu)^{\frac{n+1}{2^{b-1}}} - 1}{\mu} \quad (\text{Eq 27})$$

The difference between these input levels is:

$$\begin{aligned} \Delta x &= \frac{(1 + \mu)^{\frac{n+1}{2^{b-1}}} - 1}{\mu} - \frac{(1 + \mu)^{\frac{n}{2^{b-1}}} - 1}{\mu} \\ &= \frac{(1 + \mu)^{\frac{n+1}{2^{b-1}}} - (1 + \mu)^{\frac{n}{2^{b-1}}}}{\mu} \\ &= (1 + \mu)^{\frac{n}{2^{b-1}}} \left[\frac{(1 + \mu)^{\frac{1}{2^{b-1}}} - 1}{\mu} \right] \\ &= (1 + \mu)^{\frac{n}{2^{b-1}}} x_{MIN} \quad (\text{Eq 28}) \end{aligned}$$

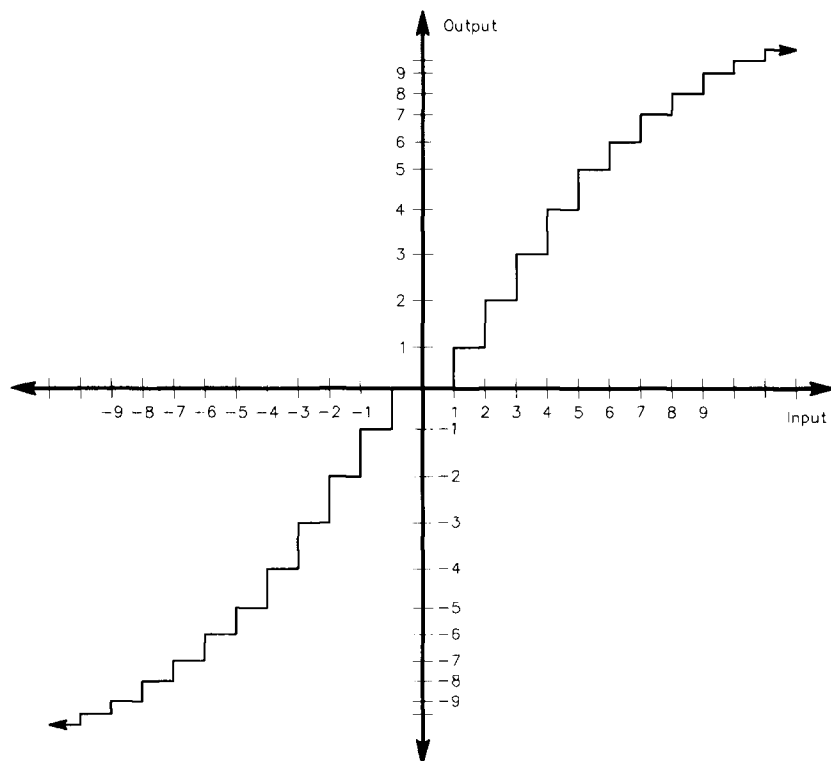


Fig 5—Nonuniform quantizer transfer characteristic.

and the expected value of the noise voltage is:

$$\sigma = \frac{(1+\mu)^{\frac{n}{2^{b-1}}} x_{MIN}}{\sqrt{12}} \quad (\text{Eq 29})$$

The SNR is the ratio of the input level x_n to the noise:

$$\begin{aligned} SNR &= \frac{x_n}{\sigma_n} \\ &= \frac{\left(\frac{(1+\mu)^{\frac{n}{2^{b-1}}} - 1}{\mu} \right)}{\left(\frac{(1+\mu)^{\frac{n}{2^{b-1}}} x_{MIN}}{\sqrt{12}} \right)} \\ &= \frac{\sqrt{12} \left[1 - (1+\mu)^{-\frac{n}{2^{b-1}}} \right]}{\mu x_{MIN}} \end{aligned} \quad (\text{Eq 30})$$

In Fig 6, it's evident that this method does a reasonably good job of holding the SNR constant as compared with straight 8-bit PCM.

As the necessity arose to increase the total traffic-handling capacity of telephone networks, both satellite and fiber-optic technologies were developed. Each offers increased bandwidth without the radiation problems associated with a twisted-pair wire transmission line. The typical fiber-optic T1 line interface has a capacity of roughly 1.54 megabits per second (Mbps), and so can handle several simultaneous calls:

$$\begin{aligned} calls &= \frac{1.54 \times 10^6}{64 \times 10^3} \\ &\approx 24 \end{aligned} \quad (\text{Eq 31})$$

We infer that a data connection using a modem at 28.8 kbps occupying the same 3 kHz bandwidth is not an efficient use of resources, since were the digital interface extended to the user, 64 kbps would be possible. Therefore, we conclude that the PSTN is not optimized for data traffic. No great shock, since this isn't what it was designed for in the first place.

However, some very bright person comes along and discovers that the bandwidth occupied by digitized audio can be reduced by coding the *difference* between the samples. The difference between samples is smaller in amplitude than the actual samples, and so can be coded with fewer bits. Bandwidth is therefore reduced.

Delta Modulation

Extending this idea, we increase the sample rate by a factor of 8 (for the 8 bits per byte) and reduce the bit-resolution by the same factor. Now we're using only a single bit each sample time, and we have a one-bit quantizer. This is called linear *delta modulation* (DM).¹⁰ The first such scheme was developed in 1946.

When the encoded bit = 1, the voltage is increasing; when the bit = 0, the voltage is decreasing. (See Fig 7.) A certain value of voltage change, dV , is associated with each bit. The encoded bit stream is integrated at the decoder to reproduce the original waveform. This design has an inherent difficulty, however: It can't reproduce waveforms that have slopes exceeding the maximum-possible integration time constant, dV/dt . This phenomenon is known as *slope overload*. The net effect is a roll-off in the high-frequency response.

Increasing the value of dV helps mitigate this problem, but it introduces *granular noise*. Large values of dV tend to mask low-amplitude signals smaller than dV . In the situation where input signals are smaller than dV , the quantizer output is an alternating sequence of ones and zeros; ie,

a square wave. Since this integrates to dc, low-level signals are lost.

Continuously-Variable Slope Delta Modulation (CVSD)

We can use adaptive techniques we learned earlier to address the issues of granular noise and slope overload. Allowing the value of dV to change adaptively—based on the input slope—largely solves the problems encountered above. This technique of CVSD was first introduced by Greefkes and Riemens in 1970.¹¹ In it, dV is altered "on the fly" based on the values of the last three or four bits in the stream. See Fig 8.

When the last three or four bits are not identical, the system is equivalent to linear DM. When continuous strings of ones or zeros occur of at least that length, however, the integration time constant is changed to increase the slope. Thus the granularity problem is no worse than in the case of linear DM, and the slope overload problem has been greatly ameliorated. Note that the figure incorporates an adaptive predictor.

The adaptive character of CVSD results in an SNR-versus-input level performance similar to the μ -law en-

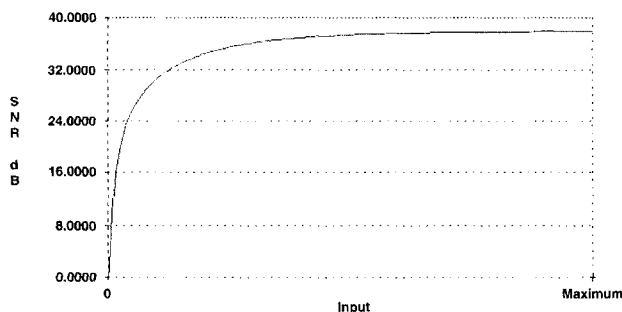


Fig 6— μ -law SNR-versus-input amplitude.

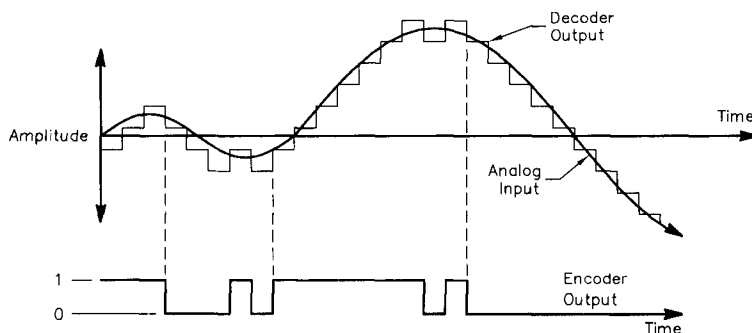


Fig 7—DM representation.

coding above. The nonlinear transfer curve in this case is due to changes in the value of dV based on past variations in the input signal. I_1 is referred to as the *primary integrator* and I_2 as the *pitch integrator*. Time constants of 1 ms and 5 ms, respectively, have been found effective.

The performance of this coding system is remarkably good. Overall, the quality of CVSD at 32 kbps is about as good as for 64 kbps PCM. Standard data modems can support 32 kbps, so the transport mechanism is readily available for use on the PSTN.

CVSD Performance

We can analyze CVSD performance by comparing it with its cousin, linear DM. When the input frequency-amplitude product doesn't exceed:

$$(Af_{in})_{MAX} = \frac{f_s dV}{2\pi} \quad (\text{Eq 32})$$

where f_s is the bit rate, the two systems are the same. For single integration, the quantization noise power¹⁰ is:

$$\sigma^2 = \frac{2dV^2 f_{BW}}{3f_s} \quad (\text{Eq 33})$$

where f_{BW} is the system bandwidth. For a signal at the slope-overload threshold, the signal power is:

$$A_{MAX}^2 = \frac{1}{2} \left(\frac{f_s dV}{2\pi f_{in}} \right)^2 \quad (\text{Eq 34})$$

and the SNR is:

$$\begin{aligned} SNR_{MAX} &= \frac{A_{MAX}^2}{\sigma^2} \\ &= \frac{3f_s^3}{16\pi^2 f_{BW} f_{in}^2} \\ &\approx 10 \log \left(\frac{f_s^3}{f_{BW} f_{in}^2} \right) - 17.2 \text{ dB} \end{aligned} \quad (\text{Eq 35})$$

For our system with $f_s = 32$ kbps and $f_{BW} = 3$ kHz, Eqs 33 through 35 are used to plot SNR versus input amplitude for $f_{in} = 1$ kHz sine wave as Fig 9. Eq 35 predicts a maximum SNR of

23.2 dB. The curve shows that the SNR peaks at an input level near the middle of the DR. Above this level, slope overload degrades SNR because of distortion; below, quantization noise is responsible.

CVSD takes care of much of the slope-overload problems, and achieves a similar maximum SNR for voice signals. Note that in all DM systems, the maximum SNR degrades as the square of the input frequency, and with the *cube* of the bit time.

To get standard data modems to pass a more or less steady stream of bytes, we must switch off their data compression and error-correction functions. Both V.42 and MNP-5 error-correction standards are commonly used by today's V.34bis, 33.6 kbps modems. Both of these algorithms break the data into blocks, and the resulting intermittent output stream causes too many buffering headaches. In addition, the total end-to-end delay becomes objectionable. Without error-correction, the noise immunity of the audio-coding

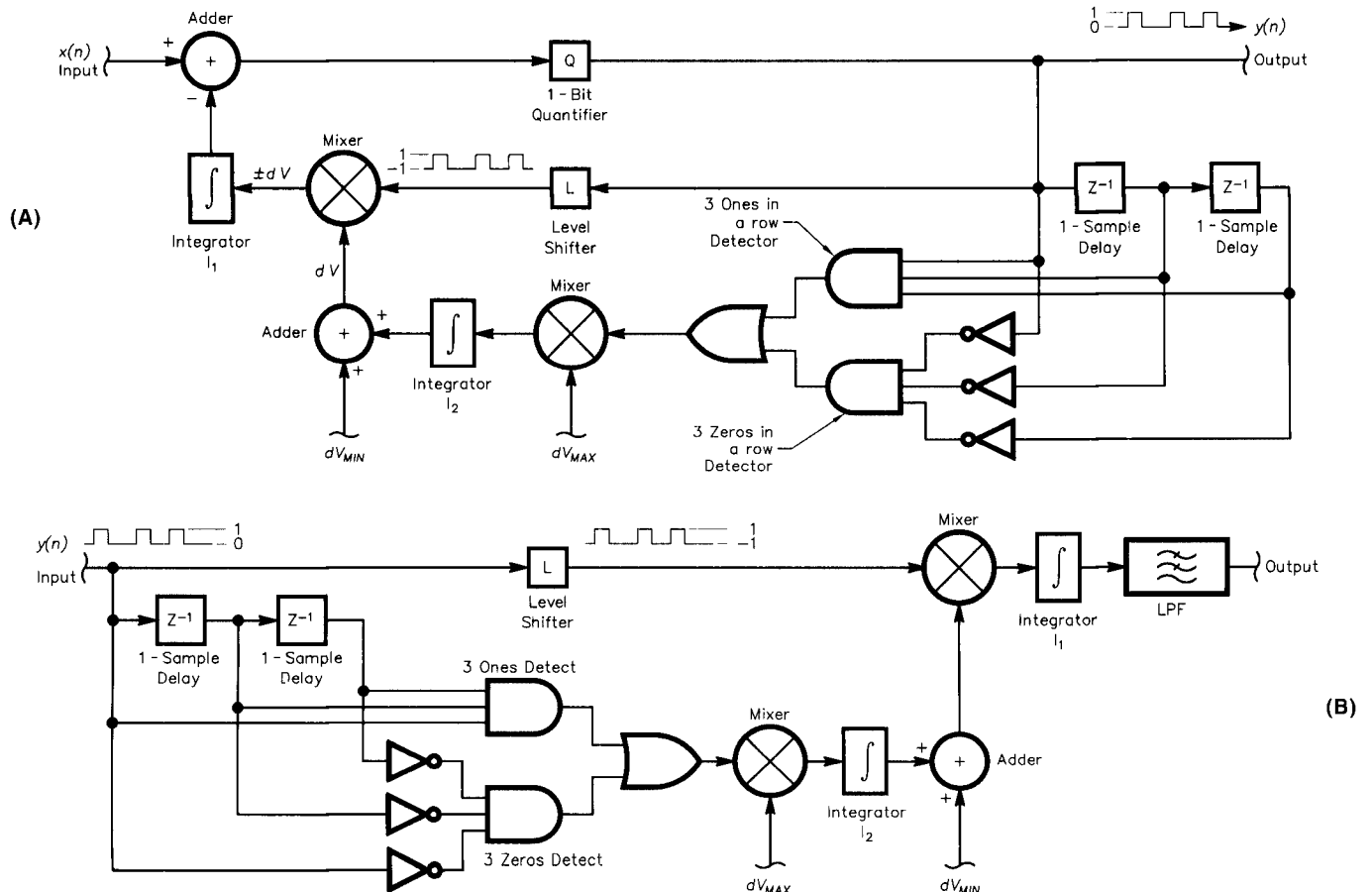


Fig 8—(A) a CVSD encoder block diagram. (B) a CVSD decoder block diagram.

scheme and that of the transceiver control protocol are of concern.

A mathematical analysis of CVSD performance in the presence of random bit errors isn't practical here. Fortunately, experiments have been performed in which subjective opinions were used to assess the perceived quality over the range of expected bit error rates (BERs).¹² On a scale from 1 to 5, listeners judged the quality of speech over BERs from 1×10^{-5} to 0.1. The scale represented the broad categories in Table 1.

Our goal of *toll quality* will be achieved with a score above four, whereas *communication quality* needs a score of at least three. This last term refers only to quality that in no way impairs intelligibility, not necessarily to good-quality audio.

In Fig 10, the results of opinion testing for the two compression methods we've discussed are plotted: μ -law PCM and CVSD. First, note that CVSD out-performs the other in the presence of errors. Second, it remains in the communications quality region until the BER rises to about 1%. This hardy performance makes CVSD an excellent choice where error-correction isn't possible.

Data Modem Performance on the PSTN

Back to the telephone company's traffic problems for a moment. Once the types of *differential quantization* such as the DM systems above were proven, "Ma Bell" decided she could double her traffic-handling capability by going to a 32 kbps system. A technique similar to CVSD called *adaptive differential pulse-code modulation* (ADPCM) was adopted as an international standard,¹³ and equipment that could be retrofitted to the existing system became available for use at tele-

phone switching centers. It's a lot less expensive to add a few boxes than to string a few thousand more miles of T1 lines! The voice quality with ADPCM remains excellent, but it ultimately limits the data rates of modems connected through it.

The new "56k" modems are capable of cross-loading information at 56 kbps, but to achieve these speeds, the bandwidth limitations of the central-office switches must be bypassed. An inherently digital line between the "uploader" and the central switch must be obtained. Because the "downloader" is still on the end of a regular telephone line, only speeds up to 33.6 kbps are possible in the other direction, and between two users without digital lines.

In fact, at my location in central Arizona, it's rare to achieve even a 33.6 kbps connection; more usually, 31.2 kbps is the best I can do. Occasionally during peak demand, the best connection possible is 26.4 kbps. This change in available connection quality occurs because the ADPCM equipment can adaptively alter its bit rate to provide greater-bandwidth connections during slack periods, and to lessen bandwidth during heavy usage to accommodate more calls. At 32 kbps, a T1 line can carry 48 calls; at 24 kbps, it'll handle 72. At 16 kbps, 96 simultaneous

calls are possible, but even the voice quality starts to suffer considerably at this rate. Very occasionally—especially right after school lets out—I encounter an "all circuits busy" message! So, I've discovered that 56k modems aren't always worth the investment.

As demand continues to increase, the telephone companies will be forced to add lines and equipment. Although recent rulings have eroded their status as "monopolies," they have been in the unique situation of providing a service, the cost of which isn't proportional to usage. I can make as many local calls as I want each month, and the bill won't change. At some point, this scenario may affect the service provider's profit, and something must give.

As the PSTN actually forms the backbone of the Internet, it makes sense for the telephone companies to become Internet service providers (ISPs) as well. Then we'll see all kinds of new equipment down at the central office and bandwidth galore! The traffic capacity of fiber-optic cable (and even twisted pairs) is inherently much greater than what's currently allowed. It's a good bet that, when phone companies can justify charging for it, the bandwidth will become available—even though it could have been there all along.

In our remote-control system, the control-data throughput rate is usually much less than that required for the digitized audio. So, we invent a byte-synchronous interleaving scheme that time-multiplexes the two data streams, and we accept the very slight degradation of audio quality. Off-the-shelf DSVD modems are optimized for the opposite situation: more data and just enough digitized audio to get communication quality. Our desire is for toll quality, which implies the type of DR and SNR we derived previously.

Table 1
Subjective Evaluation of Audio Quality versus BER

Score	Quality	Impairment
5	Excellent	Imperceptible
4	Good	Perceptible but not annoying
3	Fair	Slightly annoying
2	Poor	Annoying
1	Bad	Very annoying

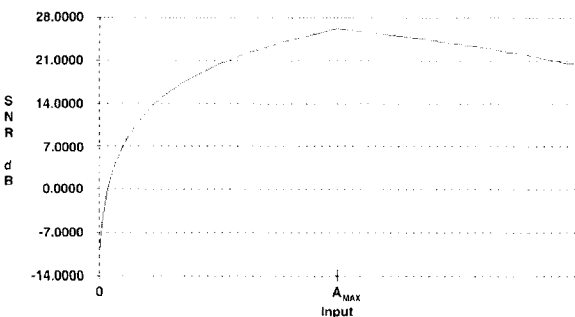


Fig 9—CVSD SNR-versus-input amplitude.

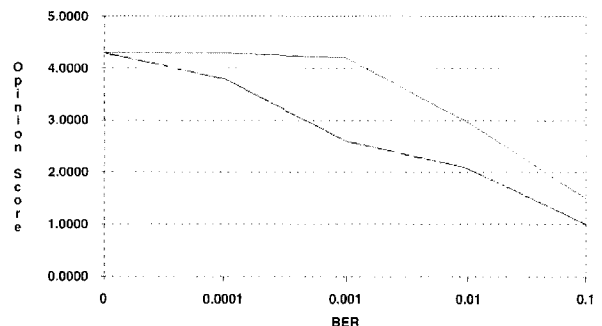


Fig 10—CVSD voice-quality score versus-BER.

Serial Remote-Control Protocols

As for the remote-control protocol, it's relatively easy to dream up byte sequences complex enough to achieve the required noise immunity. Command strings are sent from the serial port of the PC at the control point, multiplexed with any digitized audio, and transmitted to the remote site using the modem. After execution of the command, an acknowledgment is returned by the transceiver. This "handshake" is necessary to establish positive control.

Telemetry is continually passed from the transceiver to the control point using the same multiplexing method. The telemetry data indicate the received signal strength in receive mode, and the forward and reflected power in the transmit mode. Additional telemetry may be included to indicate the state of synthesizer lock, heat-sink temperature and other parameters.

Also, the byte-synchronous multiplexer can interleave control data for other devices at the remote site, such as antenna rotator controls. Over-the-air digital-mode operation of the transceiver is possible by locating the radio modem at the remote site, and interleaving the transmitted or received data into the bit stream.

Conclusion

Most of the technologies I've described in this article series are in current use by radio amateurs and others worldwide. I was motivated to write about them because the rate at which they're advancing is threatening to overcome our ability to keep up. At no point in the past have hams ever been in danger of falling behind the state of our art as much as we are today. While I believe this is true for other fields as well, it's especially true for electronics. I wish to emphasize that I *don't* believe hams will ever be very far behind the "power curve," because we're still mostly the ones pushing it forward.

Many thanks to Rudy Severns, N6LF; Bob Schetgen, KU7G, and the rest of the terrific staff of *QEX* for taking the time and having the patience to organize my ramblings into a harmonious whole. In addition, thanks to you many readers who have given me feedback. That's what it's all about!

Doug Smith, KF6DX/7, is an electrical engineer with 18 years experience designing HF transceivers, control systems and DSP hardware and software. He joined the amateur ranks in 1982 and has been involved in pioneering

work for transceiver remote-control and automatic link-establishment (ALE) systems. At Kachina Communications in central Arizona, he is currently exploring the state of the art in digital transceiver design and with this issue he becomes Editor of QEX! See Empirically Speaking for more information.

Notes

¹M. E. Frerking, *Digital Signal Processing in Communications Systems* (New York: Van Nostrand-Reinhold, 1993).

²A. V. Oppenheim and R. W. Schaffer, *Digital Signal Processing* (Englewood Cliffs: Prentice-Hall, 1975).

³D. Smith, "Signals, Samples and Stuff: A DSP Tutorial (Part 3)," *QEX*, July/August, 1998, pp 13-27.

⁴B. Widrow and S. D. Stearns, *Adaptive Signal Processing* (Englewood Cliffs: Prentice-Hall, 1985).

⁵E. Tenner, *Why Things Bite Back: Technology and the Revenge of Unintended Consequences* (New York: Alfred A. Knopf, 1996).

⁶S. M. Shinnars, *Modern Control System Theory and Application* (Reading, Massachusetts: Addison-Wesley, 1973).

⁷D. Smith, "Signals, Samples and Stuff: A DSP Tutorial (Part 2)," *QEX*, May/June 1998, pp 22-37.

⁸Part 47 CFR 97.7 and 97.109 (Washington: US Government Printing Office, 1997).

⁹N. J. Muller, *T-Carrier Compression: Adaptive Differential Pulse Code Modulation*, Strategic Information Resources, 1995; URL www.ddx.com.

¹⁰H. P. Westman, Ed., *Reference Data For Radio Engineers*, fifth edition (Indianapolis: Howard W. Sams & Co., 1968).

¹¹J. A. Greefkes and K. Riemens, "Code Modulation with Digitally Controlled Companding for Speech Transmission," *Philips Technical Review*, 1970.

¹²N. S. Jayant and P. Noll, *Digital Coding of Waveforms: Principles and Applications to Speech and Video* (Englewood Cliffs: Prentice-Hall, 1984).

¹³G.721: *Adaptive Differential Pulse Code Modulation*, International Telecommunications Union, Geneva, Switzerland, 1984. □□

DSP

Without Tears 

Multimedia Interactive CD-ROM Sale

Buy Before July, 4th 1998

Get all three CDs for \$999

This Could Be Your Last Chance!

Call Z Domain Technologies 1-800-967-5034 or 770-587-4812.

Hours: 9 - 5 EST. Or E-mail dsp@zdt.com

Ask for our CD sales price info, a free demo CD-ROM.

We also have live 3-day seminars: DSP Without Tears, Advanced DSP With a few Tears & Digital-Communications Without Tears.

<http://www.zdt.com/~dsp>

A Faster and Better ADC for the DDC-Based Receiver

A new ADC IC lets the DDC-based receiver tune from 200 kHz to 22 MHz in one tuning range.

By Peter Traneus Anderson, KC1HR

The AD6640 is the latest RF analog-to-digital converter (ADC) from Analog Devices.¹ With this converter, I doubled the ADC and DDC sample rate to 50 MSPS (million samples per second), permitting coverage from 200 kHz to 22 MHz in one band. This includes all amateur bands 160 through 15 meters, and all broadcast bands 600 through 13 meters. By changing one RF transformer, the low end can be pushed down to 20 kHz.

The AD6640 is essentially a faster AD9042 in a cheaper plastic package. It is rated for 80 dB SFDR (spurious-

free dynamic range) at 65 MSPS (90 dB SFDR with dither). The AD6640 is so new that, in August 1997, I could purchase one only on an evaluation board. Thus, this design is based on the Analog Devices AD6640ST/PCB evaluation board for the AD6640. The production part number for the ADC alone, is AD6640AST. The evaluation board (my board is serial number 8) has an AD6640XST. The "X" indicates a preproduction part.

The New Circuit

Fig 1 shows the new front end. The remainder of the receiver hardware is diagrammed in my previous *QEX* article.² Parts with identifier numbers above 100 (such as T102, U103) are located on the Analog Devices AD6640 evaluation board. The filters (FL1 and

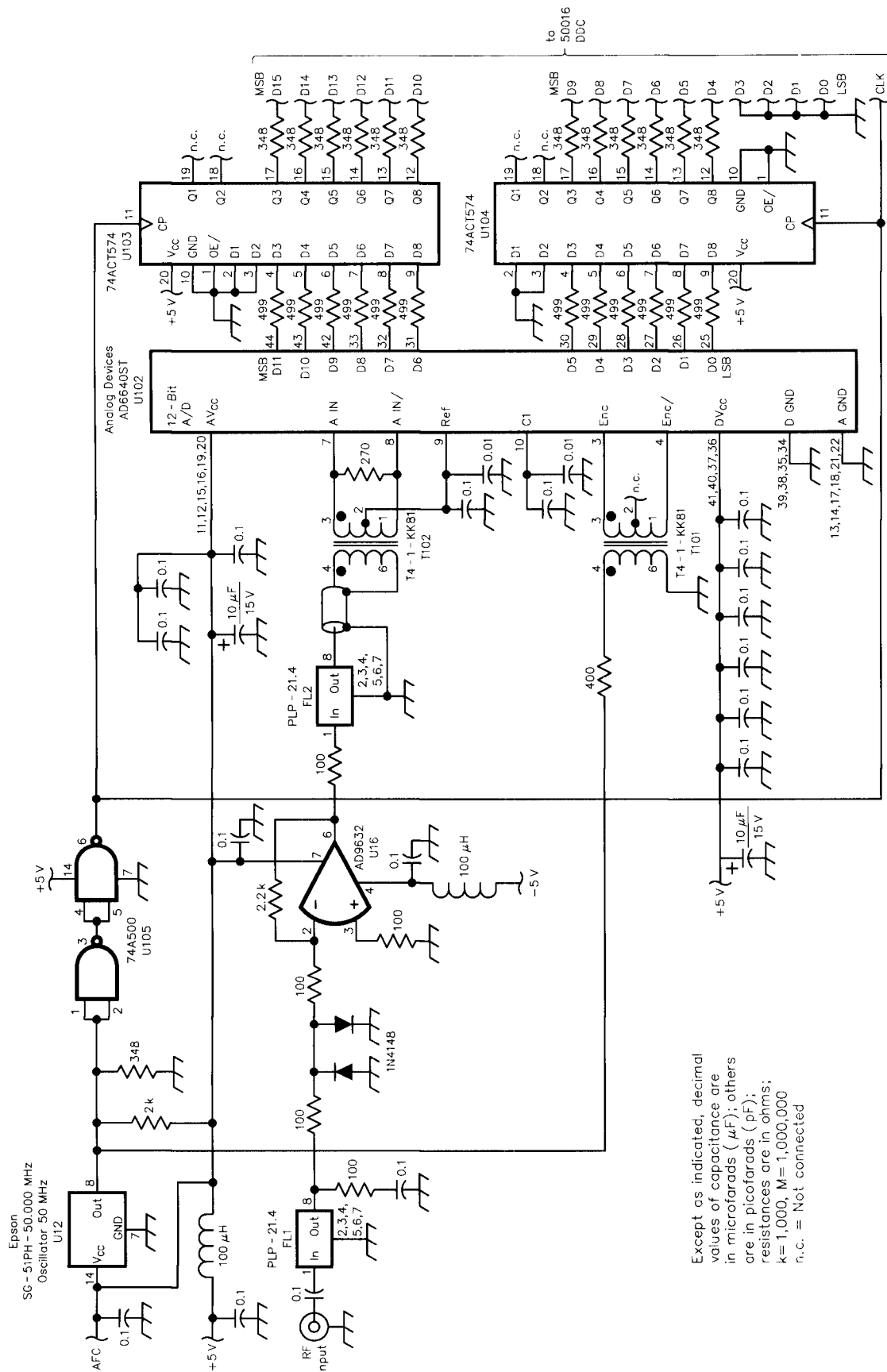
FL2) and the RF transformers (T101 and T102) are from Mini-Circuits Labs.³

The input RF signal first goes through low-pass filter FL1, which passes frequencies up to 22 MHz. Then the signal passes through op amp U16, which provides a gain of three going into FL2. The signal then goes through FL2 and T102 to the AD6640 analog input. The AD6640 has a differential input, with a full-scale range of 1 V (P-P), 350 mV (RMS).

T102 limits the low-frequency response for signals below 200 kHz. Changing T102 to a T4-6T-KK81 should lower the low-frequency limit to 20 kHz.

The 50-MHz clock oscillator, U12, is the same one that I used in my earlier article.² The associated divide-by-two

¹Notes appear on page 32.



Except as indicated, decimal values of capacitance are in microfarads (μF); others are in picofarads (pF); resistances are in ohms; k=1,000, M=1,000,000 n.c. = Not connected

Fig 1—Band-pass filter, preamplifier and ADC converter. This front end covers 200 kHz to 22 MHz in one band. To extend the low-frequency response to 20 kHz, replace T102 with a Mini-Circuits Labs T4-6T-KK81 (see Note 3). All part numbers above 100 mount on the Analog Devices AD6640 evaluation board.

flip-flop has been removed. The oscillator output drives transformer T101 and NAND gate U105. T101 provides the differential-encode signal needed by the AD6640. U105 delays and buffers the clock to U103, U104 and the DDC.

The digital outputs of the AD6640 go through 499-Ω resistors to the inputs of the D registers of U103 and U104. The resistors, according to the AD6640 data sheet, reduce the current spikes on the AD6640 outputs, to reduce the noise induced on the AD6640 analog input.

The outputs of U103 and U104 go through 348-Ω resistors to the data inputs of the DDC. The resistors, part of the evaluation board, reduce current spikes at the expense of making the propagation time to the DDC just barely fast enough.

I initially built a discrete oscillator running at 52 MHz, to run the DDC at its maximum rated speed, but I kept the clock oscillator (50 MHz) for simplicity. Also, the propagation delays from U103 and U104 to the DDC are marginally fast enough to satisfy the DDC setup-time specifications. I decided the added nanosecond (20 ns period instead of 19 ns) was worth accepting lessened alias rejection in FL1 and FL2.

Construction

Anyone building these circuits should start by checking parts availability. Most of this receiver was built in 1993, using mostly junk-box parts, so some of the parts are obsolete. The only part that is irreplaceable is the HSP50016. There are exact or functional equivalents (or improvements) in production for all other parts in the receiver.

The control software (modified for the 50 MHz clock and a simpler user interface) is available from the ARRL BBS.⁴ (The transmit VFO (DDS) code is absent because I removed the DDS to make room for the evaluation board.) This software provides bandwidths of 1709, 855, 427 and 214 Hz for CW reception, 1709 Hz for USB and LSB reception and 6836 Hz for DSB and synchronous AM reception. The 107 Hz bandwidth is no longer available, due to the doubled clock frequency to the DDC.

A User Interface

The next step in this project would be to develop a control panel for the receiver. The PC software works, but

PCs are expensive and generate EMI. At frequencies above 12 MHz or so, the antenna picks up the data transmissions from the PC to the receiver. Jean-Pierre Mallet, F5MI, has developed a microcontroller-based control panel for this receiver using a numeric keypad and alphanumeric display.⁵

The control panel is actually more difficult and more complex to design than the receiver proper. As soon as a computer or microcontroller is added to a project, most of the development time for the project will be devoted to the care and feeding of the controller and its interfaces, including the user interface.

One time-consuming issue is designing the user interface. How should the tuning controls work? Sometimes large frequency steps are needed, sometimes small steps. How should the step size be set, so the interface is easy-to-use and not diabolically aggravating? Should a direct-entry keypad be included? Should there be memories? The temptation is to keep adding complexity until the user can't remember how to use it. After all, it's "only software."

My intent has been to keep it simple, and as much like a traditional analog receiver as possible, so this receiver can be used and judged as a receiver rather than as a computer peripheral. My current thinking is to have four knobs, each a detented shaft encoder: Gain, Bandwidth/Mode, Frequency step and Frequency. An alphanumeric display would show the current settings at all times. An optional numeric keypad would permit direct entry of frequency. The control software mentioned above simulates the future knobs using pairs of keys on the PC keyboard for up/down inputs.

Other New Hardware?

The next step in hardware development is difficult: ADCs will keep getting better.⁶ However, the HSP50016 is the best DDC available.

Newer DDCs from Harris and Analog Devices are worse for this application than the HSP50016. The volume application for such chips is cell-phone base stations, where 80 dB of SFDR is plenty; there is no requirement for a noise floor below the SFDR; and the receiver output goes to a data demodulator.

The HSP50016 is rated for an SFDR of 102 dB. In this receiver, that is barely enough (this is why the bandwidths are

in 2:1 ratios). Luckily, the HSP50016 can output 32 or 38 bits of result, pushing its noise floor well below its SFDR. Newer DDCs have only 16-bit outputs because they do not attempt to push the noise floor below the SFDR.

A good DDC for HF radios would clock at 75 to 100 MSPS and have an SFDR and noise floor of 150 to 200 dB. When digital HF radios go into production, they will have DDCs built especially for HF service.

To give an extreme example, suppose we are receiving a weak CCW (coherent CW) signal using an effective filter bandwidth of 9 Hz. The signal-to-noise process gain is 25 MHz / 9 Hz = 3,000,000 = 64 dB. The AD6640 noise floor is 67 dB below full scale. When we add in the process gain, we get 131 dB of signal-to-noise dynamic range.

For a better DDC (and for a DUC for transmitting), we must make our own using CPLDs, FPGAs or ASICs. Are there any DSPers out there who want to get into hardware design?

Mission Accomplished

With the AD6640 ADC, the DDC-based receiver is fully using the capabilities of the HSP50016 DDC. The received frequency is tunable from 200 kHz to 22 MHz in one band. By changing one RF transformer, the low end can be pushed down to 20 kHz.

Notes

¹Analog Devices, One Technology Way, PO Box 9106, Norwood, MA 02062-9106, tel 617-329-4700; URL <http://www.analog.com>.

²P. T. Anderson, KC1HR, "A Simple Synchronous-AM Demodulator and Complete Schematics for the DDC-Based Receiver," *QEX*, Sep 1997, pp 3-14.

³Mini-Circuits Labs, PO Box 350166, Brooklyn, NY 11235-0003; tel 718-934-4500; URL <http://www.minicircuits.com>.

⁴You can download this package from the ARRL "Hiram" BBS (tel 860-594-0306), or the ARRL Internet ftp site: [oak.oakland.edu](ftp://oak.oakland.edu) (in the [pub/hamradio/arrl/qex](ftp://pub/hamradio/arrl/qex) directory). In either case, look for the file [ANDADC.ZIP](ftp://ANDADC.ZIP).

⁵Jean-Pierre Mallet, F5MI, "Introduction a la radio numerique," *Premiere partie: Radio REF*, Nov 1996, pp 17-22, *Seconde et derniere partie: Radio REF*, Dec 1996 pp. 19-24.

⁶A new manufacturer has entered the ADC market: Lucent Technology (<http://www.lucent.com/micro>) has just announced the CSP1152A, a 14 bit, 65 MSPS ADC with built-in dither, giving 95 dB SFDR.



Low-Noise Front-End Design with ARRL Radio Designer Example: a 23-cm Preamp

Have you tried the ARRL Radio Designer software? Here's a good example to get you started with a working project.

By John Brown, G3DVV

The ARRL Radio Designer program opens the door to finding out how circuits are going to behave before building them.¹ For me, this is the greatest step in Amateur Radio since I picked up a soldering iron. The program does even more than that: move on to Chapter 12 in the manual and reach another high.

¹Notes appear on page 36.

Boulters Barn Cottage
Churchill Rd
Chipping Norton
Oxfordshire OX7 5UT
England
e-mail John.Brown@g3dvv.demon.co.uk

The design of a low-noise front-end RF amplifier stage becomes possible, all without hassle.

The object of this exercise is a low-noise, medium-gain masthead amplifier for the 23-cm band. If you already have a number of possibilities in mind, either from articles seen or comments over the air, there remain three questions to be answered:

- Is the transistor readily available?
- Is a detailed data sheet available?
- What is your credit-card limit?

A detailed data sheet must show the impedance matching required for low-noise performance. You cannot simply plug a transistor into any circuit and expect good results: The device must

be properly noise matched. I chose an AT10135 because it has a very low noise factor and a reasonable price. Fortunately I found a couple in my junk box hiding under an 807 (*an interesting place to store your low-noise transistors.*—Ed.)

Stability

First, consider whether the device is stable at 23 cm. It is a sure bet it is not! Once upon a time, the figures had to be entered into Rollet's formula (you were lucky if you did not make an arithmetical error) to see if the answer was greater than 1. A computer program like Hewlett-Packard's *AppCad* can do the number crunching, but

better still, you can now use *Radio Designer*.

Start the program, go into Circuit Editor and note that the only component in Netlist 1 is the FET, as shown in Fig 1. Netlist 1 is based on this and the drawing below. (The Netlists are in Appendix A, and also available for download. See Note 2.—*Ed.*) Note that some of the lines are starred out (stars indicate comments in *Radio Designer* Netlists.—*Ed.*) as they will be used after the stability check has been completed.

Computer Problems

The scattering parameters for the AT10135 are copied from the AVANTEK.FLP file. I had a problem here: A red flag kept coming up on the monitor saying, "Stop. Memory Overflow" and all that jazz. This was overcome by going into the file manager and dragging the AvanteK file into Word for Windows. (Any editor would do.—*Ed.*) In Word, I copied the '10135 data and pasted it into the netlist with *ARRL Radio Designer* running. I keyed in the noise figures manually. Alternatively, I could have upgraded my computer's memory.

K Stands for Stability

Using Netlist 1, hit the Analyze button, then enter the Report Editor, click on the function that shows frequency and change this to K. Click on "Add Trace" and then "Display." The line on the graph is way below 1, exactly as I feared. Somehow, I must increase K to make it greater than or equal to one.

Stabilization

There are four ways of stabilizing FETs and BJTs: The first two are intentional impedance mismatching and negative feedback. These options are excluded by the KISS principle (Keep It Simple, Stupid). The other two remedies are a ferrite bead slipped over one of the leads and added resistance (series or parallel) in the input or output leads. The ferrite-bead approach is hardly practical with small components and SMDs so proceed by using resistors. If a resistor is put in the input, the noise factor is degraded. A series resistor in the output is preferred. This is simple and keeps the component count down. Using the Circuit Editor try a number of resistors until $K > 1$. The netlist will therefore require amendment. Remove the

star from the line starting "RES" and amend the following line to read "A:2POR 1 3." The schematic should now look like Fig 2. Try various standard resistance values in the netlist until K exceeds one. Start with say $R = 22 \Omega$ and continue upward. I found $R = 68 \Omega$ to be satisfactory.

This method of stabilization does not always work. Some transistors are so fiery that nothing can tame them at the chosen frequency. A shunt resistor across the output gives a wider range of control, but as a rule, it is a better idea to look for a different transistor.

Think Smith Chart

Analyze the new circuit (Netlist 2), which is just the FET and the resistor, and then click on the Utilities window and select Circles. Enter "s" to give you the basic lines of a Smith Chart. If you now enter S1 and S2, two pretty blue circles appear just outside the circumference of the Smith Chart. This is just what the doctor ordered; the device is 100% stable at 1.3 GHz as indicated by the circles being outside the perimeter of the chart.

To avoid the chart becoming clut-

tered with lines, enter "CLR." This wipes out everything and "s" will have to be entered again. If you prefer delete the last entry by using the command, "DEL 1" (increase the "1" to delete more than the last entry).

Now enter "GMAX" and note the reading (17.97 dB). Next enter "N 0" to obtain the optimum noise figure and note this (0.5058 dB). These points appear to be invisible on the chart so enter slightly lesser values, eg "G1 17" and "N 0.55." The gain circle has a yellow circumference and the noise circle has a purple circumference. Unfortunately, the two circles are separated, and they need to touch. Entering "G1 16" brings the circles nearer. Several tries show that with a gain of 15.5, the two circles just touch. The FET should therefore have a gain of 15.5 dB and a noise figure of 0.55 dB provided the impedance matching is correct.

Impedance Matching

Enter "RHO." You will be asked to mark a point. Move the cursor to the coincidence of the two circles. It is a little difficult to click the left mouse button without moving the cursor, so

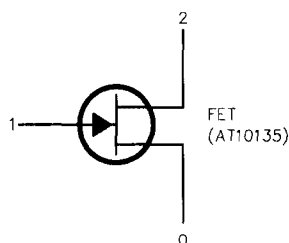


Fig 1—Netlist 1 initial schematic.

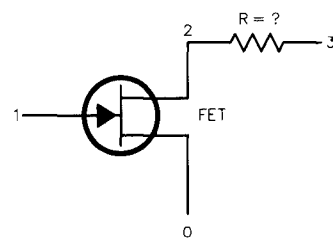


Fig 2—Install a series connected drain resistor to achieve $K > 1$.

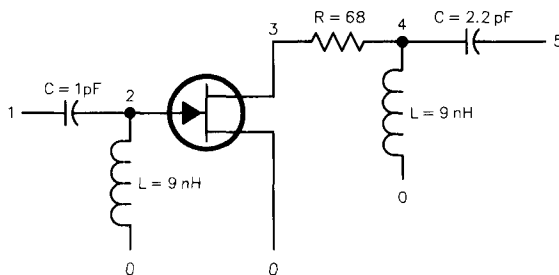


Fig 3—Complete circuit with standard values.

press "M" instead. Up comes the reading in polar coordinates: approximately 0.76 at an angle of 36°. Enter "Y" to obtain the admittance reading, which is approximately 0.15 -j0.32. Note the real part and draw in the conductance line by entering "G 0.15." This draws a green circle through RHO.

Rules of the Game

The object of the next exercise is to match the center point of the chart, which represents 50 Ω, to the RHO point. There are a number of alternatives on offer but for 23 cm, lumped constants (as opposed to microstrip line) will be used for matching.

Rule 1: You are only allowed to move the cursor along red or green lines.

Rule 2: If you move clockwise along a red line, you are calculating a series inductance. Moving ccw calculates a series capacitor.

Rule 3: If you move clockwise along a green line you are calculating a parallel capacitor, and ccw gives you a parallel inductance.

Rule 4: You must start at the center of the chart.

Matching the Input

Enter "DX" (I am not talking about clusters). You are asked to mark the first point. Press "C"; this marks the center of the chart, and then you are asked for the next point. This is where the red line going ccw meets the green line. Move the cursor to this point and press "M." Up pops the value of the capacitor: around 1.06 pF. Next enter "DB," mark the intersection and move the cursor ccw to RHO and again hit "M." This gives a value in the region of 8.94 nH. If you have ever struggled to obtain correct readings on a physical Smith Chart using a straight edge and a compass, this modern way is a delight.

If Smith Charts and matching is a little baffling, treat yourself to a copy of *RF Circuit Design* by Chris Bowick: an excellent book on the subject. Refer also to the Circles chapter in the ARRL *Radio Designer* manual.

Matching the Output

You may want to "CLR" the chart to remove some of the clutter and then reinstate the noise and input gain circles. Remembering that the gain is 15.5 dB, enter "G1B 15.5" and "RHOL 15.5." You will be asked to mark a point. Mark the intersection of the input gain and noise circle. Exercise a little care as you have already selected this point

as RHO S. Check from the narrative that you have the same figures. Note that a new marker has appeared on the output gain circle. This circle has a dashed-yellow circumference. The new marker is the output RHO and must be matched to the center of the chart. Enter "Y," move the cursor to RHOL (the new marker) and press "M." This gives the admittance reading. Note the real part only (1.2). Enter "G 1.2." A green circle now goes through RHOL.

The rules for matching the input also apply for output matching. Hit "DX" followed by "C." Then go ccw to where the red line intersects the green line and mark the intersection. Up comes the value for the series capacitor, 2.33 pF. Enter "DB," mark the intersection, go ccw to RHOL, and press "M." This gives the value of the parallel coil (9.12 nH). That is all we need to know.

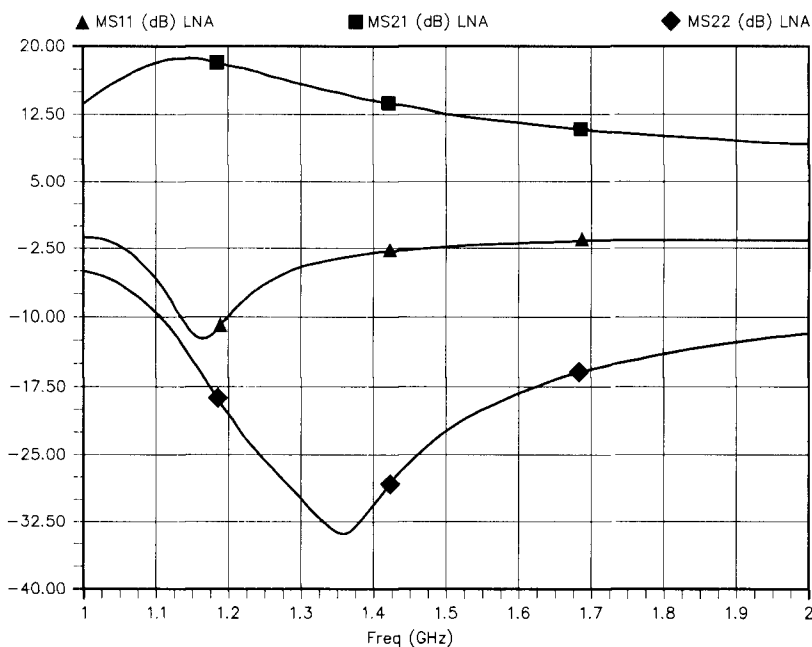


Fig 4—A plot of input return loss (MS11), output return loss (MS22) and gain (MS21) versus frequency.

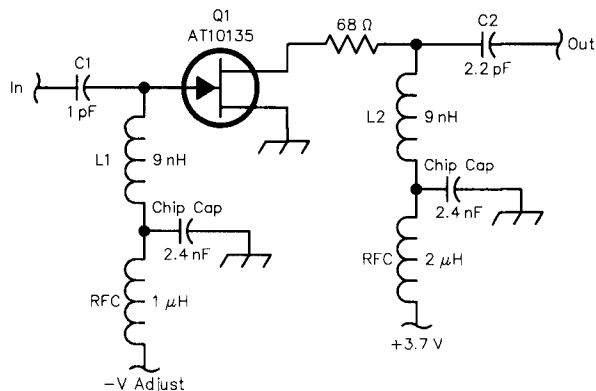


Fig 5—Completed circuit with connections for power.

The Final Circuit

The circuit to be entered into the Circuit Editor and analyzed is shown in Fig 3. See Netlist 3 in the Appendix.

The calculated values are not standard however, and Netlist 3 only shows standard values. There is also the point that good quality capacitors, ie porcelain ATC chips, must be used. However, there can be a spread in values, and the problem can be met by using a variable capacitor. A ham is not a ham if without something to adjust for peak performance, and variable capacitors may enable a better noise figure to be obtained.

After entering the Netlist (the Q figures shown have been plucked out of thin air), analyze it and bring up the Report Editor. Click on the Freq slot, enter MS11, Add Trace, click on MS21, Add Trace and finally click on MS22, Add Trace and Display. The graph in Fig 4 shows the performance in a nutshell.

Scatter Parameters

So what is MS11 etc (read as "magnitude of scatter parameter S sub one-one")? It is scatter-speak for input reflection loss. MS 21 is scatter-speak for gain, and MS22 is the output reflection coefficient. These reflection coefficients should be the most-negative values possible. A large return loss means that only a small portion of the signal is being reflected; there is, therefore, a good match, a low SWR. Chapter 6 of the *ARRL UHF/Microwave Experimenter's Manual* explains all this.³

The graphs show MS11 = -5 dB, MS21 = 15.5 dB and MS22 = -30 dB. Go back to the Report Editor, click on Freq and press "N" on the keyboard. This brings up NF (Noise Factor). Click on it, Add Trace and Display. The graph shows approximately 0.55 dB.

MS11 only gives a return loss of -5 dB at the required frequency of 1296 MHz. This indicates a moderately large SWR in the front end, which leads to increased losses. There appears to be no way of improving the match without the NF going down the chute. The poor SWR occurs because we chose to match for optimum noise rather than maximum gain. In fact, an optimum-noise match is really an impedance mismatch. This explains why it is a good idea to keep front-end losses as low as possible.

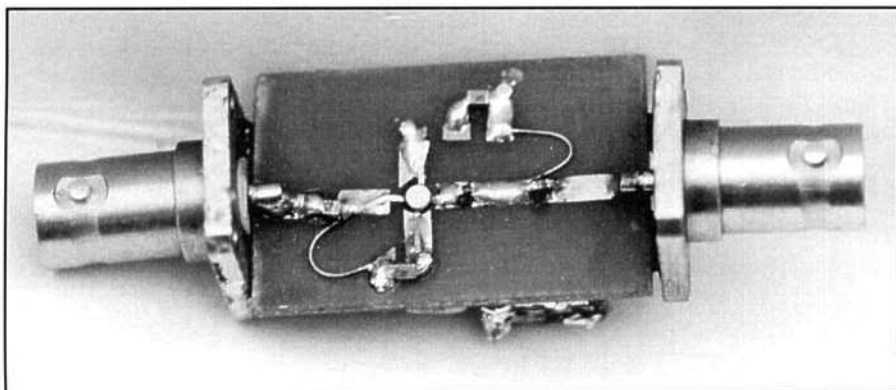


Fig 6—A photo of the completed amplifier. The RFCs and power supply are on the back of the board.

The Construction Department

The next step is to build a prototype (or more correctly, a lash-up). The final RF circuit is shown in Fig 5, which includes connections for dc power.

I used a small piece of 1/16-inch double-plated epoxy fiberglass PCB (as in Fig 6), drew in the tracks with etch-resist ink and etched the board. I soldered BNC sockets to each end, then installed the pin-mounted components, two pieces of wire as L1 and L2 (each wire is 0.64 inches long, #28 AWG enameled wire bent in a loop). Next install the SMDs—this is easier said than done—and they do not like much heat. Finally, solder in the FET. The usual precautions for avoiding electrostatic charges apply here; although I must say, I have not had any failures in this department to date (touch wood). The dc supply is mounted on the plain side of the board.

Plug in the supply, switch on the power and take some readings. First a word of warning: the figures calculated are theoretical and not easily obtainable in practice. In fact, the gain of my circuit measured 11 dB and the noise factor as 1.1 dB. Okay, that's not as good as calculated, but a step in the right direction. The main problem lies in the front-end losses caused by the high input SWR, but a more suitable dielectric for the PCB and more accurate component values would improve the figures, as would correctly photo-etched lines together with SMA sockets. I noticed that placing a metal sheet under the PCB improved the NF by a fraction, so a boxed enclosure is required.

Conclusion

Well, that's it. Once upon a time, the calculations were manipulated manually with matrix algebra and much juggling of scatter and ABCD parameters. All that has been bypassed, and in addition, the whole circuit can be simulated before building.

Acknowledgments

To Mr. Phillip Smith, Compact Software and the *ARRL Radio Designer*, thank you.

Notes

¹ARRL *Radio Designer* Ver 1.5 (for Windows 3.1 and later) is ARRL Order #6796. ARRL publications are available from your local ARRL dealer or directly from the ARRL. Mail orders to Publication Sales Dept, ARRL, 225 Main St, Newington, CT 06111-1494. You can call us toll-free at tel 888-277-5289; fax your order to 860-594-0303; or send e-mail to pubsales@arrl.org. Check out the full ARRL publications line on the World Wide Web at <http://www.arrl.org/catalog>.

²You can download this package from the ARRL "Hiram" BBS (tel 860-594-0306), or the ARRL Internet ftp site: [oak.oakland.edu](ftp://oak.oakland.edu/pub/hamradio/arrl/qex) (in the [pub/hamradio/arrl/qex](ftp://pub/hamradio/arrl/qex) directory). In either case, look for the file G3DVV.ZIP.

³The *ARRL UHF/Microwave Projects Manual*, Vol 1 (Newington: ARRL, 1994, ARRL Order No #4491). See Note 1 for purchasing information.

John was first licensed in 1947. He is a Chartered Accountant by profession, but now retired. Sometime Honorary Treasurer of the RSGB. He's never happier than when holding a soldering iron or a pint of beer.

Appendix A**Netlists 1 through 3***** NETLIST 1 Save as 23cmsA.ckt.**

*Check for stability.

*Using FET AT10135

BLK

TWO 1 2 0 q

*RES 2 3 R=68

LNA:2POR 1 2

END

FREQ

*1.3GHZ

ESTP 1GHZ 2GHZ 300

END

DATA

q: s

*AV068 AVANTEK AT10135N V=2v, I = 25mA

0.5GHZ	.98	-18	5.32	163	.020	78	.35	-9
1.0GHZ	.93	-33	5.19	147	.038	67	.36	-19
2.0GHZ	.79	-66	4.64	113	.074	59	.30	-31
3.0GHZ	.64	-94	4.07	87	.110	44	.27	-42
4.0GHZ	.54	-120	3.60	61	.137	31	.22	-49
5.0GHZ	.47	-155	3.20	37	.167	13	.16	-54
6.0GHZ	.45	162	2.88	13	.193	-2	.08	-17
7.0GHZ	.50	120	2.51	-10	.203	-19	.16	45
8.0GHZ	.60	87	2.09	-32	.210	-36	.32	48
9.0GHZ	.68	61	1.75	-51	.209	-46	.44	38
10.0GHZ	.73	42	1.52	-66	.207	-58	.51	34
11.0GHZ	.77	26	1.26	-82	.205	-73	.54	27
12.0GHZ	.80	14	1.12	-97	.200	-82	.54	15

NOI RN

1GHZ .4 .85 24 .7

2GHZ .4 .7 47 .46

4GHZ .5 .39 126 .36

6GHZ .8 .36 -170 .12

8GHZ 1.1 .45 -100 .38

END

***NETLIST 2. Save as 23cmsB.ckt**

*Input and Output matching

*10135 preamp at 23 cms

BLK

TWO 1 2 0 q

RES 2 3 R=68

LNA:2POR 1 3

END

FREQ

1.3GHZ

*ESTP .5GHZ 12GHZ 300

END

DATA

q: s

*AV068 AVANTEK AT10135N V=2v, I = 25mA

0.5GHZ	.98	-18	5.32	163	.020	78	.35	-9
1.0GHZ	.93	-33	5.19	147	.038	67	.36	-19
2.0GHZ	.79	-66	4.64	113	.074	59	.30	-31
3.0GHZ	.64	-94	4.07	87	.110	44	.27	-42
4.0GHZ	.54	-120	3.60	61	.137	31	.22	-49
5.0GHZ	.47	-155	3.20	37	.167	13	.16	-54
6.0GHZ	.45	162	2.88	13	.193	-2	.08	-17
7.0GHZ	.50	120	2.51	-10	.203	-19	.16	45
8.0GHZ	.60	87	2.09	-32	.210	-36	.32	48
9.0GHZ	.68	61	1.75	-51	.209	-46	.44	38
10.0GHZ	.73	42	1.52	-66	.207	-58	.51	34
11.0GHZ	.77	26	1.26	-82	.205	-73	.54	27
12.0GHZ	.80	14	1.12	-97	.200	-82	.54	15

NOI RN

1GHZ .4 .85 24 .7
 2GHZ .4 .7 47 .46
 4GHZ .5 .39 126 .36
 6GHZ .8 .36 -170 .12
 8GHZ 1.1 .45 -100 .38
 END

***NETLIST 3.**

* Save as 23cmsC.ckt
 * Examine preamp performance

BLK
 IND 2 0 L=9NH Q=100
 CAP 1 2 C=1Pf Q=200
 TWO 2 3 0 q
 RES 3 4 R=68
 IND 4 0 L=9NH Q=100
 CAP 4 5 C=2.2PF Q=200
 LNA:2POR 1 5

END
 FREQ
 * 1.3GHZ
 ESTP 1GHZ 2GHZ 300

END
 DATA

q: s
 *AV068 AVANTEK AT10135N V=2v, I = 25mA

0.5GHZ	.98	-18	5.32	163	.020	78	.35	-9
1.0GHZ	.93	-33	5.19	147	.038	67	.36	-19
2.0GHZ	.79	-66	4.64	113	.074	59	.30	-31
3.0GHZ	.64	-94	4.07	87	.110	44	.27	-42
4.0GHZ	.54	-120	3.60	61	.137	31	.22	-49
5.0GHZ	.47	-155	3.20	37	.167	13	.16	-54
6.0GHZ	.45	162	2.88	13	.193	-2	.08	-17
7.0GHZ	.50	120	2.51	-10	.203	-19	.16	45
8.0GHZ	.60	87	2.09	-32	.210	-36	.32	48
9.0GHZ	.68	61	1.75	-51	.209	-46	.44	38
10.0GHZ	.73	42	1.52	-66	.207	-58	.51	34
11.0GHZ	.77	26	1.26	-82	.205	-73	.54	27
12.0GHZ	.80	14	1.12	-97	.200	-82	.54	15

NOI RN
 1GHZ .4 .85 24 .7
 2GHZ .4 .7 47 .46
 4GHZ .5 .39 126 .36
 6GHZ .8 .36 -170 .12
 8GHZ 1.1 .45 -100 .38
 END



QEX Subscription Order Card

American Radio Relay League • 225 Main Street • Newington, CT 06111-1494 • USA
 QEX, the Forum for Communications Experimenters, is available at the rates shown below.

For one year (6 bi-monthly issues)
 of QEX, ARRL Member* rates:

Subscribe toll-free with your credit card
1-888-277-5289

In the US, \$18.00

Renewal New Subscription

In Canada, Mexico and US by
 First Class mail, \$31.00

Name _____ Call _____

Elsewhere by Surface Mail
 (4-8 week delivery) \$23.00

Address _____

Elsewhere by Airmail \$51.00

City _____ State or Province _____ Postal Code _____

Payment Enclosed Charge:

*Non-members add \$12 to these rates

Remittance must be in US
 funds and checks must be
 drawn on a bank in the US.
 Prices subject to change
 without notice.

Account # _____

Good thru _____ Signature _____

4/98 QX

A Remote Bandswitch for the “Bug Catcher”

Build a simple device that allows instant QSYs with the “Bug Catcher” and similar exposed-coil mobile antennas.

By Paul I. Protas, WA5ABR

After getting in and out of my car several times to change bands with the Bug Catcher I had borrowed from WD5CAY, I thought it would be nice to be able to change bands remotely. The resulting device works quite well and does not seem to deteriorate the performance of the antenna. I have not, however, tested it for long-term durability or weather extremes.

The device is divided into two parts: a switch device in the vehicle and the relay board that is attached to the Bug Catcher coil. The circuit is very straightforward as can be seen from the schematic in Fig 1. The mechanical con-

siderations are more difficult than the electrical circuitry. The capacitors were used only to bypass any stray RF that might activate the relays.

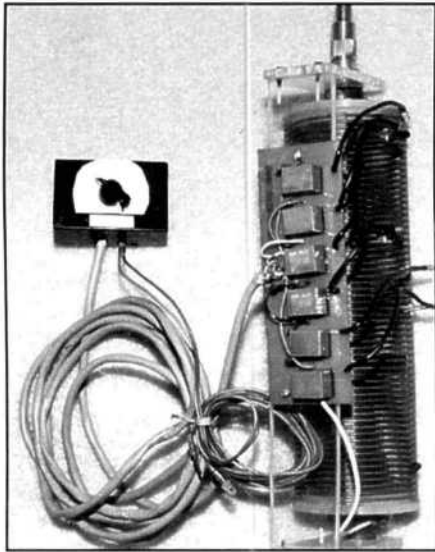
To begin construction, cut a PC board to 2 $\frac{1}{4}$ ×6 $\frac{1}{4}$ inches. Then mark, etch and drill the circuit board to specifications. Use $\frac{1}{8}$ -inch bits for large wire holes (the six clip leads and the clip lead from the Bug Catcher). Make the relay holes a little larger than actually needed (about $\frac{1}{16}$ inch) to compensate for error and make sure the relays fit flush against the board. The holes for the capacitors and other leads can be $\frac{1}{32}$ inch.

The relays will only fit on the board one way. Looking at the board from the foil side, the six separate strips of foil with a hole in each end should be on your left. (See Fig 2.) Holding a relay

with the bottom facing you, the three in-line pins should be at the top. These will correspond to the three holes on the board starting with the innermost contact of the above mentioned strips and going to the right. Solder all the relays in place.¹ Between each pair of mounted relays will be an “inverted L” of unetched foil. Mount the capacitors

¹Although this circuit doesn't show them, it's always a good idea to place a reverse-biased diode across the coil leads of each relay. Because it's reverse biased (cathode to the positive lead), the diode does not conduct when the relay is activated. When the control voltage is removed, however, the diode conducts to short the transient that results from the coil's collapsing field. Builders can easily add the diodes across the coil leads on the solder side of the board.—Ed.

between the right-most pad of the L and the long vertical bus next to it. Solder the capacitors in place and tin all exposed copper.



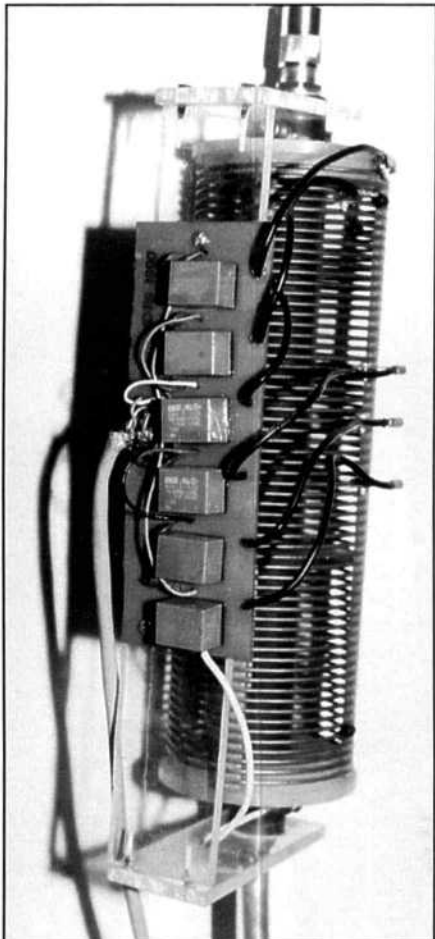
The switch box, PC board and coil together.

Cut seven pieces of the #14 insulated wire, each about 5½ inches long and strip ¼ inch of insulation from each end of each piece. (Do not substitute solid wire for stranded; it is too stiff and puts too much stress on the board.) Solder one end each—of six wires—to a B & W pinch clip. Mount and solder the other ends of the six wires, one into each of the large holes forming a vertical line along the right side (from the component side) of the PC board. Mount and solder the seventh wire into the large hole at the bottom of the board. The other end of this seventh wire receives a ⅜-inch ring terminal that will replace the clip lead connected at the bottom of the Bug-Catcher coil.

Remove about six inches of the outer gray jacket from the control cable and strip about ¼ inch of insulation, each, from six of the colored wires. Solder the six colored wires to the six holes between the relays, a different wire to each hole. Solder the ground wire and

shield to the ground on the board (GND in Fig 2). Hold the gray control-wire cable in the center of the board with a cable tie or a loop of wire through the two holes near the edge of the board. If using wire, twist the ends tightly together on the other side of the board and solder them. This will remove any strain from the board connections. If the control cable is to be pulled through a small hole in the car, you might want to insert a shielded in-line, 8-pin DIN jack and plug in the cable.

Now, drill three holes in the switch box. One hole should be in the center of the largest face of the box to accommodate the rotary switch. The next two can be on the bottom, top or side depending on the method of mounting. One hole should be about ¼ inch for the control cable and a grommet. Another ¼-inch hole and grommet permits the power and ground wires to enter the box. These should go to the vehicle fuse box or some other source of 12 V dc and a chassis ground.



A close-up of the PC board mounted to the coil.

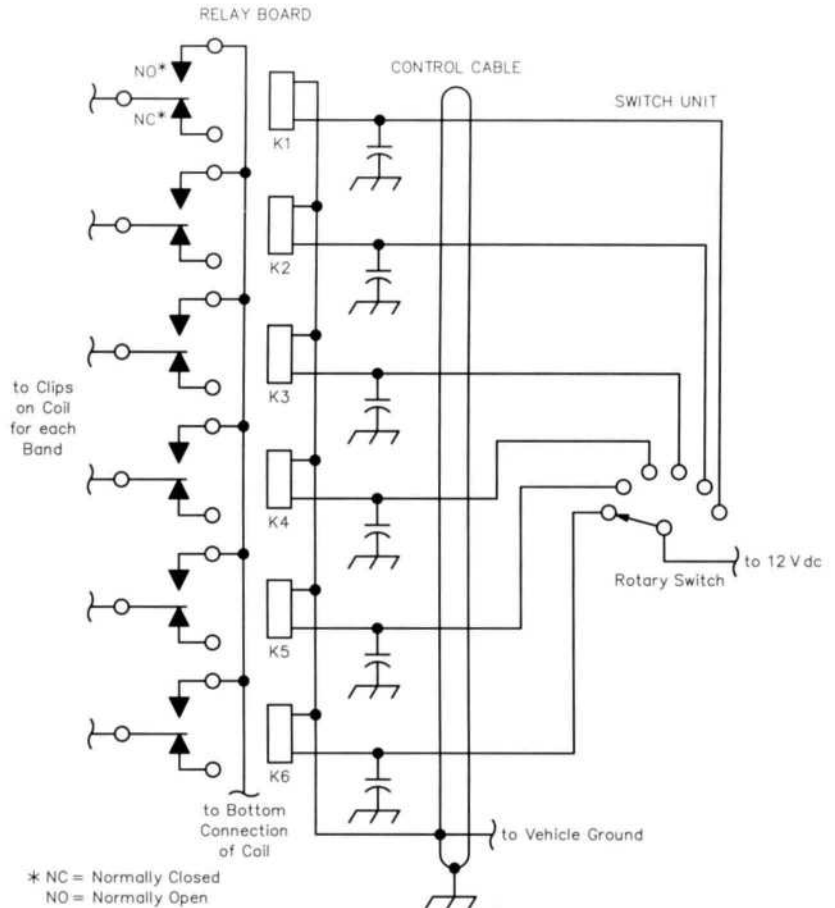


Fig 1—A schematic of the Bug Catcher Bandswitch. See the "List of Materials" for more information.

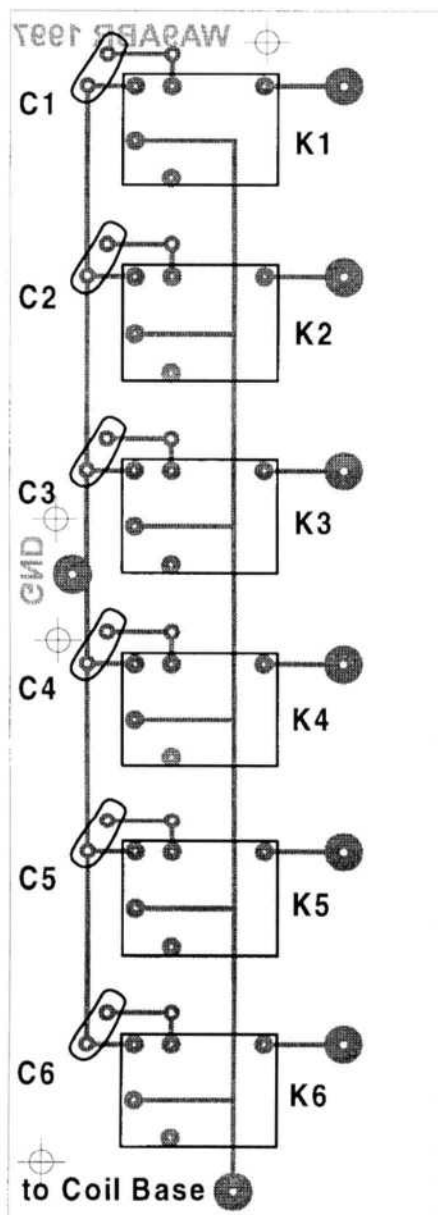
Mount the rotary switch in its hole, then pull the gray control cable through the grommet and mount them in their control-box hole. Remove about two inches of the cable jacket, then twist the ground and shield together.

Begin to wire the rotary switch by noting the color of each wire on the relay board. When the relay board is mounted on the Plexiglas, the top relay corresponds to the highest fre-

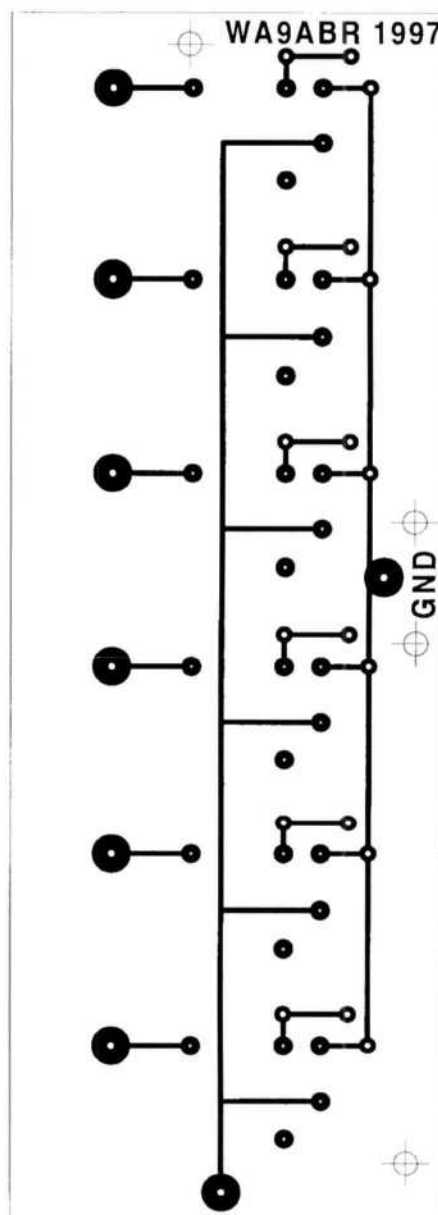
quency band. This wire color will be number one; the next color is number two and so on. Connect no wire to the first switch position, but leave it open as an "off" position. Solder wire one to the second position, proceed with wire two at position three and continue in order until all six wires are connected. Finally, solder the cable shield, cable ground wire and the power-ground wire (#14) to the common terminal of

the rotary switch. The power cable passes through a grommet and the remaining hole in the box. The power cable should be long enough to reach the fuse box, battery or other source of power (13.8 V). Label the rotary switch positions on the front of the box using your favorite method.

Next, connect the power and ground leads to a temporary source of power and check to see that each relay clicks



Parts Placement Diagram



Etching Pattern

Fig 2—Full-scale etching pattern and parts-placement diagram for WA5ABR's project. Black indicates unetched copper viewed from the trace side of the board. Etch or otherwise remove all copper from the component side of the board. The finished board size is 2 1/4 x 6 3/8 inches.

as the switch selects it. Then connect a DVM to the clip lead that goes to the bottom of the Bug Catcher and to the top pinch clip. Turn the switch to the first position and check for continuity. Remove the connection from the first pinch clip and connect it to the second. Turn the switch to the second position and check again. Successively check all positions for continuity. If the unit is working properly, paint the entire board top and bottom with exterior clear polyurethane making sure that the bottom of each relay is sealed to the board (at least two coats).

Attaching the unit to the coil is a challenge in construction ingenuity. Feel free to use your imagination, but the finished product must be light, with minimum wind load. Here's how I did it: The dimensions provided should fit a stock Bug Catcher or any other mobile loading coil up to about five inches in diameter. I used some scrap $\frac{3}{16}$ -inch-thick acrylic sheet. (Refer to Fig 3). Cut two pieces $1\frac{5}{8} \times 4\frac{1}{2}$ inches. Mark a spot one inch from the end and centered between the long sides on each piece. Carefully drill (or cut) a one-inch-diameter hole, centered on the mark, in each piece. In the opposite end, drill two holes (sized to clear the wood screws you've chosen; see the "List of Materials" sidebar) that will serve to fasten these end pieces to the large piece to be made next.

Cut a piece of the acrylic that is $1\frac{5}{8} \times 11\frac{1}{2}$ inches. Drill two holes in the face of this piece to mount the circuit board. (Size the holes to clear the bolts

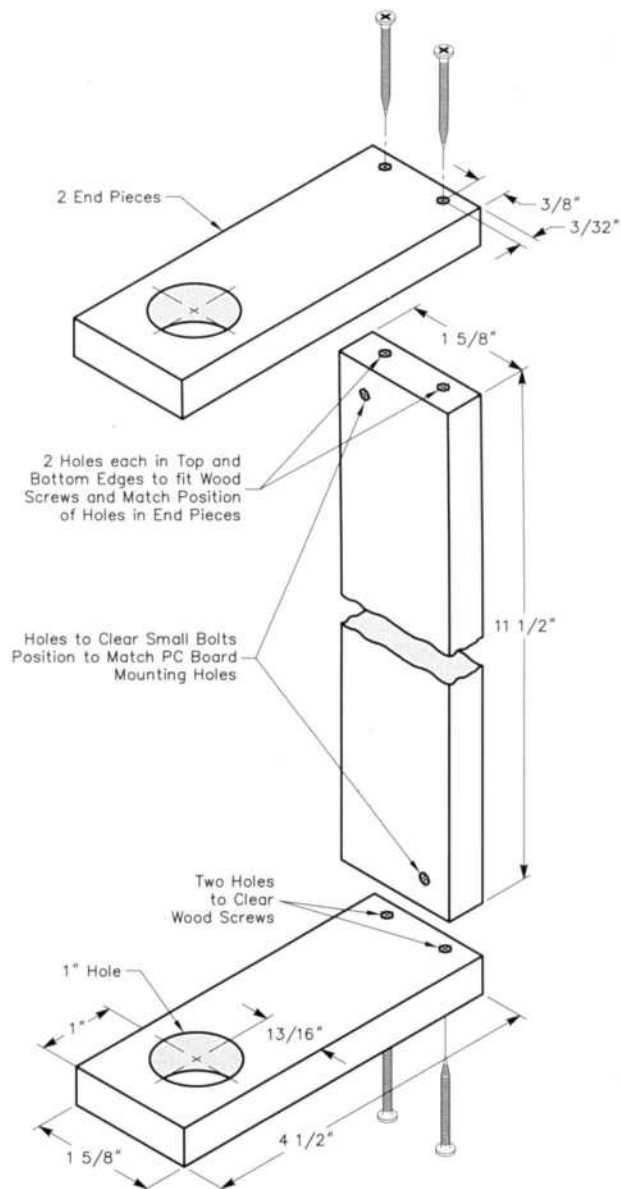


Fig 3—Acrylic mount parts for the Bug Catcher Bandswitch.

List of Materials

- 6—SPST relays 12 V dc, 10 A, PC mount (Radio Shack 275-248).
- 1—10 to 15 foot length of 10-conductor shielded cable (All Electronics 10C/S22).
- 1—12-position rotary switch (Radio Shack 275-1385).
- 6—0.005 μ F, 100 V disc capacitors.
- 1—PC board $6\frac{3}{8} \times 4\frac{1}{2}$ -inches, double sided (Radio Shack 276-1499, cut in half along its length, only one piece is used).
- 6—B & W pinch clips (similar to the clip on the tap lead of the Bug Catcher).
- 1—12-foot length of #14 stranded, insulated wire.
- 4—Small wood screws about $\frac{3}{8}$ inch long.
- 2—Small machine screws, lock washers and nuts.
- 2— $\frac{1}{4}$ -inch rubber grommets



The coil and switch assembly mounted on the author's truck.

you've chosen; see the "List of Materials" sidebar.) Using the small holes in the ends of the small pieces as guides, mark the center of two holes in each short *edge* of the large piece. Drill holes at the marks to fit the wood screws. Super-glue one of the end pieces to the large piece for extra strength. This glued piece becomes the top mount. Install the wood screws (about 3/8-inch long) only in this end. Now attach the circuit board to the mount with two small machine screws, lock washers and nuts. Make sure that the top relay corresponds to position two (remember, position one is "off") on the switch and the glued end of the mount is at the top. Slip the top mount over the Bug Catcher top insulator. Slip the lower mount over the bottom insulator and install the remaining screws. (Do not tighten the screws too much; you may crack the acrylic.) Attach the bottom wire on the board to the bottom of the Bug Catcher coil, where the tap lead was originally.

Assemble the mast, coil and whip, then mount the antenna on the vehicle. Attach the control box to power and ground. The final stage of installation is tuning the antenna for each band. This may take considerable time, but it's possible to achieve an acceptable SWR on each band. I used a two-foot mast, the Bug Catcher, and a five-foot whip. This antenna works from 80 through 10 meters. I found an eight-foot whip was too long for 10 meters; it only worked for 80 through 15 meters. If you have already labeled the switch with your favorite frequencies for each band, start with those and adjust the clip positions for resonance. Begin with the highest frequency band and work your way down to the lowest. Once this is done, the project is finished, and you can enjoy mobile operation with instant QSY.

Paul I. Protas, WA5ABR, Extra class licensee, was first licensed in 1961. A full time pharmacist, he likes to chase DX and experiment with antennas. □□

Surface Mount Chip Component Prototyping Kits—
Only **\$49.95**

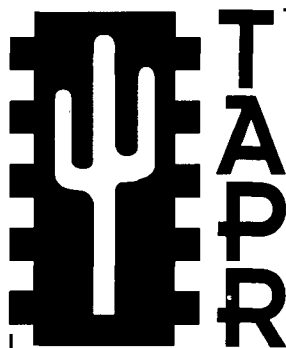
INDIVIDUAL VALUES AVAILABLE



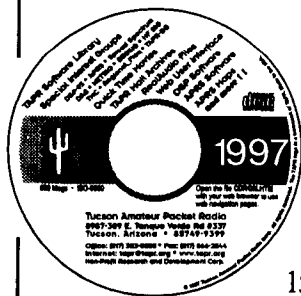
CC-1 Capacitor Kit contains 365 pieces, 5 ea of every 10% value from 1pf to 33µf. CR-1 Resistor Kit contains 1540 pieces, 10 ea of every 5% value from 10Ω to 10 megΩ. Sizes are 0805 and 1206. Each kit is ONLY \$49.95 and available for immediate One Day Delivery!

Order by toll free phone, FAX, or mail. We accept VISA, MC, COD, or Pre-paid orders. Company PO's accepted with approved credit. Call for free detailed brochure.

COMMUNICATIONS SPECIALISTS, INC.
426 West Taft Ave. • Orange, CA 92665-4296
Local (714) 998-3021 • FAX (714) 974-3420
Entire USA 1-800-854-0547



Join the effort in developing Spread Spectrum Communications for the amateur radio service. Join TAPR and become part of the largest packet radio group in the world. TAPR is a non-profit amateur radio organization that develops new communications technology, provides useful/affordable kits, and promotes the advancement of the amateur art through publications, meetings, and standards. Membership includes a subscription to the *TAPR Packet Status Register* quarterly newsletter, which provides up-to-date news and user/technical information. Annual membership US/Canada/Mexico \$20, and outside North America \$25.

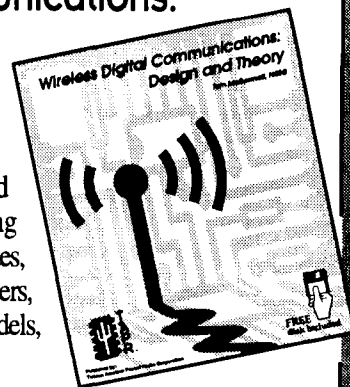


TAPR CD-ROM

Over 600 Megs of Data in ISO 9660 format. TAPR Software Library: 40 megs of software on BBSs, Satellites, Switches, TNCs, Terminals, TCP/IP, and more! 150Megs of APRS Software and Maps. RealAudio Files. Quicktime Movies. Mail Archives from TAPR's SIGs, and much, much more!

Wireless Digital Communications: Design and Theory

Finally a book covering a broad spectrum of wireless digital subjects in one place, written by Tom McDermott, N5EG. Topics include: DSP-based modem filters, forward-error-correcting codes, carrier transmission types, data codes, data slicers, clock recovery, matched filters, carrier recovery, propagation channel models, and much more! Includes a disk!



Tucson Amateur Packet Radio

8987-309 E. Tanque Verde Rd #337 • Tucson, Arizona • 85749-9399
Office: (940) 383-0000 • Fax: (940) 566-2544 • Internet: tapr@tapr.org www.tapr.org
Non-Profit Research and Development Corporation

The CYLOAD

Cylinder-Loaded Dipole

*An electrically shortened antenna
for your backyard or attic.¹*

By Hal Wright, W9UYA

Have you ever wanted to put up a short capacity-loaded backyard vertical antenna without having to put a wagon wheel on top of it? How about putting up a short vertical or horizontal antenna without the losses associated with loading coils? Do you want to put up something different just to see if it will radiate?

What I am about to describe will meet any or all of the above objectives. I first designed it in this particular way when I was planning to install a 14.06 MHz antenna in my townhouse attic. I looked at the standard formu-

las in Chapters 2, 6 and 16 of *The ARRL Antenna Book (15th edition)* and asked myself, "Would it be possible to so proportion the conductors that the ends of a dipole were, in effect, cylindrical loads?"

The answer is the CYLOAD short dipole, each side consisting of a wire element end-loaded by a cylinder. The length of the wire (in inches) is 1476 divided by frequency in megahertz. The reactances of the wire and cylinder sections are equal, and their lengths are proportioned² to fit into a recommended minimum space (in inches) of $3280 / \text{frequency}$.

CYLOAD is an experimental antenna that performs well. It does not offer any practical advantage over other short dipoles, but it does re-open an area of

antenna design not often mentioned in current Amateur Radio literature.

The configuration shown in Fig 1 not only proved possible, but it also radiates extremely well. My new 14.06 MHz antenna is comprised of a 105-inch length of #14 (AWG) wire on each side of center, end-loaded by cylinders—9 inches in diameter and 20 inches long—made of aluminum-sheet flashing.

Don't be intimidated by the math involved in designing a CYLOAD dipole. If you have a computer and *HAMCALC*³ (Version 25 or later) you can design a CYLOAD antenna in a few seconds and skip to the last paragraph of this article. Otherwise, here's a design procedure: First set these variables:

Desired operating frequency, f (MHz)

¹Notes appear on page 46.

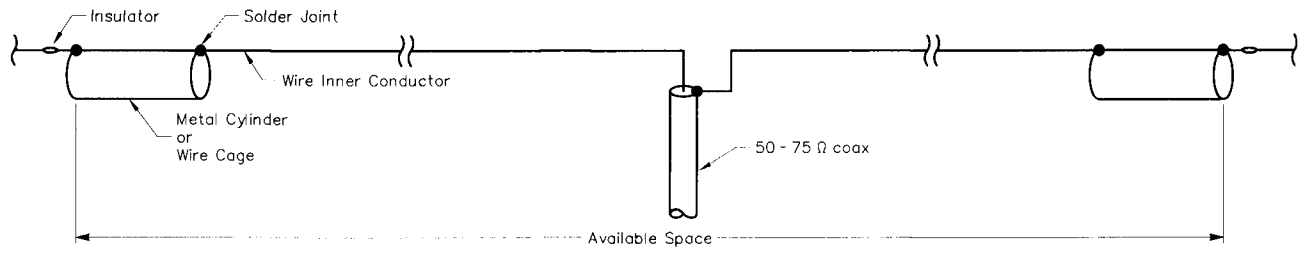


Fig 1

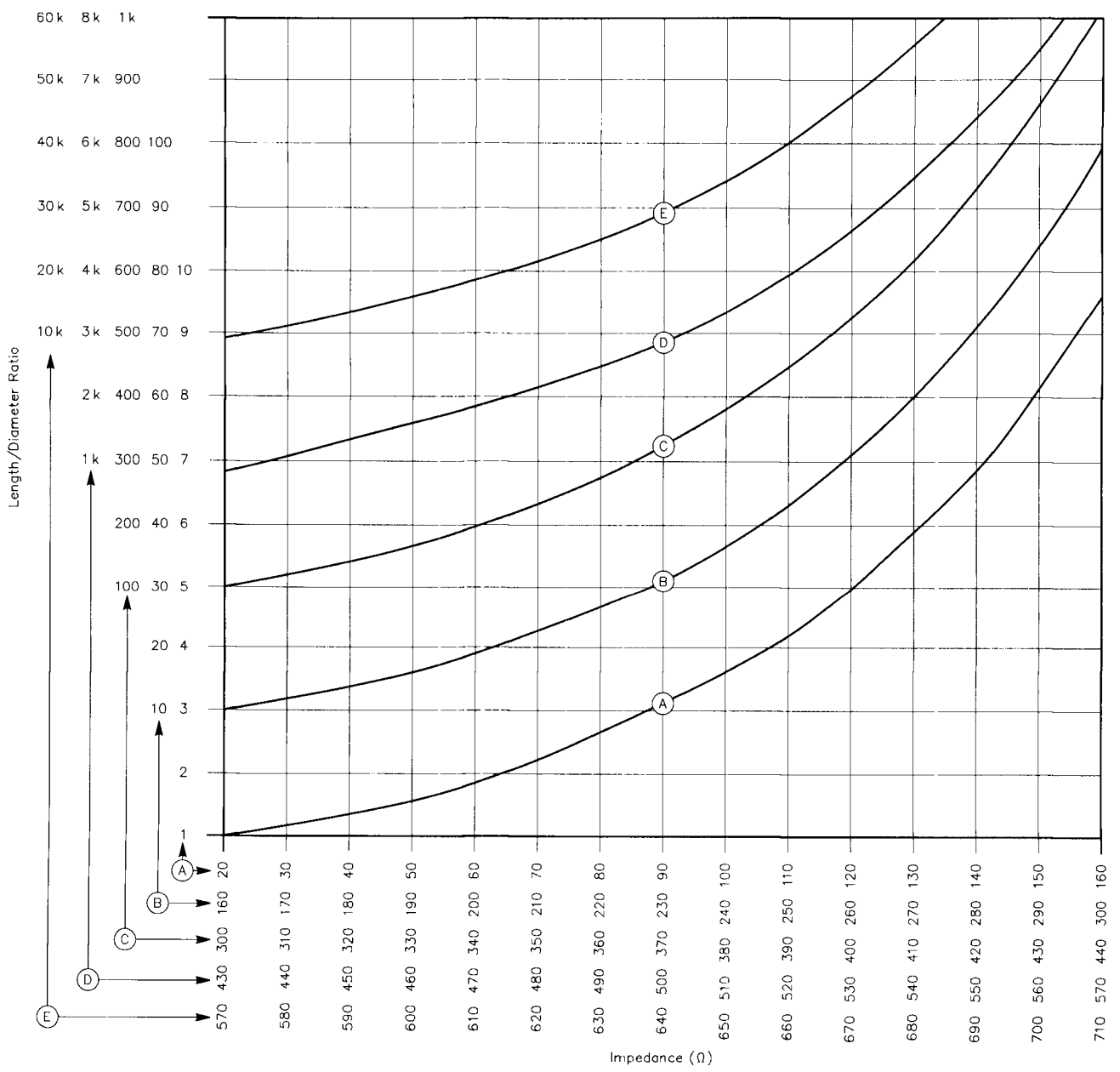


Fig 2

Length of proposed antenna, L (inches)

Diameter of wire section conductor, D_W (inches)

Then calculate the following:

The minimum space required, L_{min} (inches)

The factor for conversions to electrical degrees, L_{deg} (inches)

Length of wire section, L_W (inches)

Length of cylindrical load, L_{Cyl} (inches)

Length-to-diameter ratio of wire section, L/D_W

Characteristic impedance of wire section, Z_{0W} (ohms)

Characteristic impedance of cylindrical load, Z_{0Cyl} (ohms)

Diameter of the cylindrical load, D_{Cyl} (inches)

Regarding wire diameter, you need only know that the diameter of #12, #14 and #16 are approximately 0.08, 0.064 and 0.05 inch, respectively. For the next sixth size larger or smaller than any of these wire sizes, multiply the known diameters by 2 for larger sizes or divide by 2 for the smaller sizes. Thus, with reference to #12, #6 wire has a diameter of 0.16 inch and #18 a diameter of 0.04 inch, and so on.

Now, let's say we have 25 feet (300 inches) of space for a 14.06 MHz horizontal dipole that will be made from #14 (0.064-inch) wire. The minimum recommended length for a CYLOAD dipole is:

$$L_{min} = 3280 / f \quad (\text{Eq 1})$$

The minimum length for this example is $3280 / 14.06 = 233$ inches.

If we allow 25 inches on each end for an insulator, fastening to whatever support we may be using and pruning, we have enough space left for an antenna 250 inches long. This is 17 inches more than the minimum required, so we are all set to design a 250-inch CYLOAD dipole, with each side being 125 inches.

In order to design the antenna, we need to convert some of the dimensions to electrical degrees. To find the length in inches of one degree:

$$L_{deg} = 32.8 / f \quad (\text{Eq 2})$$

Therefore, $1^\circ = 32.8 / 14.06 = 2.33$ inches.

To find the minimum recommended length of the wire section in inches:

$$L_W = 1476 / f \quad (\text{Eq 3})$$

Therefore, wire length = $1476 / 14.06 = 105$ inches.

To find the minimum recommended length of the cylinder in inches:

$$L_{Cyl} = L - L_W \quad (\text{Eq 4})$$

Cylinder length = $125 - 105 = 20$ inches.

To find the length of the cylinder in degrees:

$$Cyl_{deg} = L_{Cyl} / L_{deg} \quad (\text{Eq 5})$$

The cylinder length, in degrees, = $20 / 2.33 = 8.6^\circ$

To find the length-to-diameter ratio of the wire:

$$L/D = L_W / D_W \quad (\text{Eq 6})$$

$$L/D = 105 / 0.064 = 1641:1$$

To find characteristic impedance, Z_{0W} , of the wire, look at Fig 2. An L/D of 1641 on curve D of Fig 2 gives an impedance of 460Ω .⁴

To find characteristic impedance Z_{0Cyl} of the cylinder:

$$Z_{0Cyl} = Z_{0W} \times \tan(Cyl_{deg}) \quad (\text{Eq 7})$$

Impedance $Z_{0Cyl} = 460 \times \tan 8.6^\circ = 70 \Omega$

To find the L/D ratio of the cylinder, look at Fig 2. A 70Ω impedance is on curve A of Fig 2. It corresponds to an L/D of 2.2:1.

To find the cylinder diameter:

$$D_{Cyl} = L_{Cyl} / (L/D) \quad (\text{Eq 8})$$

The cylinder diameter = $20 / 2.2 = 9$ inches.

Each of our dipole sides consists of a wire section 105 inches long (3) that is end-loaded by a cylinder 9 inches in diameter (8) and 20 inches long (4). We need only assemble the thing and fire it up for a trial run.

Conclusion

Amateur literature about capacitive end-loaded antennas goes back at least as far as 1934,⁵ but little has been written specifically about cylinder loaded short dipoles. The material presented here will enable you to build efficient experimental CYLOAD antennas, but the operative keyword is "experimental." Much development is still to be done, and I would appreciate hearing from anyone with any comments, experience or interest in this subject.

In concept, there is nothing original about CYLOAD, except use of the basic formulas

$$k_m = 60 [\ln(2h/a) - 1] \text{ and}$$

$$jkm_2 (\cot h_2) = -jkm_1 (\tan h_1),$$

to determine the load dimensions. One can expect that there will be limitations in the use of this formula for this

purpose. It works well in the HF range, but becomes less accurate above 21 MHz. Its true boundaries and any corrective factors that may extend its useful frequency range are areas for future experimentation. Boyer's article in *Ham Radio* provides excellent background material for anyone interested in further experimentation.⁶

Thanks to George Murphy for writing the *HAMCALC* program for CYLOAD and for invaluable aid in writing this article. Thanks also to L. B. Cebik, W4RNL, for extensive computer modeling that confirmed the validity of this approach to computation of capacitive-end loading in the low to mid-HF ranges and pointed to possible inadequacies of the approach at VHF and beyond.

Notes

¹...or anywhere else. As with any other electrically shortened dipole, make it as long as possible and mount it as high as possible. A "rubber duckie" in the depths of a mine will work, but not as well as a CYLOAD in an attic, which will also work, but not as well as a $1/2$ -wave dipole mounted $1/4$ -wave above perfect ground, which will also work, but not as well as.....etc.

² $Z_{02} = Z_{01} \tan h_1^\circ \tan h_2^\circ$ where:

Z_{01} and h_1° are the impedance and length of the wire section.

Z_{02} and h_2° are the impedance and length of the cylinder section.

³*HAMCALC* is free software containing more than 160 Amateur Radio related programs including a "Short Cylinder-Loaded Dipole" program (in Versions 25 and later) that performs all the mathematical gyrations used to design a CYLOAD antenna.

For a *HAMCALC* 3 $1/2$ -inch, 1.44 Mb MS-DOS floppy send US \$5 check or money order (to cover cost of diskette, packaging and airmail postage to anywhere in the world) to its author: George Murphy VE3ERP, 77 McKenzie St, Orillia, ON L3V 6A6, Canada. Murph and I have had a lot of fun collaborating on the CYLOAD design program. *HAMCALC* Version 27 is available from the ARRL "Hiram" BBS (tel 860-594-0306), or the ARRL Internet ftp site: [oak.oakland.edu \(in the pub/hamradio/arrl/bbs/programs directory\)](http://oak.oakland.edu/pub/hamradio/arrl/bbs/programs). In either case, look for the file HCAL-27.ZIP.

⁴The curves in Fig 2 are plotted from the equation $Z_0 = 60 [\ln(4h/d) - 1]$ where h/d is the length-to-diameter ratio of the wire.

⁵R. B. Dome, "Increased Radiating Efficiency for Short Antennas," *QST*, Sep 1934, pp 9-12.

⁶Joseph M. Boyer, W6UYH, "The Antenna-Transmission Line Analog," *Ham Radio*, 1977; Part 1 Apr, pp 52-58; Part 2 May, pp 29-39. The copyright to *Ham Radio* is now held by *CQ* magazine. □□

A Concise Calculation Method for Pi-L Networks

The ARRL Handbook equations provide Q-based Pi and Pi-L network design. Take another step forward with simplified Pi-L network design.

By Karl Gerhard Lickfeld, DL3FM

The presentation of methods for calculating the Pi-L circuit has been, and still is, rare and of apparently secondary importance in Amateur Radio publications for do-it-yourselfers. Generally speaking, the published information raises questions regarding their mathematical transparency.

The network under discussion is shown in Fig 1. The Greek capital letters Π and Γ are used in place of Pi and L, respectively, in this paper because they more accurately reflect the appearance of the two low-pass networks dealt with here.

Wingfield¹ has made great contributions to the development of a chain of equations, leading to a complete solution. The question remains, however, whether a less extensive but clear-cut sequence of equations may exist.

Mathematical analysis can demonstrate that a "classically" calculated Π network cannot be matched to a resonant transformation Γ network. The effort always ends with the result:

$$\begin{aligned} X_{C2\Pi} &\neq X_{C\Gamma} \\ X_{C2\Pi} &\neq X_{JM} \\ X_{JM} &\neq X_{C\Gamma} \end{aligned} \quad (\text{Eq 1})$$

The variables are defined in Fig 1. With the help of a parallel connection of $X_{C2\Pi}$ and $X_{C\Gamma}$, thereby giving up

¹Notes appear on page 49.

the mathematically pure:

$$X_{JM} = \sqrt{R_1 \cdot Z_L} \quad (\text{Eq 2})$$

A makeshift bridge can be obtained, matching between the Π and Γ networks.¹ Another way out of the dilemma is, to set $X_{C2\Pi} = X_{C\Gamma}$, thus also giving up the pure X_{JM} .²

The author has been thinking over these matching problems and much to his surprise has found a way to simplify the calculation of Π - Γ networks—a way free from compromises. The simplification lies in dividing the two-piece Π - Γ network into three Γ networks for the calculation. This step may be symbolized by " $\Gamma \] \ \Gamma$." (See the bottom of Fig 1.) The inspiration to do this came from Orr,³ who prefers to calculate Π networks via two Γ networks, which are then combined,

corresponding to the symbol arrangement “[..].”

The image reactance plays an essential role in the calculations, in so far as it needs to be calculated first for the input of the Γ network. If this is not done first, it is impossible to calculate the Π network in such a way that its output reactance matches the input reactance of the final Γ network.

In contrast to this prerequisite, the middle Γ network can always be designed so that its output reactance equals that of the input reactance of the final Γ network, thus meeting the basic requirement of a perfect match with $C_{2\Pi} = C_{\Gamma}$. This requires the use of only one variable capacitor at point X_{IM} .

Only two parameters are required for the calculation of a Π - Γ tank output circuit. They are calculated before the main calculation, which can then be performed rapidly. The parameters are R_1 and X_{IM} .

We have:

1. $R_1 = E_p / (n \cdot I_p)$, where E_p is the plate voltage of the tube (in volts) and I_p is the plate current (in amperes). The factor n is 2 for class-C operation, 1.57 for class B and 1.5 for class AB.

2. The image reactance,

$$X_{IM} = \sqrt{R_1 \cdot Z_L},$$

is the geometric mean of both factors.

One problem when designing this network to work over the HF range (80 through 10 meters) is the minimum capacitance of the vacuum capacitors often used. This can force the use of a somewhat higher Q. Typically a Q in the range of 10 to 12 is sufficient. Higher quality factors should not be required.

The following equations satisfy the postulates discussed above:

$$X_{L\Gamma} = \sqrt{(X_{IM} \cdot Z_L) - Z_L^2} \quad (\text{Eq 3})$$

$$X_{C\Gamma} = \frac{X_{IM} \cdot Z_L}{X_{L\Gamma}}$$

$$X_{C2\Pi} = X_{L2\Pi} = X_{C\Gamma} \quad (\text{Eq 4})$$

$$X_{C1\Pi} = \frac{R_1}{Q} \quad (\text{Eq 5})$$

$$X_{L1\Pi} = X_{L1\Pi}$$

A Design Example

If $R_1 = 3125 \Omega$; $Z_L = 50 \Omega$; $X_{IM} = 395.28 \Omega$; $Q = 12$, and $f = 3.65 \text{ MHz}$, the desired resonant frequency, we have:

$$X_{L\Gamma} = 131.39 \Omega; L_{\Gamma} = 5.73 \mu\text{H}$$

$$X_{C\Gamma} = 150.42 \Omega; C_{\Gamma} = 290.03 \text{ pF}$$

$$f = 3.90 \text{ MHz (cutoff frequency)}$$

$$X_{C2\Pi} = 150.42 \Omega; C_{2\Pi} = 290.03 \text{ pF}$$

$$X_{L2\Pi} = 150.42 \Omega; L_{2\Pi} = 6.56 \mu\text{H}$$

$$f = 3.65 \text{ MHz}$$

$$X_{C1\Pi} = 260.42 \Omega; C_{1\Pi} = 167.52 \text{ pF}$$

$$X_{L1\Pi} = 260.42 \Omega; L_{1\Pi} = 11.36 \mu\text{H}$$

$$f = 3.65 \text{ MHz}$$

$$L_{1\Pi} + L_{2\Pi} = 17.92 \mu\text{H}$$

$$\frac{C_{1\Pi} \cdot C_{2\Pi}}{C_{1\Pi} + C_{2\Pi}} = \frac{167.52 \cdot 290.03}{167.52 + 290.03} = 106.19 \text{ pF}$$

$$f = 3.65 \text{ MHz}$$

Putting together the three separate parts, each of which has the same resonant frequency, forms the complete network.

Three transformation ratios characterize a Π - Γ network. These are:

$$r_{\Pi} = \sqrt{\frac{R_1}{X_{IM}}}$$

$$r_{\Gamma} = \sqrt{\frac{X_{IM}}{Z_L}}$$

$$r_{\Pi\Gamma} = \sqrt{\frac{R_1}{Z_L}}$$

The following conditions must be met: $r_{\Pi} = r_{\Gamma}$ and $r_{\Pi} \cdot r_{\Gamma} = r_{\Pi\Gamma}$

In this example:

$$r_{\Pi} = \sqrt{\frac{3125 \Omega}{395.28 \Omega}} = 2.81$$

and

$$r_{\Gamma} = \sqrt{\frac{395.28 \Omega}{50 \Omega}} = 2.81$$

By way of a check:

$$r_{\Gamma} = \sqrt{\frac{3125 \Omega}{50 \Omega}} \approx 7.9$$

$$r_{\Pi} \cdot r_{\Gamma} = 2.8^2 \approx 7.9$$

\therefore the Π - Γ network transforms flawlessly.

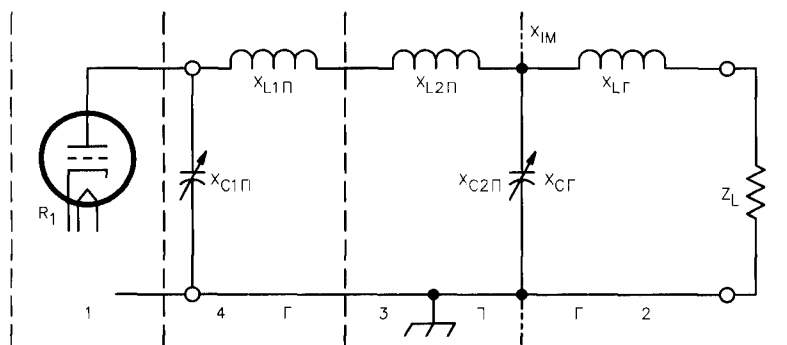


Fig 1—The small numbers and shapes (Γ , Π) indicate the order of calculation and orientation of the three G networks, respectively.

Notes

¹Robert Schetgen, KU7G, Ed., *The 1996 ARRL Handbook* (Newington: ARRL, 1995), pp 13.5-13.8.

²Karl Lickfeld, DL3FM, *CQ DL* 1996, #12, pp 966-969; *CQ DL* 1997, #7, p 537.

³William Orr, W6SAI, *Radio Handbook 1995*, pp 14-17 through 14-20.

Karl G. Lickfeld, DL3FM, was first li-

censed in 1943. He began VHF experiments in 1941, while still in secondary school. On returning from captivity in Russia in 1946 he began his activities as a radio amateur using the call DA3JD. He received his doctorate in natural sciences from Bonn University. From 1950 to 1964 he was the VHF man-

ager of DARC and visited ARRL Headquarters in 1961 as a DARC representative. Karl was Chairman of the IARU Region I VHF Committee from 1956 to 1964. He is a retired professor in the field of electron microscopy. Active on short waves, CW only. He has been an ARRL member since 1953. □□

Conference Proceedings Available

The Central States VHF Society Conference

The Central States VHF Society Conference was held July 24-26, 1998, in Kansas City, Missouri. Here is a summary of papers presented. Conference proceedings are available from ARRL. ISBN: 0-87259-691-5; cost is \$15, plus shipping; ARRL order number: 6915.

A Brief History of the Central States VHF Society

Chambers Award Recipients

Wilson Award Recipients

A Pair of 3CX800s for Six Meters; Dick Hanson, K5AND

A Simple Self-Contained Beacon Keyer; Robert J. Carpenter, W3OTC

FM-TV Station Search Software; Robert J. Carpenter, W3OTC

The RF Safety Rules Two Years Later: A Retrospective View; Wayne Overbeck, N6NB

The May 1998 Tropo "Openings of the Decade"; Jon K. Jones, NØJK

High Speed CW via Meteor Scatter—A Primer; Jim McMasters, KM5PO
Abstract: A Hydrogen-Line Receiver

for Radio Astronomy and SETI; Dr. H. Paul Shuch, N6TX

Transverter IFs?—Answers to Some Questions!; Steve Kostro, N2CEI

An Andrew Cable Primer; Tom Whitted, WA8WZG

Blown Preamp in your Radio Shack HTA-20?; Kent Britain, WA5VJB

M/A-Com and The RF Connection Introduce New Cables; Jeff Embry, WI2T

FC-11Z

FC-14Z

FC-20Z

FC-28Z

FC-38Z

FC-48Z

RM-9267, Comments of the Central States VHF Society

Central States VHF Society 1997 Antenna Gain Results

Central States VHF Society 1997 Noise Figure Results

Southeastern VHF Society Conference Proceedings

The Southeastern VHF Society Conference was held April 3-4, 1998, in

Atlanta, Georgia. Here is a summary of papers presented. Conference proceedings are available from ARRL. ISBN: 0-87259-675-3; cost is \$15, plus shipping; ARRL order number: 6753.

A Pair of 3CX800s for the Magic Band; Dick Hanson, K5AND
Surge Protection; Fred Runkle, K4KAZ

Converting a Dentron MLA-2500 HF Amplifier to Six Meters; Jim Worsham, W4KXY

A Compact Helix Antenna; Michael Barts, N4GU

The WD4MBK Multi-Band Microwave Beacons Move to North Georgia; Charles Osborne, WD4MBK

What Frequency Am I Really On?; Charles Osborne, WD4MBK

SVHFS Conference 98: Antenna Gain Measurements; Dale Baldwin, WBØQGH

High Speed CW via Meteor Scatter—A Primer; Jim McMasters, KM5PO

Control Circuits, Gerald Johnson; KØCQ

Waveguide Interdigital Filters; Paul Wade, N1BWT

SVHFS Conference 97: Antenna Gain Results

SVHFS Conference 97: Noise Figure Results □□

Upcoming Conferences

16th Space Symposium and AMSAT Annual Meeting

The 16th Annual Meeting and Space Symposium will be held October 16-18 1998 at the Park Inn International in Vicksburg, Mississippi. Proceedings of the Symposium will be printed by the ARRL and made available at and after the meeting. Information

regarding Vicksburg area attractions and details on arrangements for the 16th Space Symposium and AMSAT Annual Meeting can be found at <http://pages.prodigy.com/DXHF93A>, or you can e-mail vbvburg98@amsat.org.

17th Annual ARRL and TAPR Digital Communications Conference

The 1998 ARRL and TAPR Digital Communications Conference will be held September 25-27, 1998, in Chicago, Illinois. This year's conference location is the Holiday Inn Rolling Meadows, just minutes from O'Hare Airport.

The conference is an international forum for radio amateurs in digital communications, networking and related technologies, who meet, publish their work and present new ideas and techniques for discussion. The conference is not just for digital experts, but

for digitally oriented amateurs at all levels.

This year's conference again provides multiple-session tracks for beginning, intermediate and advanced presentations on selected topics in digital communications. Topics will include APRS, satellite communications, TCP/IP, digital radio, Spread Spectrum and many others. Don't miss this opportunity to listen and talk to others in these areas.

Full information on the conference and hotel information can be obtained by contacting Tucson Amateur Packet Radio, 8987-309 E Tanque Verde Rd, Tucson, AZ 85749-9399; tel 940-383-0000, fax 940-566-2544; e-mail tapr@tapr.org; or visit <http://www.tapr.org/tapr/html/dccconf.html>. □□

Harmonic Filters, Improved

Are you satisfied with traditional, table-based low-pass filter designs? Modern circuit-analysis tools let us tweak those designs to better meet our needs.

By James L. Tonne, WB6BLD

The author has been involved with a project involving harmonic-attenuating output filters for an amateur-band transmitter in the 3.5 to 29.7 MHz region. This article grew from a study of various options for those filters and attempts to maximize the performance from a given topology.

The typical final amplifier in amateur service uses a transistor or tube (or a pair of same) driving either a matching network or a tuned tank circuit. The magnitudes of the harmonics present in the output of the final amplifier must be suppressed to a greater degree than the matching network or tank alone can provide. For this reason, a low-pass filter must be installed between the network or tank and the antenna. The design process can be broken into two frequency re-

gions: the passband and the stopband. The passband is that region containing signals we want to pass (logically) and the stopband is that region where we want to attenuate or reject signals.

The stopband portion of the design involves measuring (or at least approximating) the magnitudes of the various harmonics leaving the output of the final-amplifier output network. Then we must determine the allowable magnitudes of each of the harmonics exiting the filter. With knowledge of these two items, the stopband attenuation requirements for the output low-pass filter itself are indirectly specified. For the purposes of this article, I assume two things: First, the signal applied to our low-pass filter has high harmonic levels; and second, we must meet the FCC spurious output requirements. The stopband will be considered here to mean integer multiples of the passband.

The passband portion of the design

involves consideration of the maximum allowable insertion-loss levels, along with the filter's input SWR through that band. Insertion loss will manifest itself as heat dissipated in the filter. High input SWR taxes the final amplifier stage by presenting an incorrect—possibly reactive—load. The common path is to specify a design that has uniformly good performance from dc to its cutoff frequency. That is, the passband extends down to dc. By good performance, we mean satisfactorily constant input impedance with an acceptably flat magnitude response from dc to cutoff. This design approach is popular because design tables in the literature can be used. Most programs for automating the design of a low-pass filter use this same approach.

For amateur applications, however, good performance is not needed over the entire passband from dc up to the operating frequency. Good passband performance is needed only over an amateur band or bands. (The stopband

performance requirements remain unaltered.)

The First Design

Let's design a filter to pass the band from 3.5 to 4.0 MHz with some small value of insertion loss over that range. We want the final RF amplifier to look into a nearly resistive load, and the filter to attenuate harmonics of signals in the passband by 40 dB. This will allow us to meet the requirements of the present¹ FCC Rule 97.307(d) for transmitters with output powers up to 500 W. (The author's project is a transmitter with only 250 W of output.) By designing for 40 dB of attenuation to all harmonics in the filter itself, any harmonic suppression in the final amplifier proper and/or its matching network or tank can be considered as a margin or bonus. If our filter fails to meet the 40-dB design goal, any inherent suppression in the final RF amplifier may bring the system within the regulatory requirements.

For a first pass at a filter design, let's use the Caue family. This filter is best known for its good shape factor. The schematic of such a filter, with no parts values, is shown in Fig 1. Let us specify the order to be five, the bandwidth to be 4.0 MHz and the cutoff to be 7.0 MHz. Set the minimum attenuation in the stopband as 40 dB.

¹In response to action at WRC-97, we can expect the FCC to adopt more stringent spurious-emission requirements in the next five years or so. For details, see "WRC 97 An Amateur Radio Perspective," *QST*, Feb 1998, pp 31-34. Given the life span of equipment, it's wise to start designing for the new limits now.—Ed.

The passband ripple then works out to be 0.006 dB, corresponding to an input SWR of 1.08:1 or a return loss of 28 dB. These latter figures are the result of using a computer; the complete design of a Caue filter is impractical without one.

Such a design should pass the band from 3.5 to 4.0 MHz and reject the second harmonic of that band, the stopband starting at 7.0 MHz. However, an experienced designer would immediately see that we have—using real-world inductors with their inherent losses—a loss problem at 4.0 MHz. Further, if the component tolerances are non-ideal—and they will be in practice—then our goal of 40 dB of attenuation at 7.0 MHz might not be met. However, the filter-response plot for this blue-sky filter design is shown in Fig 2.

The Second Design

We must "tighten the screws," so to speak, and slightly overdesign. Our first overdesign steps are to lower the stopband frequency from 7.0 MHz to 6.8 MHz and increase the stopband minimum attenuation from 40 dB to 43 dB. We will also raise the passband

from 4.0 MHz to 4.3 MHz. Monte Carlo analysis reveals that our goals have been met in that the attenuation to all harmonics will be better than 40 dB even with component-value variations. The frequency-response and return-loss plots for this modified filter are shown in Fig 3.

A characteristic of this kind of design (the usual textbook approach) is that the passband performance is uniformly good from the cutoff frequency down to dc. By specifying the passband to be only a small percentage of the bandwidth from cutoff downward (instead of from cutoff down to dc), the filter's performance can be increased significantly. What I propose in this article is to design a low-pass filter that has especially good passband performance only over the region just below the cutoff frequency, and at the same time better performance in the stopband. Below the lower edge of the passband, we can relax all of the specifications. The various characteristics at 2 MHz, for example, are irrelevant. We can increase the performance in the stopband by sacrificing performance in that portion of the original passband where it doesn't matter. This can all be done

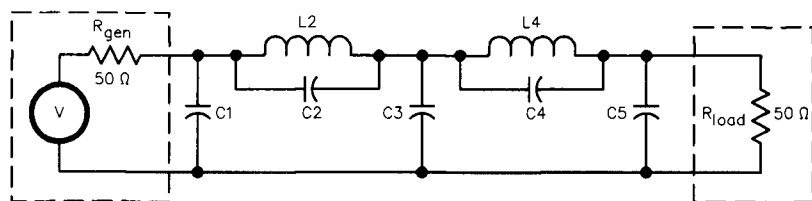


Fig 1—Schematic sans parts values.

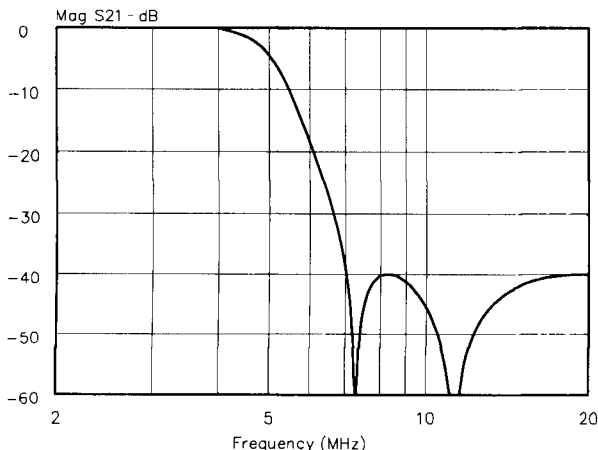


Fig 2—Frequency response of first-pass blue-sky filter.

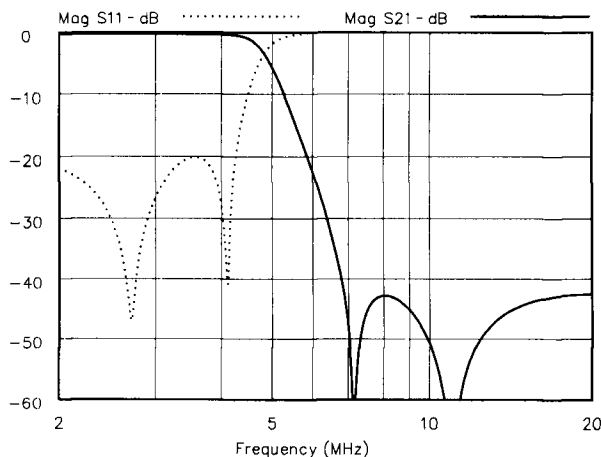


Fig 3—Frequency response and return loss of second-pass filter.

by a modest deviation from the values obtained from the usual design tables. The result might very well be called a *pseudo-band-pass* filter.

This technique is most useful for transmitters operating in narrow bands (15% or so bandwidth), such as the amateur bands. Obviously, this is not a constraint for amateur service.

Improved Designs

The transmission loss of our new filter is shown in Fig 4. On this plot, we have marked the passband, the second- and the third-harmonic regions. Whereas the transmission loss was flat from cutoff down to dc on the first and second designs (see Figs 2 and 3), this design has increased attenuation below the area we are now calling the passband. The return-loss plot is shown in Fig 5. Notice how the return loss becomes quite poor below our region of interest. Compare that with the usual design technique, whose return loss can be seen in Fig 3. In our new design, we simply don't care what happens below our region of interest. That fact enables us to optimize performance within the amateur band (better return loss and less insertion loss) and at harmonics of that band (greater attenuation). It forms the basis for this article.

The schematic of our new filter is shown in Fig 6. This is the minimum-inductor design. That topology would be used when inductors are less expensive than capacitors. The minimum-capacitor version is shown in Fig 7. Coupling among the five inductors may be problematical when using the

topology of Fig 7. If component Q values and any possible inter-inductor coupling are both ignored, the two topologies have the same responses excepting the input impedance and its angle. Even with Q values considered, the responses are quite similar. The stopband input-impedance values are quite different for the two designs and may be a factor in topology selection. Fig 8 illustrates the minimum-inductor schematic using the nearest standard values. C3 has been trimmed by using two capacitors in parallel.

The insertion loss of the minimum-inductor design is about 0.25 dB at 4 MHz, using inductor Q values of 150. If the inductors are built as air-cored solenoids and placed in an enclosure, their Q values may drop to perhaps 100 and the filter's insertion loss would then increase to about 0.37 dB at 4 MHz. In either case, attenuation is better than 55 dB at the second and third harmonics of the passband.

Adjustment

I paid considerable attention during the design of the filter to make it adjustment free. For most applications, the design can be used as presented, simply by using the nearest available values. For best stopband performance, adjust C2 or L2 for resonance at 2.83 times the lower passband frequency. Adjust C4 or L4 for resonance at 2.03 times that same frequency. For minimum input SWR, an additional adjustment may be made: Adjust C3 in the minimum-inductor topology, or L3 in the minimum-capacitor topology, for minimum SWR in the middle of the passband.

Scaling

The ideal values are shown for a 50- Ω filter covering a 3.5 to 4.0 MHz band. To find the capacitor values for another band, divide each of the capacitor values shown by the ratio of the new passband *lower* edge to 3.5 MHz. To find the inductor values for another band, divide each of the inductor values shown by the ratio of the new passband lower edge to 3.5 MHz. To change to a different characteristic impedance, divide each of the capacitor values shown by the ratio of the new impedance to 50 Ω , and multiply each of the inductor values by the ratio of the new impedance to 50 Ω . These techniques hold true for both the minimum-inductor and minimum-capacitor topologies.

For example, to scale either of these filters up to the 40-meter band, divide all the component values by two (7.0 MHz divided by 3.5 MHz). To change to a 100- Ω design, *multiply* the *inductor* values by two (the ratio of the new impedance to 50 Ω), and *divide* the *capacitor* values by two (the ratio of the new impedance to 50 Ω).

Normalized Values

For those accustomed to using normalized values to design filters, or who have a computer automate the process, the recommended normalized values for this optimized design are shown in Table 1. Using these values will result in a low-pass filter as presented, normalized to a bandwidth of one radian/second when terminated at each end with one ohm. To denormalize these values, use the bottom edge of the passband for the frequency entry, along with the impedance of the

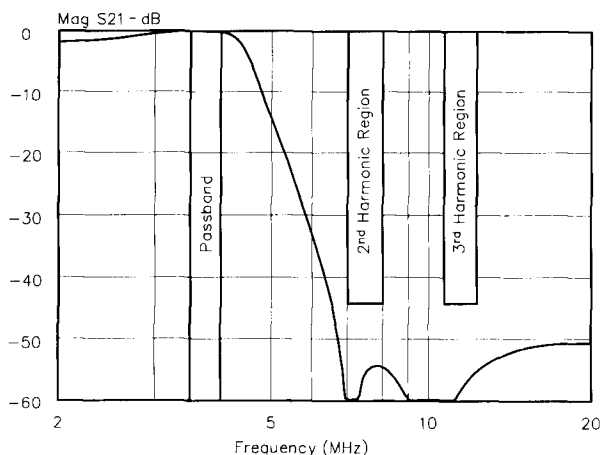


Fig 4—Frequency response of new design.

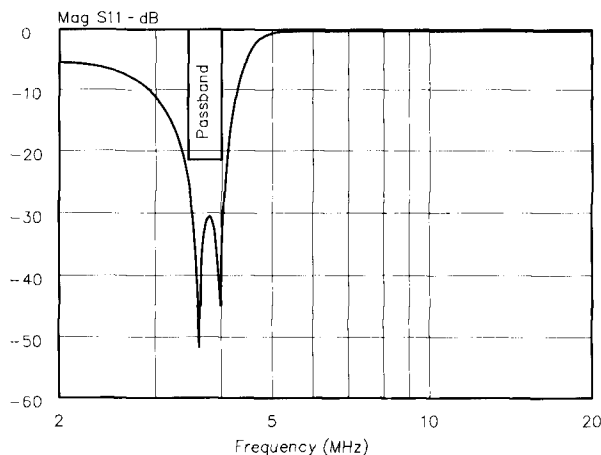


Fig 5—Return loss of new design.

Table 1

Normalized values for a one-radian/second bandwidth, one-ohm termination low-pass filter. These values are normalized to the bottom edge of the passband. "On" is the ratio of the notch frequency (transmission zero) to the passband bottom edge. Both the input and the output terminations are assumed to be one ohm.

N:	C_n	L_n	On
1	1.3808		
2	0.1952	0.6408	2.8276
3	2.6781		
4	0.4447	0.5473	2.0270
5	1.2251		

circuit where the filter is inserted.

Summary

The component values for the filter as shown in this article were obtained by starting with a fifth-order Cauer low-pass filter. That design was then optimized for a return-loss goal from 3.4 MHz to 4.2 MHz of 23 dB. In addition, the attenuation goals from 6.8 MHz to 8.0 MHz and from 10.5 MHz to 12 MHz were set to 55 dB. These goals result in an overdesign. If very tight tolerances are assigned to each of the components, the filter performance could be increased noticeably. The method of optimization is immaterial; it could be optimizing software (that has been properly instructed) or manual optimization, preferably with the aid of a computer for the math. The optimizing goals could be modified to change the stopband minimum attenuation, to change the return loss, etc. The deliberate overdesign of this filter allows the use of real-world components with a minimum of adjustment, while still maintaining respectable performance. The filter design, as presented, can be scaled to any amateur band, up to and including the 10-meter band. At higher frequencies, the mandated filtering requirements become more stringent.

The design as presented is an odd-order Cauer-type design. A characteristic of that filter family is that the descent rate into the far stopband is only 6 dB per octave. Another approach to this filtering problem raises this ultimate rolloff rate to 30 dB per octave. It requires another component, however. The merit of this improved rolloff rate is debatable.

We have not touched on lumped-element component failure at the

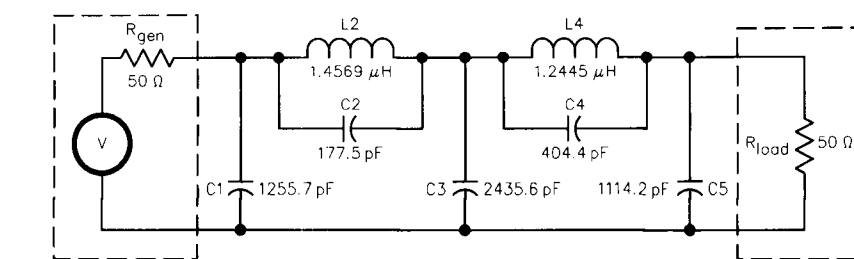


Fig 6—Schematic of minimum-inductor version of new design.

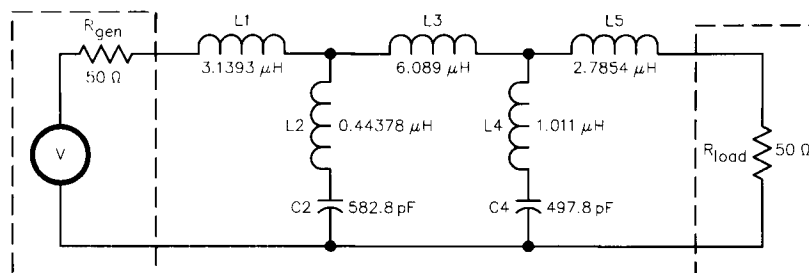


Fig 7—Schematic of minimum-capacitor version of new design.

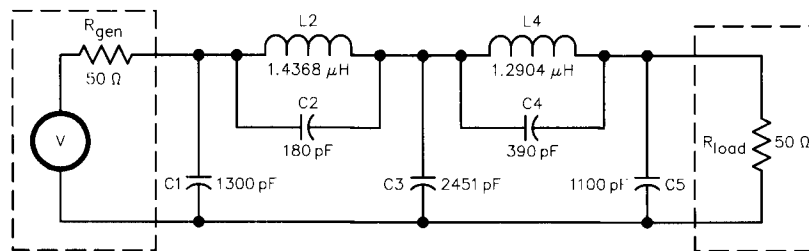


Fig 8—Schematic of minimum-inductor version using nearest available values.

higher frequencies. This problem starts to become significant at frequencies above about 50 MHz. The exact frequency depends on the components and construction techniques used; it is not unique to this design. The filter's performance at UHF can be improved by the use of an additional separate TVI filter, probably of a unique construction, cascaded with this filter.

An assumption has been made here that could have some impact on the results: We have assumed an input termination of 50 ohms in the design of our filter. This is the impedance seen looking back into the amplifier. If this value is not 50 ohms, the results will be worse than anticipated. Fortunately, they will not be completely out of the ballpark; the filter will likely be quite

useful. In addition, the load is assumed to be resistive and of modest SWR. These assumptions are not unique to this filter design; they are commonly made in the literature.

We have not dealt with impedance-matching transmission-line effects, coil winding and related construction techniques, packaging and so on. Most of those items are critically dependent on the power level and the available components and facilities. Netlists for *ARRL Radio Designer*, HP/EEsof's *Touchstone* and Microsim's *PSPice* are available from the author.

First licensed in 1951 as W5SUC, the author is an engineer at an electronics firm near Balch Springs, Texas. He can be reached at 972-475-7132 or by mail at 7801 Rice Dr, Rowlett, Texas 75088.



A Test for Ambient Noise

Receivers are often judged by their sensitivity specifications, but ambient noise may far outweigh a receiver's internal noise. After we ask, "How sensitive is this receiver?" perhaps we should consider "Do I actually need that much receiver sensitivity?"

By Peter Lefferson, K4POB
Electronic Design Consultant

Recceiver sensitivity is limited by many familiar factors. In very general terms, we speak of thermal noise and amplifier input noise. When the receiver is taken from the lab to its working environment, it sees new noise sources. Galactic, atmospheric and background transmissions all contribute to ambient noise that puts a new limit on receiver sensitivity. We compare receivers by their many specifications: One of the first we consider is receiver sensitivity. Possibly, other parameters are more important if real-world sensitivity is determined more by the environment than by the receiver.

I have discovered several quick ways to compare the ambient noise to the receiver noise that defines its specified sensitivity. The following two methods have the receiver connected to its normal antenna.

Attenuator Method

Setup

Connect the receiver to the antenna in the manner you plan to use the receiver. (See Fig 1.) Set up a test antenna at a "far field" distance from the first. (See Appendix 1.) The actual distance is not at all critical, but since the received noise source is a "far field" distance from the receiver antenna, the test antenna must also be in the "far field." Connect the test antenna to a calibrated signal generator as shown in Fig 1.

Procedure

Measure receiver sensitivity through this radio link. (Any definition of receiver sensitivity that is appropriate to your receiver is correct.¹) Record this as sensitivity #1. The sensitivity is often a difficult measurement to make because the ambient noise is not constant. To overcome this problem, make the measurement 5 or 10 times and average the results. Next, insert an accurate, large-value attenuator (say 20 dB; see Appendix 2) between the receiving antenna and the receiver. Measure receiver sensitivity again and record this as sensitivity #2. You will need to increase the generator signal amplitude to com-

¹Typical measures of sensitivity are minimum-discernable signal (MDS) or 10 dB signal-to-noise ratio (SNR). $SNR = (s+n)/n \approx s/n - Ed$

pensate for the added attenuation when measuring sensitivity #2. Sensitivity #2 will appear to be better than sensitivity #1 if you subtract the attenuator insertion loss.

Calculation

In this method the attenuator can be thought of as acting as a noise reducer. In the first sensitivity measurement, the receiver saw all of the ambient noise. In the second measurement, the ambient noise was greatly reduced by the attenuator, but the signal generator output was increased to overcome much of the attenuator loss. That is, the ambient-noise level changed greatly at the receiver, but the received signal was changed by a small amount.

Fig 2 is a simple block diagram of the first measurement. The signal to noise ratio is:

$$\frac{s}{n} = \frac{S1}{Na + Nt + Nr} \quad (\text{Eq 1})$$

The second measurement can be modeled as shown in Fig 3. The signal to noise ratio is:

$$\frac{s}{n} = \frac{\frac{S2}{A}}{\frac{Na}{A} + Nt + Nr} \quad (\text{Eq 2})$$

Receiver sensitivity is measured to a specific SNR. Therefore these two expressions can be set equal to each other and solved for a ratio of the ambient noise to the thermal and receiver noise.

$$\frac{Na}{Nt + Nr} = \frac{1 - A \left(\frac{S1}{S2} \right)}{\frac{S1}{S2} - 1} \quad (\text{Eq 3})$$

Note, if the sensitivity ratio ($S2/S1$) is the same as the attenuation, there is no ambient noise. This would be the lab sensitivity measurement, where the signal generator simulates the antenna signal.

An actual example might use a 20-dB pad and get sensitivities of:

- S1 dBm = -65.8 dBm
- S2 dBm = -52.7 dBm
- S2 dBm = -S1 dBm = 13.1 dBm

or 20.417 as a pure power ratio for the equation. This gives the noise ratio as 6.126 dB. The ambient noise is approximately 6 dB greater than the sum of thermal and receiver noise.

Resistive Power-Divider Method

The second method does not require a second antenna but does require a 6-dB resistive power divider. (See Appendix 3.) This time the ambient noise

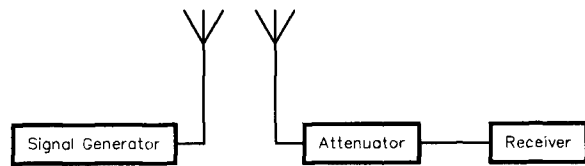


Fig 1—Block diagram of the setup for Attenuator Method ambient-noise measurement.

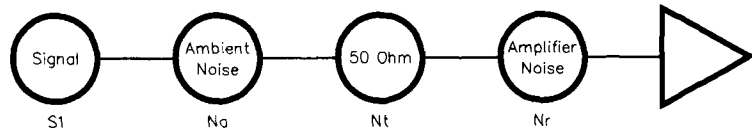


Fig 2—A model of the first Attenuator Method SNR measurement.

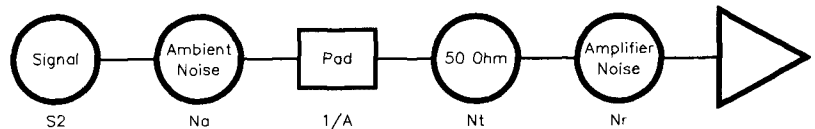


Fig 3—A model of the second Attenuator Method SNR measurement.

and signal generator output are added directly.

Setup

Connect the 6-dB resistive power divider to the receiver. Connect the receiver's normal antenna and a calibrated signal generator to the other two ports of the resistive divider.

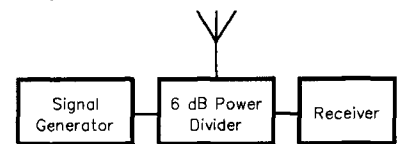


Fig 4—Block diagram of the setup for Power-Divider Method ambient-noise measurement.

Appendix 1

Far-Field Distance

The electric and magnetic fields of all antennas are a uniform plane wave in the "far field," but are quite different close to the antenna. The transition from "near field" to "far field" is gradual, but one can estimate the "far field" distance from equations found in most antenna handbooks. One approach assumes a rough knowledge of the antenna gain as follows:

The apparent antenna area is:

$$A = \frac{\text{gain} \cdot \lambda^2}{4\pi} \quad (\text{Eq 7})$$

Where gain is a power ratio; that is, *not* dB. The apparent diameter squared (D^2) is $(4A) / \pi$. Then the range equation gives $R = (2D^2) / \lambda$.

For example, a 14-MHz dipole will have a nominal gain of 2.14 dB (1.64:1 as a power ratio) over an isotropic antenna. The wavelength is:

$$\begin{aligned} \lambda &= 300 / \text{frequency (MHz)} \\ &= 300/14 = 21.4 \text{ meters} \end{aligned}$$

The area is $A = 59.8$ meters square.

The apparent diameter squared is $D^2 = 76.2$ meters square.

The "far field" distance is $R = 7.11$ meters, or 23.3 ft.

Procedure

Measure receiver sensitivity and call it sensitivity #1. Remove the antenna from the resistive divider and attach a dummy load in its place. Measure receiver sensitivity again and call it sensitivity #2.

Calculation

The block diagrams will again be used to evaluate ambient noise as compared to receiver and thermal noise. The noise is attenuated by 6 dB as it passes through the resistive divider. Therefore, using the ratio of the two sensitivities is not correct.

In simple blocks, the first measurement can be modeled as shown in Fig 5. The signal to noise ratio is:

$$\frac{s}{n} = \frac{\frac{S1}{4}}{\frac{Na}{4} + Nt + Nr} \quad (\text{Eq 4})$$

The second sensitivity measurement can be modeled as shown in Fig 6. The signal to noise ratio is:

$$\frac{s}{n} = \frac{\frac{S2}{4}}{Nt + Nr} \quad (\text{Eq 5})$$

These two expressions can be set equal to each other and solved for the ratio of ambient noise to the thermal and receiver noise.

$$\frac{Na}{Nt + Nr} = 4 \left(\frac{S1}{S2} - 1 \right) \quad (\text{Eq 6})$$

An actual example might yield:

S1 dBm = -101.1 dBm

S2 dBm = -104.0 dBm

This gives the noise ratio as 5.8 dB. The ambient noise is still approximately 6 dB greater than the sum of thermal and receiver noise. (Note that S1 and S2 in Eq 6 are gain ratios, *not* decibels. That is S1 is 77.6×10^{-12} , and S2 is 39.8×10^{-12} . S/N is then 3.79, which is 5.8 dB.—Ed.)

Note that we have not considered the gain of the receiver antenna. Receiver antenna gain would surely be a factor of received noise level. For these noise-ratio calculations, we assume that the receiver antenna is the one to be used in a communication link with the tested receiver. Therefore, our interest is only in the noise ratio for that application.

Acknowledgement

I want to acknowledge an old friend, Jim Olivenbaum and his colleague, Bob Pucket for their helpful review of this paper.

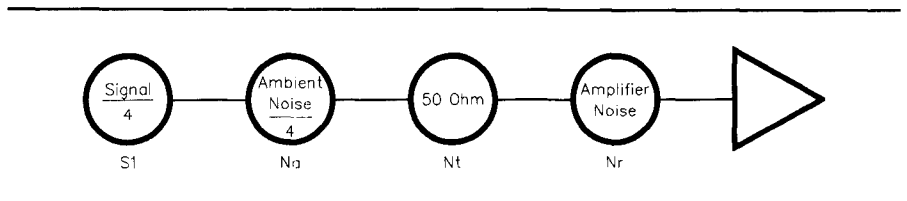


Fig 5—A model of the first Power-Divider Method SNR measurement.

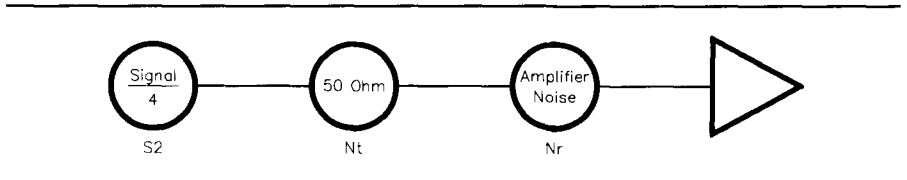


Fig 6—A model of the second Power-Divider Method SNR measurement.

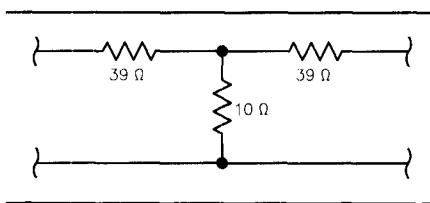


Fig 7—A wideband 20 dB attenuator; 1/8-W resistors should be fine for the power levels common in receiver tests.

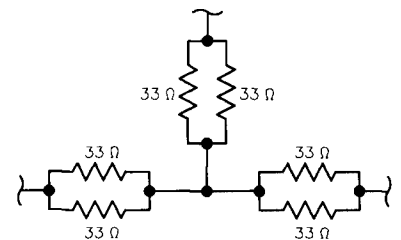


Fig 8—Schematic of a resistive, 6-dB power divider.

Appendix 2

20-dB Attenuator

A good reliable wideband 20-dB attenuator is easily constructed using chip resistors on microstrip lines. The handbooks provide formulas and construction examples. For example, (using standard values) a T pad in a 50 Ω line would look like Fig 7.

Appendix 3

6-dB Resistive Power Divider

An accurate 6-dB power divider is handy for many RF measurement applications because it presents the correct line impedance at any one port when the correct impedance termination is connected to the other ports. An example (using standard part values) would look like Fig 8.

Ham radio started Pete's interest in electronics in 1957, with the Novice call KN2SHS. He expanded his interest into a profession with Bachelor's and Master's degrees in electronics from the University of Florida. The 32 years of practice since then have seen

the design of receivers, transmitters, antennas, controls systems, high-voltage, high-power power supplies and many other exciting projects. Pete is grateful to Amateur Radio for his start so many years ago.

□□

RF

By Zack Lau, W1VT

A Narrow 80 Meter Band-Pass Filter

A common problem during Field Day is interference between SSB and CW transmitters on the same band. Clever antenna design helps a lot, but a sharp filter would also help make operating more pleasant. This design should help out an 80-meter CW receiver. The goal was to achieve a reasonable trade-off between cost, performance and practicality. With a 3.56 MHz center frequency, it has a 59 kHz -3 dB bandwidth and 2.3 dB of insertion loss, using self-shielding toroidal inductors. Signals above 3.75 MHz are attenuated by another 26 dB, for an insertion loss of at least 28 dB.

I did some experimenting and decided that 23 turns of #14 (AWG) enameled wire on a T-130-6 core offers the best trade-off between unloaded Q and cost, for an 80-meter inductor. I wound several samples and found worst case Q s of 371, 410 and 412 at 4.0 MHz; Q s are slightly higher at 3.5 MHz. I tried thinner wire, but this noticeably decreased the Q from 371 to 330. The filter was built using the two inductors that exhibit the highest Q s.

The resonating capacitors are 330 pF silver-mica capacitors (with

#22 wire leads) in parallel with Johnson trimmer capacitors. Thicker leads would work even better; avoid capacitors with thinner leads that have more loss. There are chip capacitors with higher Q s and silver strap leads for easy installation, but they can be difficult to obtain. Silver micas can usually be found if you look for them in places that cater to parts for

building RF circuits. The Johnson trimmer capacitors feature relatively high Q , and appear to still be in production, unlike many other air variable capacitors.

Due to component tolerances, it may be necessary to try several different parts as C4. Alternately, one could substitute an air variable trimmer capacitor for C4.

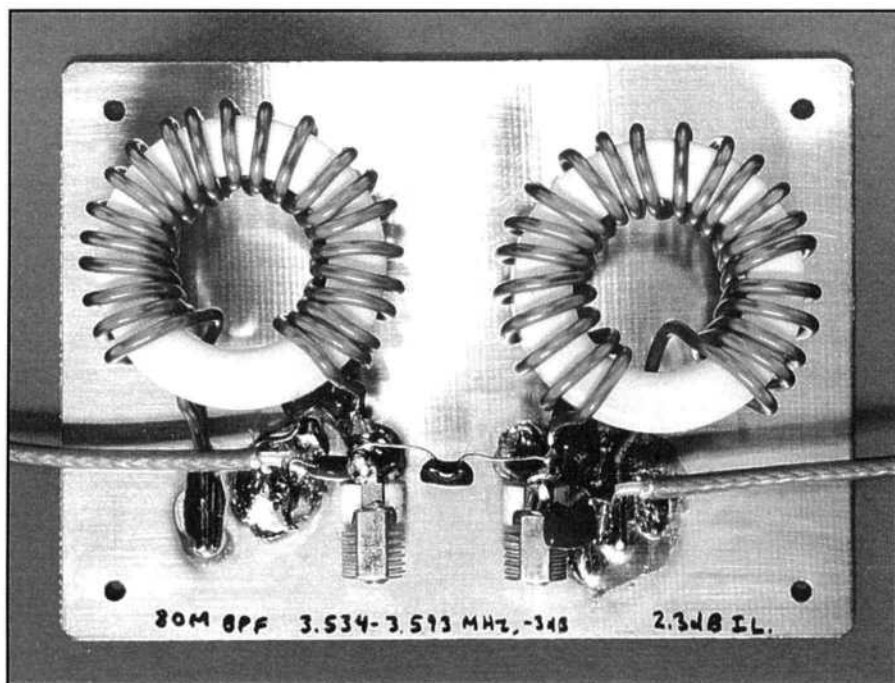


Figure 2—The 80-meter band-pass filter.

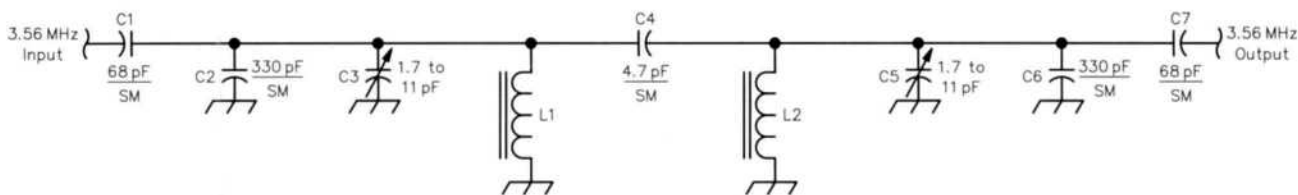


Fig 1—80 meter band-pass filter with 59-kHz bandwidth.

C1, C7—68 pF, silver mica.
C2, C6—330 pF, silver mica.

C3, C5—Johnson T6-5 air variable trimmer. 1.7 to 11 pF; $Q = 2000$ at 1 MHz.
C4—4.7 pF, silver mica.

L1, L2—23 turns, #14 enameled wire on T-130-6 iron-powder toroid core.

Letters to the Editor

About Wave Interference and Impedance Matching

◇ To Walt Maxwell: I want to thank you for your excellent article in the Mar/Apr 1998 issue of *QEX*.¹ I haven't finished studying it completely, but your clear statements in the first example stimulated me to do something that I have thought about since I first started teaching some time-domain reflectometry topics in a class some years ago. Your statement at the beginning of the article, "By wave interference resulting from superposition," reminded me of an earlier attempt to treat the problem as a sinusoidal multiple-reflection problem. My first inept attempt, by hand calculation of your stub example, convinced me to set up a spreadsheet for the computations. I chose a simple example of a $\lambda/4$ of 50 Ω line driven by an ideal voltage source ($1 \angle 0$ RMS phasor) with a 150 Ω load. Using complex voltage and current reflection coefficients at both ends of the line and the delay due to propagation time, I calculated 18 successive forward and reflected voltage and current phasors at the input to the line.

I then applied superposition by phasor addition of the forward and reflected voltages and currents. Using this result, I calculated forward, reflected and total power, as well as line impedance at the sending end. The results, of course, agree with those predicted by the Smith Chart.

While it maybe some time before I get around to modeling your first example, I am sure that—if it is set up correctly—it will directly demonstrate that wave interference causes total reflection of the reverse power at the match point. Thanks again for the lucid presentation, which clarified points that I had previously missed.—*Warren Weingarten, W9VKG, 216 Clark St, Houghton, MI 49931; e-mail alweing@mail.portup.com*

◇ I was honored to find my *QEX* article between the same covers as that of my greatest mentor and unknow-

ing Elmer, Walt Maxwell, W2DU. I would like to put my two-cents worth in, editorially, in his defense, not that he needs any. For whatever it's worth, here it is:

Follow the Heat

There is a fond saying in the world of physics research: "If you want to know what's really happening, follow the heat."

Whenever we speak of energy, we are really speaking of heat. Eventually, no matter how many contortions and gyrations an electrical or electromagnetic wave may undergo, the bottom line is, how much heat are we generating, and where is it getting hot? If we want to speak of *power*, we simply reconfigure our question to "How fast is it getting hot?" This is not rocket science; it's just good physics and good definitions. With all the debate about whether or not reflected RF power gets "burned up in the plates of the finals," we seldom see evidence of anyone actually measuring this supposed increase in dissipation that results when we have a high-SWR condition.

I have worked closely with high-powered transmitters for a quarter of a century, in both broadcasting and research (where we use megawatts of HF power for ionospheric-heating experiments). In ionospheric research, it's critically important to know how much power you're putting into the region of interest, and therefore critically important to know your transmitter performance. Also, the nature of the research requires considerable frequency agility, which often requires operation well outside the "low SWR" region of the antenna system, and yet with optimum performance. Seldom do we have the luxury of looking into a flat impedance, and often the match is abysmal. We rely on our wide-range output Pi-networks to take up the slack.

Fortunately, our giant water-cooled transmitters do offer us another luxury: We have the ability to measure the plate dissipation very accurately, simply by measuring the rise in water temperature over time, with an accurately known water flow. This

is standard calorimetry—again, not rocket science. We can, and do, measure the plate dissipation of our finals under wildly varying load conditions. As long as we take care to resonate and load our finals properly, we have never seen any difference in plate dissipation between operation at the natural resonant frequency of our antennas and under conditions exceeding 6:1 SWR! This conforms precisely with everything Walter Maxwell, W2DU, has been telling us for decades! If anyone says that operating into a "high SWR" automatically results in poor transmitter efficiency, I would like to see some empirical evidence. I'm confident that I won't see any, however, because there is none. Although the raging debate over SWR makes for lively discussion, seldom does it shed any real light on the subject, and more often than not, it propagates fallacy and vain imagination. Uncle Walt has taken the alternate route, hard science. I choose to remain thoroughly entrenched in his camp.—*Eric Nichols, KL7AJ, PO Box 56235, North Pole, AK 99705; e-mail enichols@gci.com.*

◇ As someone who has had the experience and fun of modeling antennas with computer programs over the years, I wish to point out that it is not necessary to spend a lot of money to get started. Recent articles in *QEX* have focused on the use of packages that are commercially available. The commercial packages have many desirable features, especially in the ease of input and output. However, for people who wish to dabble or even hardcore fanatics there are many quite usable older computer codes available for free on the World Wide Web such as *NEC-2*, *MININEC* and more exotic less heard of codes. Most of these are not *Windows* point-and-click programs, but they are usable if you are not scared off by the idea of having to format your own input with ASCII editors and format the output with editors and spreadsheet programs.

A good place to start looking for these codes is on the University of Missouri - Rolla Electromagnetic Compatibility Web site at: <http://www.emclab.umar.edu/> (see the link for Numerical Electromagnetic Modeling). This site has many items and links of interest to hams in addition to the antenna modeling software.—*Ray Cross, WK0O, Cedar Rapids, Iowa; e-mail rlcross@inav.net* □□